CHARLES UNIVERSITY

FACULTY OF PHARMACY IN HRADEC KRALOVE

DEPARTMENT OF PHARMACOLOGY AND TOXICOLOGY

Resistance mechanisms in therapy of acute myeloid leukemia

Doctoral thesis

Hradec Králové 2022   Mgr. Simona Suchá

ACKNOWLEDGEMENT

Although my PhD journey was turbulent and not always a bed of roses, I have found my love for science and research. And for that, I would like to thank everyone that accompanied me along the way.

I would like to thank my supervisor Assoc. Prof. PharmDr. Martina Čečková, PhD. for giving me the opportunity to work in the research field, for allowing me to participate in interesting projects, for your guidance, support, and critical reflection. Many thanks to my colleagues from our research group, Simona, Fahda, Lenka, Vikrant, for your support, motivation and help along the way. I am incredibly grateful to PharmDr. Aleš Šorf, PhD., with whom I worked on most of the projects. Thank you for your patience, for sharing your skills and knowledge, for endless discussions and, most importantly, your friendship. I would like to thank Assoc. Prof. RNDr. Jakub Hofman, PhD., who was there at the beginning of my scientific journey, introduced me to the lab work and guided me in the early days.

I would like to thank Prof. Jacqueline Cloos for welcoming me in Amsterdam and allowing me to do my internship in her research group. Thank you for the opportunity, for your guidance during my stay, and for broadening my perspective and knowledge.

My PhD journey would not have come to an end if it wasn't for the continuous support of my friends and family. I am especially thankful to Martin, who was there by my side (literally) from day one, and to Tomáš, Yousef, Verča, who kept me going and encouraged me even in tough times. I feel incredibly lucky to have these amazing people by my side.

ABSTRACT IN ENGLISH LANGUAGE

Candidate: Mgr. Simona Suchá

Supervisor: Assoc. Prof. PharmDr. Martina Čečková, PhD.

Title of the doctoral thesis: Resistance mechanisms in therapy of acute myeloid leukemia

Acute myeloid leukemia (AML) is a hematologic cancer known for its extensive heterogeneity, poor treatment outcomes and high relapse rate. Therapy outcome is often compromised by highly resistant leukemic clones present at diagnosis, which evade chemotherapy and continue to spread the disease. Identification of their cellular features is, therefore, a key in successful targeting and eliminating of these resistant leukemic cells. AML cells can, however, develop drug resistance even overtime due to prolonged drug exposure. Extremely high adaptability of leukemic cells enables them to survive whenever therapeutic stress stimuli occur. Uncovering molecular mechanisms that cells utilize to activate their survival mode is crucial in selection of treatment leading to maximal efficacy.

Based on these grounds, two main aims of this thesis were set. First, to determine clinical relevance of ABC efflux transporters in AML and to evaluate the effect of targeted agents on chemotherapy. The focus was put on agents belonging to either FLT3 inhibitors (midostaurin) or CDK4/6 inhibitors (abemaciclib, palbociclib, ribociclib). Second aim was to evaluate transcriptome and proteome changes in AML cell line after having acquired resistance to gilteritinib, another drug from the group of FLT3 inhibitors. Lysosomes were further explored as mediators of gilteritinib resistance in more detail.

In the first part, we focused on ABCB1 transporter widely recognized for its role in cancer resistance. In peripheral blood mononuclear cells isolated from patients *de novo* diagnosed with AML, increased *ABCB1* gene expression was identified in patients not responding to anthracycline-based induction therapy, and therefore, not achieving complete remission. Patients highly expressing *ABCB1* were predominantly CD34 positive and belonged to a patient group with adverse cytogenetic risk. Activity of ABCB1 was diminished by all tested kinase inhibitors (midostaurin, abemaciclib, palbociclib, ribociclib), which was reflected in elevated intracellular anthracycline concentrations while at the same time providing evidence of ABCB1 being their off-target. Moreover, exposure of ABCB1-overexpressing leukemic cells to midostaurin and anthracycline led to induction of apoptosis. We also found a direct linkage

between ABCB1 efflux activity and miR-9 expression, which post-transcriptionally regulates ABCB1 in AML. Collectively, we provide evidence that ABCB1 gene expression and function is highly related to resistant AML phenotype and that miR-9, if used as a biomarker, could be helpful in identifying such patients.

The second part elaborated on gilteritinib-resistant HL-60 G75 cell line developed in our lab. Cells developed resistance, which was transient, and upon gilteritinib withdrawal, it was completely reversed only after four weeks. Distinct transcriptome and proteome profiles were revealed in HL-60 G75 when compared to gilteritinib-sensitive HL-60 WT. Although the resistance appeared to be resulting from modification of multiple cellular processes, some stood out more than the others. Lysosomes-related processes as one of the most deregulated ones were explored further. Lysosomes-specific staining revealed increased number of lysosomes in HL-60 G75, however, gilteritinib withdrawal led to immediate decrease. Sunitinib, a drug with similar mechanism of action and physicochemical properties as gilteritinib, but fluorescent, was utilized to detect sequestering capacity of lysosomes. Sunitinib was fully sequestered in lysosomes in HL-60 G75 but seemed to be predominantly spread within cytosol upon gilteritinib withdrawal. Fluctuation of lysosomal mass and/or activity appeared to be highly dependent on gilteritinib presence. Although the exact mechanism is not yet known, we suppose that gilteritinib might have a direct or indirect impact on lysosomal biogenesis.

In summary, data presented in this thesis brought new insights into mechanisms of resistance, which to this day presents one of the most challenging obstacles in AML pharmacotherapy.

ABSTRAKT V SLOVENSKOM JAZYKU

Kandidát: Mgr. Simona Suchá

Školiteľ: doc. PharmDr. Martina Čečková, Ph.D.

Názov dizertačnej práce: Mechanizmy rezistencie v terapii akútnej myeloidnej leukémie

Akútna myeloidná leukémia (AML) patrí medzi hematologické ochorenia známe pre svoju rozsiahlu heterogenitu, nedostatočnú odpoveď na liečbu a vysokú mieru relapsov. Terapia častokrát zlyháva kvôli mimoriadne rezistentným leukemickým klonom prítomným v čase diagnózy. Vďaka ich schopnosti vyhnúť sa terapii sa môže ochorenie voľne šíriť ďalej v tele. Dôkladná charakteristika týchto buniek je preto kľúčová v ich úspešnom odhalení a následnom zničení. AML bunky však dokážu nadobudnúť rezistenciu na prítomné látky i počas prebiehajúcej liečby, a to vďaka ich dlhodobému vystaveniu týmto látkam. Extrémne vysoká adaptabilita leukemických buniek im umožňuje prežiť zakaždým, keď sa stres v podobe liečiv objaví. Preto je nevyhnutné odhaliť molekulárne mechanizmy, ktoré bunky využívajú k tomu, aby sa týmto vonkajším vplyvom prispôsobili.

Na základe týchto poznatkov boli stanovené dva primárne ciele tejto práce. Prvým bolo zistiť klinickú relevanciu ABC efluxných transportérov v AML a vyhodnotiť možný vplyv cielenej terapie na chemoterapiu. Dôraz bol kladený na liečivá zo skupiny FLT3 inhibítorov (midostaurin) a CDK4/6 inhibítorov (abemaciclib, palbociclib, ribociclib). Druhým cieľom bolo charakterizovať zmeny v transkriptóme a proteóme AML bunkovej línie, ktorá si časom vybudovala rezistenciu voči gilteritinibu, ďalšiemu liečivu zo skupiny FLT3 inhibítorov. Jedným z mechanizmov, ktoré boli študované ďalej boli lyzozómy a ich podiel na rezistencii voči gilteritinibu.

V prvej časti tejto práce sme sa zamerali na ABCB1 transportér známy pre svoj značný podiel na liekovej rezistencii. K tomu boli využité mononukleárne bunky vyizolované z periférnej krvi pacientov s *de novo* diagnostikovanou AML. U pacientov, ktorí nereagovali na indukčnú liečbu pozostávajúcu z antracyklínu a cytarabínu, bola zistená zvýšená expresia *ABCB1* génu. U týchto pacientov nebol dosiahnutý stav kompletnej remisie. Pacienti s vysokou génovou expresiou *ABCB1* boli prevažne CD34 pozitívni a patrili do skupiny pacientov s nepriaznivými cytogenetickými zmenami. Aktivita ABCB1 bola efektívne zablokovaná prostredníctvom všetkých štyroch testovaných inhibítorov (midostaurin, abemaciclib, palbociclib, ribociclib), čo

sa prejavilo i na zvýšenom intracelulárnom množstve antracyklínov. Súčasne tak bol ABCB1 identifikovaný ako jeden z možných sekundárnych terapeutických cieľov týchto liečiv. Navyše kombinácia midostaurinu a antracyklínu spôsobila prechod leukemických buniek s nadmernou expresiou ABCB1 do apoptózy. Taktiež bol odhalený priamy vplyv miR-9 na efluxnú aktivitu ABCB1, ktorá sa podieľa na posttranskripčnej regulácii ABCB1 v AML. Výsledky tejto časti teda naznačujú, že génová expresia a taktiež funkčná aktivita ABCB1 súvisia s rezistenciou AML pacientov, a že miR-9 by mohol napomôcť v identifikácií týchto pacientov v čase diagnózy.

Druhá časť tejto práce sa zaoberala bunkovou líniou rezistentnou na gilteritinib, ktorá bola vytvorená v našich laboratóriách a nesie označenie HL-60 G75. Bunky dlhodobo kultivované v prítomnosti gilteritinibu si časom vytvorili rezistenciu na túto látku, hoci len dočasnú, keďže už štyri týždne po vysadení gilteritinibu sa rezistencia kompletne stratila. Transkriptóm a proteóm HL-60 G75 a HL-60 WT, bunkovej línie senzitívnej na gilteritinib, sa pritom výrazne líšili. Napriek tomu, že sa na vytvorení a udržaní rezistencie podieľalo niekoľko rôznych bunkových mechanizmov, niektoré z nich sa prejavili viac ako iné. Jedným z najviac deregulovaných boli procesy súvisiace s lyzozómami. Mikroskopická a cytometrická analýza s priamym označením lyzozómov odhalila výrazne vyšší počet lyzozómov v HL-60 G75, ktorý však klesol okamžite po odobraní gilteritinibu. Pre overenie schopnosti lyzozómov sekvestrovať sa využil sunitinib, čo je liečivo s podobným mechanizmom účinku i fyzikálno-chemickými vlastnosťami ako gilteritinib, avšak na rozdiel od gilteritinibu fluoreskuje. V HL-60 G75 sa všetok sunitinib sekvestroval v lyzozómoch. Keď sa týmto rezistentným bunkám odobral gilteritinib z kultivačného média, sunitinib zmenil svoju lokalizáciu a prednostne sa vyskytoval v cytozole. Tieto výsledky naznačujú, že fluktuácia množstva a/alebo aktivity prítomných lyzozómov je závislá na prítomnosti gilteritinibu. Hoci presný mechanizmus, ktorým k tomuto javu dochádza, nie je známy, zdá sa, že gilteritinib by mohol priamo alebo nepriamo ovplyvňovať biogenézu lyzozómov.

Výsledky tejto práce prispievajú k lepšiemu porozumeniu mechanizmov rezistencie leukemických buniek, ktorá i v dnešnej dobe predstavuje jednu z najväčších prekážok farmakoterapie AML.

TABLE OF CONTENTS

1 INTRODUCTION

Hematopoiesis - a lifelong blood cell production - is a highly regulated process. Hematopoietic stem cells have the ability to self-renew and give rise to all blood lineages. These cells maintain the homeostasis of the hematopoietic system and are involved in crucial processes such as immunity, hemostasis, and oxygen supply. Progenitor cells originating from a hematopoietic stem cell follow a specific path to develop into mature blood cells. Any abnormalities or disruption of the developmental process can lead to hematological diseases. This dissertation focuses on acute myeloid leukemia (AML), a disease characterized by uncontrolled division of abnormal myeloid progenitors [1, 2].

2 ACUTE MYELOID LEUKEMIA

AML is a hematologic malignity arising from immature myeloid blasts that are rapidly proliferating and partially or fully arrested in their immature stage. Eventually, the blasts accumulate in the bone marrow and by replacing healthy stem cells lead to bone marrow failure. Rapid spillage into the bloodstream may spread the disease to other body tissues [3].

2.1 Epidemiology

According to the annual report of American Cancer Society, AML is the second most common type of leukemia in both adults and children. In the US, in 2022 20,050 new AML cases are expected to be diagnosed, accounting for 1.0 % of all new cancer cases, and a total of 11,540 deaths, accounting for 1.9 % of all estimated deaths. Over the years, rates of new cases and deaths (Fig 1) have been stable, while 5-year survival has been continuously increasing. Nevertheless, with an overall 5-year survival of 30.5 %, AML still belongs to life-threatening malignancies especially in the elderly since median age at diagnosis is 68 and 73 at death [4, 5].
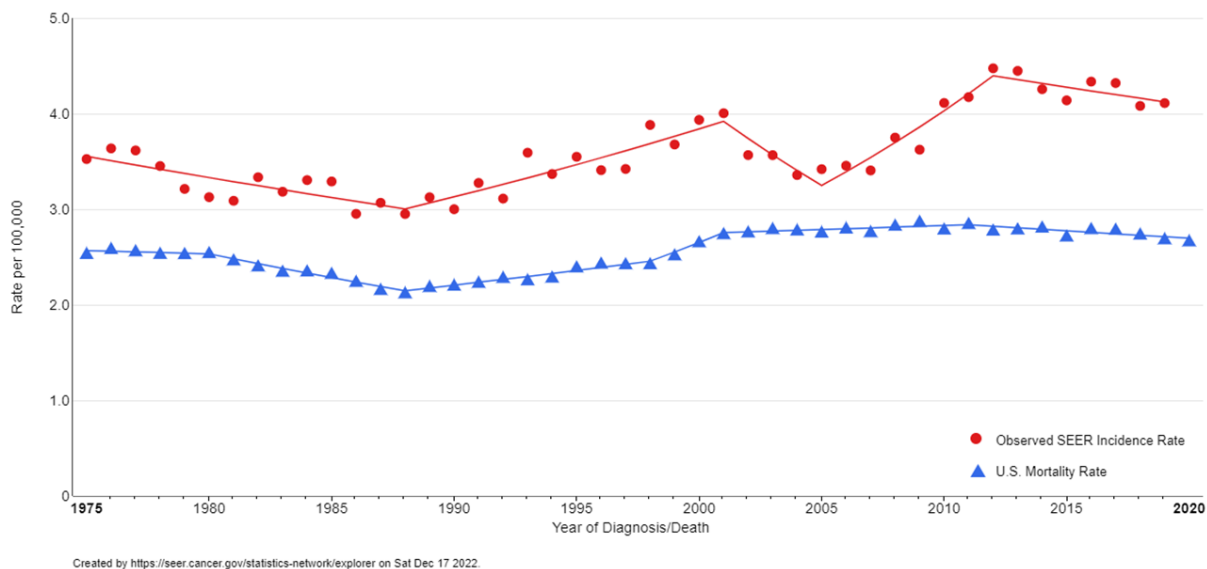
Fig 1. Rates of new AML cases (red) and deaths (blue) over the years. Modified from [5].

2.2 Diagnosis, prognosis, and classification

Since AML interferes with blood cells, it predominantly presents with leukocytosis, thrombocytopenia, neutropenia, or anemia, which can result in bleeding and bruising problems, susceptibility to infections, fever, breathlessness, pallor, or overall weakness. If untreated, it can have devastating effects on human body [6]. AML is typically diagnosed when blasts in peripheral blood or bone marrow exceed 20 %, however, blast threshold for AML-defining recurrent genetic abnormalities is only 10 %. Besides blast count, immunophenotyping, cytogenetic and molecular analyses are routinely performed to establish the diagnosis and identify therapeutic targets for treatment selection [7, 8].

2.2.1 Immunophenotyping

Detection of cell surface and intracellular markers by flow cytometry is necessary to not only accurately identify AML subtypes, but to distinguish AML from different types of leukemia. Implementation of flow cytometry has become essential in the assessment of leukemia stem cells (LSC) as well as measurable residual disease (MRD). LSC are the most therapy-resistant subpopulations of the bulk leukemic cells present at diagnosis. These cells eventually outgrow and initiate the relapse (Fig 2). Typically, they're defined by the $CD34^+CD38^-$ immunophenotype and are assessed at diagnosis and at follow-up. MRD refers to the persistent leukemic cells that remain present in the body after the initial treatment. MRD is detected at the apparent complete remission (CR) and is believed to include subpopulations of LSC. MRD is

now being implemented into routine diagnostics as a prognostic factor valuable in post-diagnosis decision-making and relapse prediction [9-11].
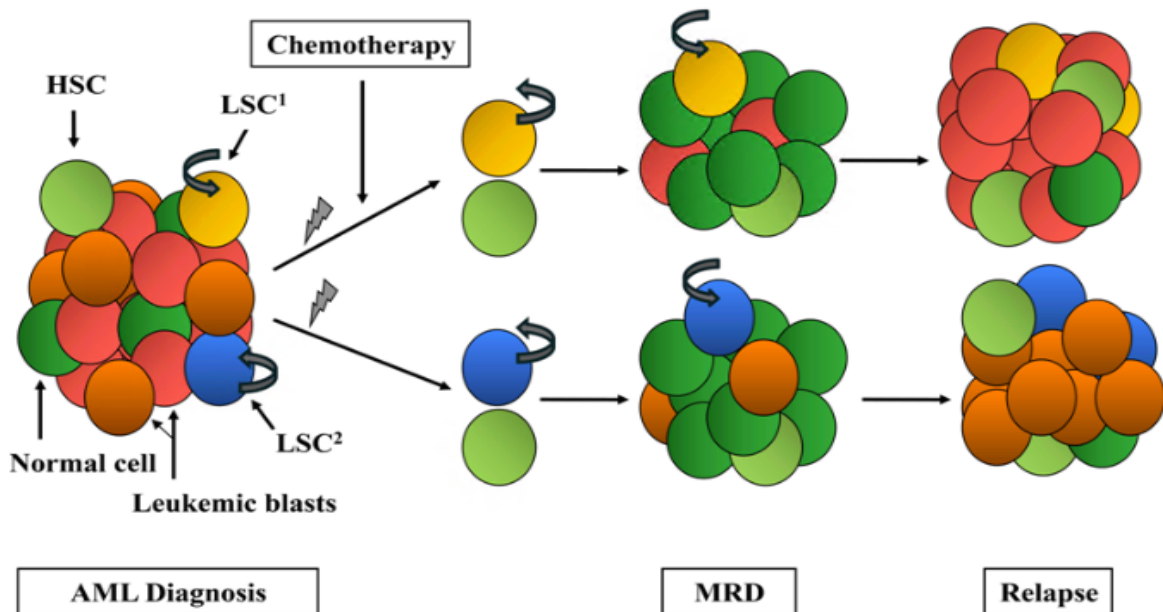
Fig 2. The role of leukemia stem cells (LSC) and measurable residual disease (MRD) in AML. At diagnosis, a heterogenous population of cells can be identified including normal and leukemic cells. After treatment, only chemotherapy-resistant cells remain in a patient and are assessed during MRD detection. Resistant leukemic cells can include different subpopulations of LSC (referred to as LSC[1] and LSC[2] in the figure) of which any can cause relapse [11].

2.2.2   Cytogenetics

Karyotype and cytogenetic abnormalities represent key indicators in diagnosis of AML. As mentioned above, patients with certain recurrent cytogenetic abnormalities are considered to have AML even if their blast count does not reach the threshold of 20 %, since occurrence of such abnormalities has an immense impact on patient's prognosis. While some aberrancies affect the prognosis positively (e.g., t(8;21), t(16;16), inv(16) or t(15;17)), others affect it negatively (such as inv(3), t(3;3) or complex karyotype that involves 3 or more chromosomes). Nevertheless, almost 50 % of adult AML patients have a normal karyotype (Fig 3), yet very heterogenous therapeutic outcomes [12, 13].

2.2.3   Gene mutations

AML development can be driven by mutations in several genes that have been identified in patients with normal karyotype but can be found in other cytogenetic groups as well. Recurrent

somatic mutations and their cooccurrence tremendously influence prognostic outcome and treatment selection. Internal tandem duplication in the fms-like tyrosine kinase 3 (*FLT3*-ITD), a receptor tyrosine kinase with a crucial role in normal hematopoiesis, occurs in a third of all AML cases. Its presence is associated with overall poor survival and high relapse rate; therefore, focus is put on development of FLT3-targeted therapy (see chapter 2.4.1). Prognostic impact of *FLT3*-ITD can be positively influenced by concurrent mutations in the nucleophosmin (*NPM1*) gene, which overall demonstrates favorable outcomes. Most frequent mutations in AML are depicted in Fig 3 [13-15].
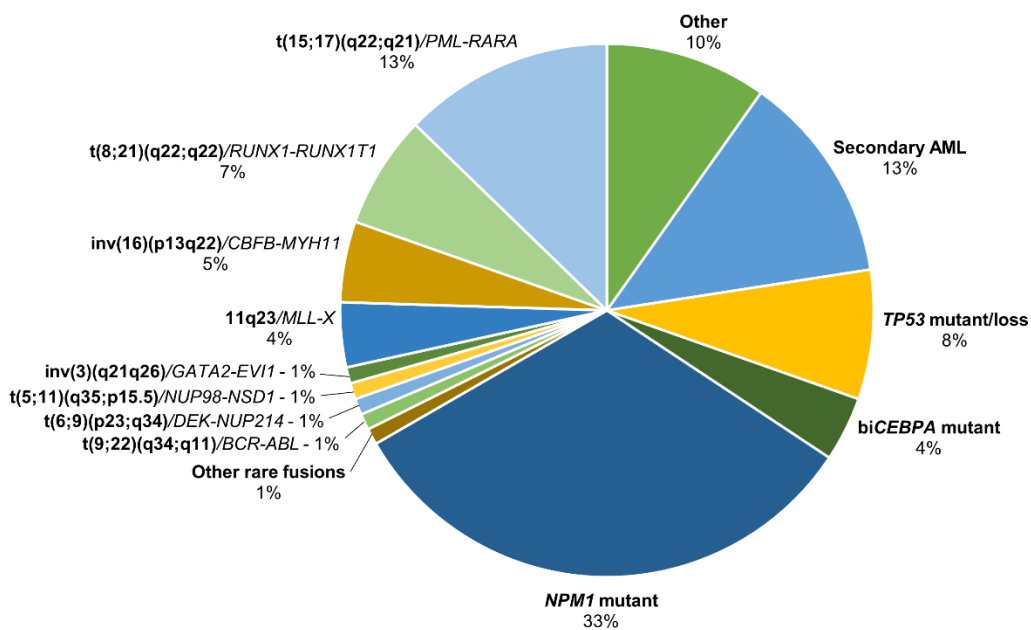
Fig 3. Overview of frequently occurring cytogenetic alterations and gene mutations in adult AML. Somatic chromosomal abnormalities (e.g., t(8;21)), that give rise to chimeric fusion genes (e.g., BCR-ABL) and genes encoding transcription factors (e.g., PML-RARA, RUNX1), epigenetic regulators (e.g., MLL-X) and others are in bold, while encoded genes are in italic. Modified from [15].

2.2.4 Classification

AML is organized into various classification systems used by clinicians as well as researchers. These systems provide recommendations for diagnosis of AML in adults and inform of the prognosis and treatment options. The French-American-British (FAB) classification is the oldest, yet still commonly used system primarily based on the morphology of the leukemic cells. Recently, the WHO classification has come to the fore. Besides cell morphology, it considers cytogenetic and molecular aspects as well as immunophenotyping [7]. The European LeukemiaNet (ELN) constructed a risk stratification system which, unlike FAB and WHO,

reflects the patient's prognosis. Patients are divided into three risk categories (favorable, intermediate, adverse) according to their cytogenetics and mutational status (Fig 4) [8].

	ELN	WHO	FAB
Favorable	• t(8;21)(q22;q22.1)/*RUNX1::RUNX1T1* • inv(16)(p13.1q22) or t(16;16)(p13.1;q22)/*CBFB::MYH11* • Mutated *NPM1* without *FLT3*-ITD • bZIP in-frame mutated *CEBPA*	• AML with recurrent genetic abnormalities • AML with myelodisplasia-related changes • Therapy-related myeloid neoplasms • AML, Not otherwise specified • Myeloid sarcoma • Myeloid proliferations related to Down syndrome	M0 Undifferentiated AML M1 AML with minimal maturation M2 AML with minimal maturation M3 Acute promyelocytic leukemia (APL) M4 Acute myelomonocytic leukemia M5 Acute monocytic leukemia M6 Acute erythroid leukemia M7 Acute megakaryocytic leukemia
Intermediate	• Mutated *NPM1* with *FLT3*-ITD • Wild-type *NPM1* with *FLT3*-ITD (without adverse-risk genetic lesions) • t(9;11)(p21.3;q23.3)/*MLLT3::KMT2A* • Cytogenetic and/or molecular abnormalities not classified as favorable or adverse		
Adverse	• t(6;9)(p23.3;q34.1)/*DEK::NUP214* • t(v;11q23.3)/*KMT2A*-rearranged# • t(9;22)(q34.1;q11.2)/*BCR::ABL1* • t(8;16)(p11.2;p13.3)/*KAT6A::CREBBP* • inv(3)(q21.3q26.2) or t(3;3)(q21.3;q26.2)/*GATA2, MECOM(EVI1)* • t(3q26.2;v)/*MECOM(EVI1)*-rearranged • −5 or del(5q); −7; −17/abn(17p) • Complex karyotype, monosomal karyotype • Mutated *ASXL1, BCOR, EZH2, RUNX1, SF3B1, SRSF2, STAG2, U2AF1, and/or ZRSR2* • Mutated *TP53*		

Fig 4. AML organization according to the European LeukemiaNet (ELN), WHO, and the French-American-British (FAB) classification systems. Modified from [8, 13].

2.3 Treatment

Standard treatment of AML has not changed for the past five decades. After being diagnosed with AML, medically fit patients receive an anthracycline-based chemotherapy in combination with cytarabine. The combination is commonly referred to as the 7+3 regimen since it consists of a continuous 7-day administration of cytarabine with the infusion of daunorubicin on days 1 to 3. If insufficient to achieve CR, the 7+3 cycle can be repeated. Patients who are unable to tolerate intensive induction therapy receive a non-intensive alternative. Preferably, hypomethylating agents (e.g., decitabine, azacitidine) alone or in combination with venetoclax are administered [8, 16]. An additional drug can be incorporated into the induction therapy of patients with identified mutations or specific targets, e.g., midostaurin for *FLT3*-mutated AML (see chapter 2.4.1) [17] or gemtuzumab ozogamicin for CD33-positive AML [18-20].

Following successful achievement of CR, consolidation (post-remission) therapy is given. Standard protocols recommend the administration of an intermediate-dose cytarabine (IDAC). In cases of *FLT3*-mutated AML or CD33-positive AML, targeted agents (midostaurin or

gemtuzumab ozogamicin) can be incorporated into the consolidation. Hematopoietic cell transplantation (HCT) is considered as another option after successful induction therapy. Although allogeneic (cells from the donor) and autologous (cells from the patient) stem cell transplantations have been found to prevent relapse more effectively than IDAC, transplantations are still associated with higher morbidity and mortality. Therefore, the risk/benefit evaluation is crucial for consolidation therapy selection [8, 16, 20].

If the induction treatment fails to eradicate all leukemic cells, the disease can persist or come back. Unresponsiveness to the induction therapy and inability to achieve CR is called refractory AML. In cases when a patient was in CR, but the disease returned, we speak of relapsed AML. In patients with relapsed or refractory (R/R) AML, reinduction of remission by IDAC with or without anthracycline can be tried, although patients are unlikely to respond. At this stage of the disease, newly emerged targets, that were not present at diagnosis, are often detected. Their evaluation is crucial in order to tailor the treatment. Mutations in *FLT3,* isocitrate dehydrogenase 1 *(IDH1)* and isocitrate dehydrogenase 2 *(IDH2)* are the most frequently identified genetic alterations. Gilteritinib is currently used to treat *FLT3*-mutated R/R AML [21], while ivosidenib is selected for *IDH1*-mutated R/R AML [22] and enasidenib for R/R AML with *IDH2* mutation [23]. Despite many treatment options being available, allogeneic HCT is recommended to all patients considered eligible for HCT. According to the recent study comprising the worldwide HCT activity, leukemia is the most indicated disease for allogeneic HCT with AML being the most frequent one out of all leukemias [24]. Nevertheless, it does not guarantee fully cured patients since they do relapse even after receiving the allograft. On the other hand, patients who achieve a second remission can undergo another HCT or get donor lymphocyte infusion and be cured that way. One more option not only R/R patients, but all AML patients have is to take part in clinical trials if a suitable trial is currently enrolling patients and potentially benefit from treatments not yet approved [25].

2.4 Targeted therapy

Traditional chemotherapy might effectively diminish cancer cells, but it also affects healthy cells and tissues due to its non-specificity. Therefore, more specific agents have come to the forefront in the recent years. As the name targeted therapy indicates, these agents differ in the mechanism of action since they act on specific molecular targets. The goal of the targeted therapy is to not only recognize cancerous cells from healthy ones, but to be ideally utilized in

multiple cancers that share the same targets. Targeted therapy can be divided into three main groups - small molecule inhibitors, monoclonal antibodies, and immunotoxins [26]. This thesis elaborates on small molecule inhibitors, agents that target inappropriate kinase activity, which is often responsible for non-functional or abnormally functional downstream signaling pathways. In the next subchapters, the focus will be put on tyrosine kinase FLT3 and protein kinase CDK4/6.

2.4.1 FLT3-mutated AML

FLT3 belongs to a family of type III receptor tyrosine kinases, and it is expressed in immature hematopoietic cells, placenta, brain, and gonads. In bone marrow, FLT3 expression seems to be exclusive to early progenitors as most of CD34 positive cells express FLT3. Moreover, the expression of FLT3 was found to be decreasing upon differentiation [27, 28]. Wild-type FLT3 (FLT3-WT) is a crucial element in regulatory processes of hematopoietic cells, including proliferation, apoptosis, transcription, or leukemogenesis. Typically, FLT3-WT stays in its inactive form unless activated by the ligand, which leads to phosphorylation of the tyrosine kinase domain and activation of all downstream pathways. In leukemia, FLT3-WT has been found to be overexpressed in almost 100 % of AML cases and its activation results in constitutive activation of the receptor, which promotes proliferation and survival of leukemic cells [29].

Recently, activating mutations in the *FLT3* gene have been identified as the most frequently occurring genetic abnormalities in AML accounting for a third of all AML cases. These mutations either occur as internal tandem duplications (ITD) or point mutations in tyrosine kinase domain (TKD). Nevertheless, both mutations lead to ligand-independent constitutive activation of FLT3 receptor and eventual survival of leukemic cells [30-32]. When it comes to prognostic value, AML patients with *FLT3*-ITD have higher probability of relapse and reduced chances of overall survival [33, 34], while the impact of *FLT3*-TKD on prognosis has not been determined most likely due to its low frequency but appears to be more favorable nonetheless [35]. Several studies have demonstrated positive effects of coexisting mutations, such as *NPM1*, on the prognostic impact of *FLT3*-ITD [36-38], which was implemented in the ELN classification. However, based on the recent study [39], the most recent ELN risk classification does not consider concurrent mutations as a risk-determining factor [8].

Given the frequency of *FLT3* mutations in AML, targeting this kinase appears as a promising treatment strategy. Currently, many tyrosine kinase inhibitors (TKi) are either under development, in clinical trials or have already been approved and established in the therapy of AML. FLT3 inhibitors (FLT3i) can be divided into the first- and second-generation. The first-generation FLT3i target not only FLT3, but also other downstream receptor tyrosine kinases, which may result in overall antileukemic effect or lead to various off-target toxicities. On the other hand, second-generation FLT3i have been developed to be more FLT3-specific and less toxic by having fewer off-targets. The first-generation FLT3i include midostaurin, sorafenib or sunitinib, while quizartinib, gilteritinib or crenolanib belong to the second-generation FLT3i. These inhibitors can be also divided into two groups based on their target mutation, that is type I FLT3i, which are active against both *FLT3*-ITD and -TKD, and type II FLT3i only active against *FLT3*-ITD [32, 40].

Midostaurin

Midostaurin is a multikinase inhibitor showing activity against FLT3 but also c-KIT, PKC, VEGFR-2 and PDGFRB [41]. It is the first oral FLT3i approved for the treatment of newly diagnosed *FLT3*-mutated AML and advanced systemic mastocytosis. In AML cases, it has been implemented into the induction therapy in which cytarabine and anthracycline are administered for 7 days and midostaurin is given on days 8-21 [42, 43]. Approval of midostaurin was based on international randomized phase III "RATIFY" trial. The study revealed a higher 4-year survival of AML patients with either *FLT3*-ITD or *FLT3*-TKD on midostaurin than patients on placebo with the most beneficial effects in *NPM1*-WT and *FLT3*^{high} patients [17]. In the recent retrospective study, which included the same patients who were enrolled in the RATIFY trial, a beneficial effect of midostaurin was observed across all ELN risk groups regardless of concurrent mutations or FLT3 allelic ratio [39].

Gilteritinib

Gilteritinib belongs to the group of type I FLT3i. It is more selective than midostaurin but besides FLT3, it also shows activity against AXL, ALK, and ALT [32]. Based on the phase III "ADMIRAL" clinical trial [21], it was approved as monotherapy for the treatment of R/R *FLT3*-mutated AML by the FDA in 2018 [44] and by the EMA in 2019 [45]. The ADMIRAL study demonstrated longer survival of patients on gilteritinib than those receiving chemotherapy. Also, a higher number of patients on gilteritinib achieved CR compared to those treated with chemotherapy.

2.4.2 Cyclin-dependent kinases

Cyclin-dependent kinases (CDK) are regulatory units crucial in the maintenance of cell cycle, which can be divided into 4 phases: G1, S, G2, and M (Fig 5). In cooperation with cyclins and cyclin-dependent kinase inhibitors (CDKi), they ensure appropriate cell cycle transitions from one phase to another. Cell cycle comprises two major checkpoints that control G1/S and G2/M transitions, which determine whether cells enter the next phase or not. CDK4 and CDK6 are two enzymes driving the progression from G1 to S phase [46, 47].
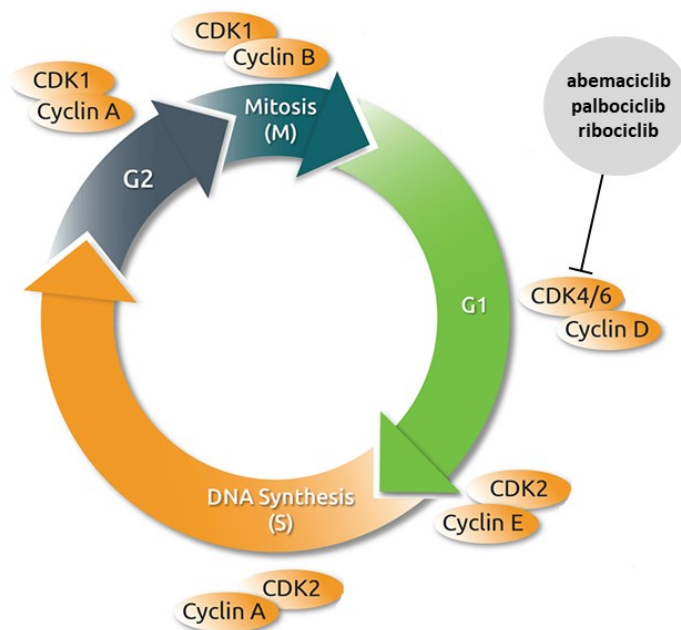
Fig 5. Cell cycle phases, their regulatory units consisting of cyclin-dependent kinases (CDK) and cyclins, and CDK4/6 inhibitors (abemaciclib, palbociclib, ribociclib). Modified from [48].

CDK4/6 dysregulation resulting from gene alterations has been associated with many different cancers, including leukemias. Mutated and overexpressed CDK4/6 fail to control the cell cycle and lead to uncontrolled proliferation of cancer cells [49, 50]. Therefore, the search for effective CDKi has become important in the therapy of not only leukemias, but also other cancers. This thesis focuses on 3 selective CDK4/6 inhibitors - abemaciclib, palbociclib, ribociclib - currently approved for the treatment of breast cancer [51-54]. At the time of our study, ribociclib and palbociclib were subjected to multiple clinical trials with patients suffering from acute leukemias. In the meantime, some of these studies got canceled, however, palbociclib remains to be implemented in several trials mostly concerning patients with R/R AML and ALL (acute

lymphoblastic leukemia) [55]. CDK6 has been linked to *FLT3*-ITD mutation commonly present in AML. It appears that *FLT3*-mutated AML cells require CDK6 for their successful proliferation and downstream signaling since decreased CDK6 led to a downregulation of FLT3 and its downstream signaling pathways [56-59].

3   RESISTANCE IN AML

Chemoresistance is one of the biggest obstacles in achieving successful cancer therapy. Even with the continuous development of newer and newer drugs, cancerous cells can rapidly adapt to new agents, which leads to eventual acquirement of drug resistance. In leukemia, even patients with apparent CR may relapse and it happens mainly due to chemoresistance. It can be caused by various mechanisms, but this thesis elaborates only on two of them - pharmacokinetic resistance associated with ATP-binding cassette (ABC) transporters and resistance mediated by lysosomal sequestration.

3.1   ABC transporters

ABC transporters create one of the largest groups of transporters. These transporters are localized in cell membranes and enable transport of various substrates across them, including nutrients, ions, and other endogenous molecules as well as toxins, drugs, and other exogenous compounds. ABC transporters can function either as importers (transporting molecules into organelles) or exporters (transporting molecules out of cells). Regardless of the direction, energy obtained from ATP hydrolysis is required to power the transport across membranes (Fig 6) [60].
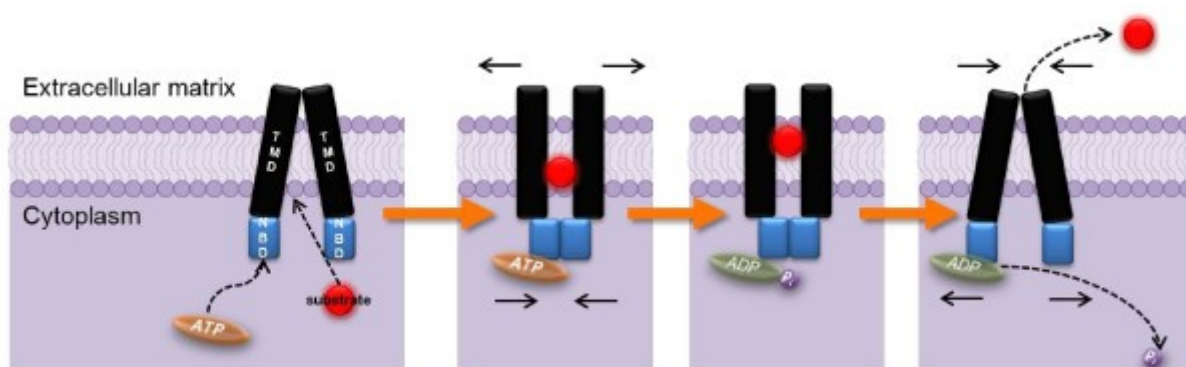
Fig 6. General mechanism of ABC transporters. ABC transporters consist of two nucleotide-binding domains (NBD) and two transmembrane domains (TMD). Upon substrate binding, conformational changes of all subunits are initiated. Hydrolysis of ATP provides energy required for the transport of

substrate until it's fully translocated. Afterwards, the transporter restores its original configuration for another cycle [61].

ABC transporters are localized in multiple tissues of the human body, predominantly in organs of excretory system. In intestines, they play important role in absorption of oral drugs into blood stream since the transport of drugs, which are substrates of ABC transporters, may be largely limited in intestines. Transporters localized in hepatocytes export bile salts or cholesterol into bile and thereby ensure biliary excretion, while renal transporters handle elimination of the drugs and its metabolites by urine. Besides excretory organs, ABC transporters can also be found in biological barriers (blood-brain barrier and blood-testis barrier) and in placenta, where they provide a protective role for the brain, testis, and fetus [62, 63].

The superfamily of ABC transporters contains 49 known membrane proteins, which are organized into 7 subfamilies ABCA - G [64]. Two ABC transporters have been widely associated with cancer resistance in general and their contribution to drug resistance has also been seen in AML. Following subchapters disclose details on these two ABC transporters - ABCB1/P-glycoprotein and ABCG2/breast cancer resistance protein.

3.1.1   ABCB1 & its role in AML

ABCB1, commonly known as P-glycoprotein (P-gp), is the most studied and characterized transporter frequently expressed in cancer stem-like cells, including leukemic cells. In leukemia and other cancers, ABCB1 has been found to be upregulated and its expression has been detected even in tissues in which ABCB1 is normally absent. This upregulation presents an effective way of how cancer cells evade chemotherapy and avoid cell death. Several chemotherapeutics, including anthracyclines used in the treatment of AML, have been described as substrates of ABCB1. Due to the ABCB1-mediated efflux, or in other words constant pumping of drugs out of cells, suboptimal drug concentrations are present in cancer cells, which impairs therapy response [65].

Overexpression of ABCB1 has been identified in approximately 30 % of AML cases at diagnosis of which majority was found to be chemotherapy-resistant [66, 67]. High ABCB1 levels have been associated with lower CR rate, worse event free survival and worse overall survival [68-71]. ABCB1 has been described as predominantly hyperactive in immature leukemic cells with CD34 positivity [72-74].

Regulation of *ABCB1* expression as well as expression of any other gene in the human body is essential. In the recent years, epigenetic modulation of *ABCB1* has been greatly explored since mechanisms such as histone modifications, DNA methylation or microRNA (miRNA/miR) seem to be involved in its regulation [75-77]. MiRNAs are short non-coding RNAs involved in regulation of multiple cellular processes (e.g., proliferation, apoptosis, differentiation, or development). MiRNAs bind with the 3'untranslated region sequences of the target mRNA, which leads to translational repression or mRNA degradation [78, 79]. In this thesis, we looked closely at three miRNAs which control ABCB1 expression - miR-9-5p, miR-27a-5p, and miR-331-5p (referred to as miR-9, miR-27, and miR-331, respectively). Moreover, these miRNAs have been associated with chemotherapy resistance in AML [80-83].

3.1.2 ABCG2 & its role in AML

ABCG2, also known as breast cancer resistance protein (BCRP), is another frequently expressed transporter in AML, yet his clinical relevance is not clear as studies have brought very inconsistent data. Some did not find any linkage of its expression to CR rate, event free survival or overall survival [84-86], while others observed association with some prognostic factors, although mostly in pediatric AML [86-88]. Nevertheless, what most of the studies agree on is that ABCG2 is predominantly expressed on CD34$^+$ leukemic cells [89-91] and that coexpression of multiple ABC transporters presents rather unfavorable prognosis and may increase the chances of relapse [92, 93].

3.2 Lysosomes

For a long time, lysosomes were believed to function only as recycle bins for degraded macromolecules such as lipids, polysaccharides, proteins, or their building blocks. Later, their involvement in autophagy regulation, signal transduction, homeostasis as well as in pathological processes, tumorigenesis, or immune responses was uncovered. To function properly, lysosomes require acidic lumen which is maintained by lysosomal V-ATPase located in the lysosomal membrane [94, 95]. Lysosomes are closely intertwined with endosomes (early, late and recycling endosomes) and together they create endolysosomal system. These lysosomes, also called secondary lysosomes, can result from a fusion with late endosomes or phagosomes, or maturate from late endosomes. They are generally larger in size, contain active digestive enzymes and are able to eliminate their content out of the cell by exocytosis [95]. Primary lysosomes represent another type of lysosomes which originate from the Golgi

apparatus. These lysosomes are generally smaller, function as storage vacuoles and do not release its content or waste products. During cancer progression, cancer cells increase their lysosomal mass and enhance lysosomal activity (enzyme activity and lysosomal biogenesis) to cope with demanding energy requirements of the cell. These processes, however, make lysosomes of cancer cells more fragile and susceptible to disruption than those of normal cells since normal cells typically activate compensatory mechanisms to prevent cell death. In cancer cells, destabilization of lysosomes can be caused by accumulation of lysosomotropic drugs. That leads to lysosomal membrane-cell permeabilization, release of lysosomal contents and eventual cell death. Drug accumulation in lysosomes can, however, also contribute to drug resistance by reducing effect of drugs on their targets. Therefore, targeting lysosomal integrity and function could present a way to induce activation of programmed cell death while simultaneously allowing drugs to reach their molecular targets and contribute to cell death [96, 97].
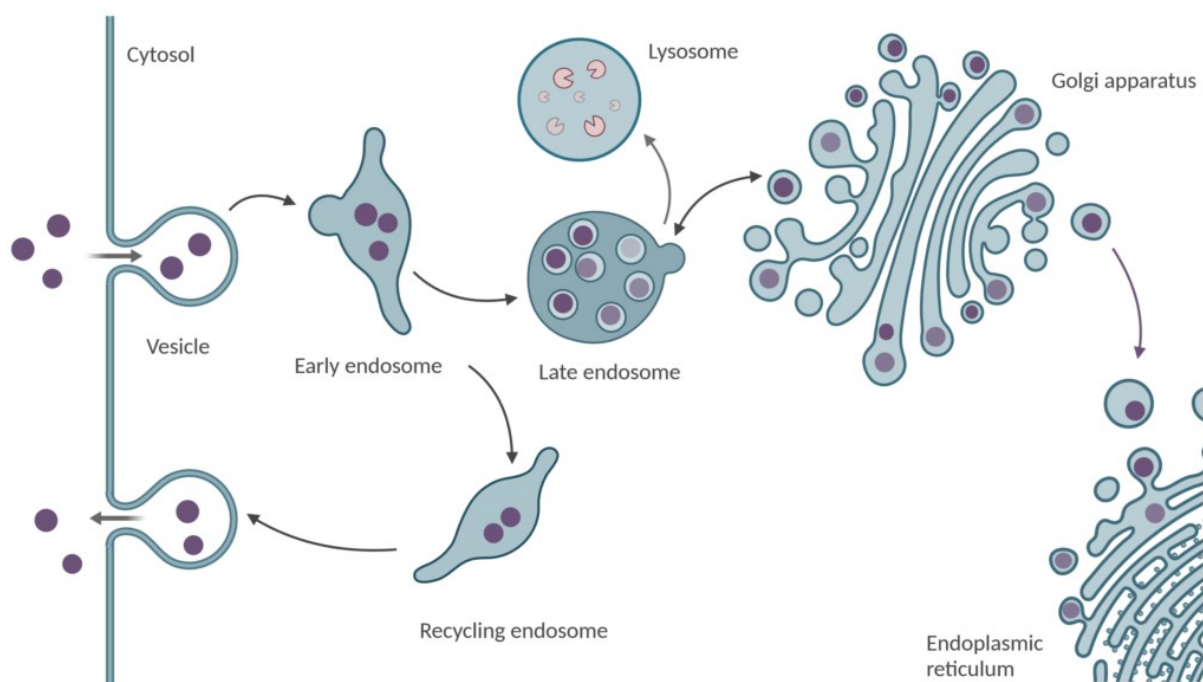
Fig 7. Endolysosomal system & formation of secondary lysosomes. Cargo molecules enter the cell and form a vesicle, which is delivered to an early endosome. Content of the early endosome can be either recycled back to the plasma membrane by endocytosis or can follow the endosomal pathway. Early endosome matures into a late endosome and later a lysosome, which degrades its content. Molecules

can be also transported from the Golgi apparatus to endosomes and further form a lysosome or they can be recycled back to the Golgi apparatus [98].

3.2.1 Lysosomal sequestration

Resistance mechanism provided by lysosomes is called lysosomal sequestration or lysosomal trapping. Drugs that are lipophilic weak bases can either freely enter the lysosome by passive diffusion or can cross the lysosomal membrane through ABC transporters embedded in the membrane, predominantly through ABCB1. Once the weak-base drugs enter the lysosome, they are rapidly protonated, and therefore, prevented from exiting the lysosome (Fig 8). This results in their accumulation within the lysosome and inability to reach their targets [99-101]. Due to their lysosomal entrapment, higher drug concentrations are required to ensure their desired therapeutic effects. Not only anticancer drugs have been found to be subjects of lysosomal sequestration, but also agents such as antidepressants or antimalarials [102]. A great variety of anticancer drugs is associated with lysosomal sequestration, e.g., topoisomerase inhibitors (topotecan, daunorubicin, mitoxantrone), antimicrotubular agents (vinblastine, vincristine), antimetabolites (methotrexate), or TKi (sunitinib, sorafenib, erlotinib) [96, 99]. For gilteritinib, a TKi targeting primarily FLT3 in AML, involvement with endolysosomal system has been proposed, yet not confirmed [103].
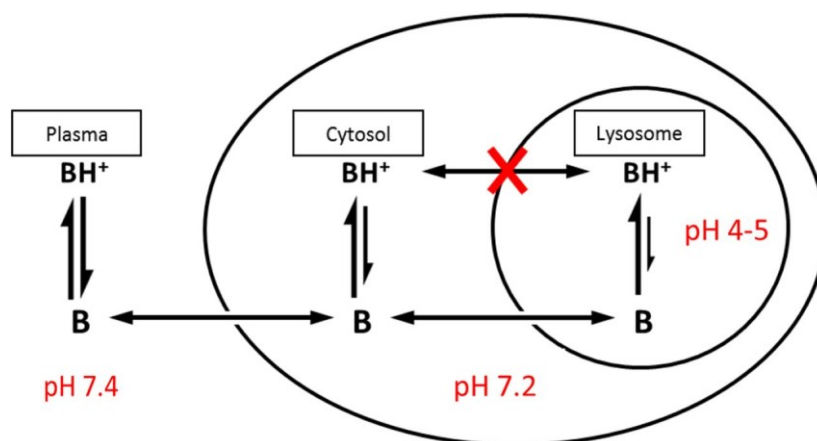
Fig 8. Drug movement into the cell and within the cell. Lipophilic weak bases can enter the cell in the unionized form (B) by passive diffusion across the cell membrane. These drugs can also freely diffuse across the lysosomal membrane into the lysosome. Once in lysosome, the drug is protonated (BH+) and unable to exit the lysosome in this form [104].

4   AIMS OF THE DISSERTATION THESIS

This thesis elaborated on different mechanisms of resistance involved in AML. In particular, it comprises the following aims:

1. To establish clinical relevance of ABC transporters (ABCB1, ABCG2) in AML patients and to investigate their epigenetic regulation by miRNAs. To evaluate the effect of midostaurin on anthracycline-based therapy.

2. To evaluate CDKi (abemaciclib, palbociclib, ribociclib) in relationship to ABC transporters (ABCB1, ABCG2) and study their effect on anthracycline-based therapy in AML patients.

3. To characterize transcriptome and proteome profiling of gilteritinib-resistant AML cell line and study lysosomes as mediators of drug resistance.

5 MATERIALS AND METHODS

5.1 Appliances

- Flow box Jouan (Saint-Herblain, France)
- Humidified incubator Sartorius Stedim Biotech (Göttingen, Germany)
- Laboratory scales Radwag (Radwag, Radom, Poland)
- Centrifuges: Hettich Universal 32R, Hettich Mikro 22R (A. Hettich GmbH & Co. KG, Tuttlingen, Germany) & Boeco C-28 (Boeckel+Co GmbH+Co, Hamburg, Germany)
- Bio-Rad TC20™ Automated Cell Counter (Bio-Rad, Hercules, CA, USA)
- SONY SA3800 Spectral Cell Analyzer (SONY Biotechnology, San Jose, CA, USA)
- BD FACSCanto™ II flow cytometer (BD Biosciences, San Jose, CA, USA)
- Hidex Sense Beta Plus 425-311 Microplate Reader (Hidex, Turku, Finland)
- QX200™ Droplet Digital™ PCR System (Bio-Rad, Hercules, CA, USA)
- T100 Thermal Cycler (Bio-Rad, Hercules, CA, USA)
- QuantStudio™ 6 Flex Real-Time PCR System (Thermo Fisher Scientific, Waltham, MA, USA)
- NanoDrop® ND-1000 (Thermo Fisher Scientific, Waltham, MA, USA)
- Nikon A1+ confocal laser scanning microscope (Nikon, Tokyo, Japan)

5.2 Chemicals and reagents

Cell culture reagents - Roswell Park Memorial Institute (RPMI) medium, L-Glutamine, fetal bovine serum (FBS) - were purchased from Merck KGaA (Darmstadt, Germany). Trypan blue, phosphate-buffered saline (PBS), dimethylsulfoxide (DMSO) as well as Ficoll-Paque™ Plus gradient solution were also purchased from Merck KGaA (Darmstadt, Germany). Opti-MEM was bought from Gibco BRL Life Technologies (Rockville, MD, USA). Isopropanol, absolute ethanol, and hydrochloric acid were obtained from Penta (Prague, Czech Republic).

Abemaciclib was bought from Selleckchem (Houston, TX, USA), while ribociclib, palbociclib, midostaurin, gilteritinib, daunorubicin and mitoxantrone were purchased from MedChemExpress (Monmouth Junction, NJ, USA). LY335979 (LY) and Ko143 were obtained from Toronto Research Chemicals (North York, ON, Canada) and Enzo Life Sciences

(Farmingdale, NY, USA), respectively. Sunitinib and Hoechst 33342 were purchased from Merck KGaA (Darmstadt, Germany).

Propidium iodide (PI), 3-(4,5-dimethylthiazol-2-yl)-2,5-diphenyltetrazolium bromide (MTT), RNAse A, annexin V-FITC/PI apoptosis kit, FITC-dextran (MW 4000) were obtained from Merck KGaA (Darmstadt, Germany). Caspase-Glo® 3/7 assay was bought from Promega (Madison, WI, USA) and anti-human CD34 antibody (4H11) from Invitrogen (Carlsbad, CA, USA). Lysotracker™ Deep Red and Lysosensor™ Yellow/Blue DND-160 were purchased from Thermo Fisher Scientific (Waltham, MA, USA).

Other chemicals and materials used in the study, but not listed in this subchapter are enclosed within detailed description of each method.

5.3   Cell lines

HL-60 WT cell line and its ABCB1- and ABCG2-overexpressing variants were provided by Dr. Balasz Sarkadi (Hungarian Academy of Sciences, Budapest, Hungary) and cultured in RPMI medium supplemented with L-glutamine and 10 % FBS. Gilteritinib-resistant HL-60 G75 cells were developed in our lab by stepwise increase of gilteritinib concentration up to 1.8 µM when the highest resistance was acquired. These cells were maintained in RPMI medium with L-glutamine, 10 % FBS and addition of 1.8 µM gilteritinib. All cell lines were kept in a humidified incubator (37 °C, 5 % CO_2).

5.4   Patient samples & isolation of mononuclear cells

AML patients were diagnosed and their samples of peripheral blood were collected at the 4th Department of Internal Medicine - Hematology, University Hospital Hradec Kralove. All patients included in this thesis provided a signed informed consent for the participation in the study which was approved by the University Hospital Research Ethics Committee (No. 2OL7OS7 LLP). Detailed characteristics of the patients are included in Table 1. A cutoff value of 20 % was used for CD34 positivity. All samples were collected at diagnosis prior to any treatment. Patients classified as acute promyelocytic leukemia were not included in the study.

Peripheral blood mononuclear cells (PBMC) were isolated by density gradient centrifugation as described previously [105, 106]. Before any experiment, PBMC were thawed and kept in RPMI with 20 % FBS and L-glutamine in a humidified incubator for at least 30 min to allow cell recovery.

Table 1. Characteristics of acute myeloid leukemia (AML) patients at diagnosis (the list comprises patients included in this thesis).

UPN	Sex	Age	FAB	ELN	WHO	Mutations	Cytogenetic profile	CD34
1	M	72	M2	N/A	Therapy-related AML	none	N/A	+
2	M	67	M2	Fav	AML with recurrent genetic abnormalities	AML1/ETO	46,XY,der(2;8;21)[28]/46 ,XY[2]	−
3	F	69	M4	Adv	AML, NOS - Acute myelomonocytic leukemia	none	44,XX,del(5)(q13q34),+6 ,-7,-10, +der(11)t(11;11), -15,-16, add(17)(p13), -18,+20[24]/46, XX[1]	+
4	F	73	M2	Adv	AML, NOS - AML with maturation	none	76-91<4n>,XX,-X,-8, i(17)(q10), del(X)(q?),+1 -3 mar[cp16]/46, XX[4]	+
5	M	31	M2	Adv	AML with recurrent genetic abnormalities	NPM1	46,XY	−
6	F	66	M2	Int	AML with recurrent genetic abnormalities	FLT3, NPM1	46,XX	−
7	M	55	M4	Int	AML with recurrent genetic abnormalities	FLT3, NPM1	46,XY	+
8	F	59	M2	Int	AML, NOS - AML with maturation	NPM1	46,XX	−
9	F	47	M2	Adv	AML with myelodysplasia-related changes	FLT3, NPM1	46,XX	+

10	M	67	M2	Adv	AML with myelodysplasia-related changes	TP53	44,XY,del(2)(q?21q?31), del(5)(q12q34),del(6)(q21q25),add(8)(q24),der(9)t(8?;9),dic(16)t(16;17)(?;q10),del(20q) [25]	+
11	F	68	M2	Adv	AML with myelodysplasia-related changes	TP53	44,XX,-2,del(5)(q21q34), der(13)t(2;13;?),?del(17p),-18, del(20)(q12)[30]	+
12	M	33	M2	Int	AML with recurrent genetic abnormalities	NPM1	46,XY	−
13	F	71	M4	Int	AML, NOS - Acute myelomonocytic leukemia	none	46,XX	+
14	M	62	M4	Fav	AML with recurrent genetic abnormalities	NPM1, IDH2	46,XY	−
15	F	77	M5a	Int	AML with recurrent genetic abnormalities	KMT2A/ MLLT3	46,XX, t(9,11)	−
16	F	75	M2	Fav	AML with recurrent genetic abnormalities	FLT3, NPM1	N/A	−
17	M	70	M5a	Fav	AML with myelodysplasia-related changes	NPM1	46,XY	−
18	F	69	M1	Int	AML with recurrent genetic abnormalities	FLT3, NPM1	46,XX	−
19	F	60	M4	Int	AML, NOS - Acute myelomonocytic leukemia	none	46,XX	−

20	F	52	M2	Int	AML, NOS - AML with maturation	none	46,XY	−
21	M	65	M1	Fav	Therapy-related AML	AML1/ETO	46,XY	+
22	M	54	M1	Int	AML with recurrent genetic abnormalities	FLT3	46,XY	−
23	F	58	M4	Int	AML, NOS - Acute myelomonocytic leukemia	DNMTA, IDH1	46,XX	−
24	M	62	M4	Adv	AML, NOS - Acute myelomonocytic leukemia	none	N/A	−
25	M	29	M2	Int	AML with recurrent genetic abnormalities	FLT3, NPM1	46,XY	−
26	M	23	M4	Int	AML, NOS - Acute myelomonocytic leukemia	MLL-PTD	46,XY	−
27	M	63	M2	Int	Therapy-related AML	none	46,XY,t(1;3)(p36;q21), der(1)t(1;3)(p36;q21)[25]	+
28	M	64	M2	Adv	Therapy-related AML	FLT3	46,XY	−
29	F	64	M4	N/A	Therapy-related AML	FLT3, NPM1	N/A	-
30	F	64	M4	Fav	AML with recurrent genetic abnormalities	FLT3, NPM1	46, XX	+

Abbreviations: UPN, unique patient number; M, male; F, female; FAB, French–American–British classification; ELN, European LeukemiaNet cytogenetic risk stratification; N/A, not available; NOS, not otherwise specified; Fav, favorable; Int, intermediate; Adv, adverse; (+), positive; (−), negative

5.5   qRT-PCR & droplet digital PCR

Total RNA from PBMC was isolated by TRI Reagent® (Molecular Research Center, Cincinnati, OH, USA) according to manufacturer's instructions. RNA concentration and purity was evaluated using NanoDrop® ND-1000. RNA (1 µg) was transcribed to cDNA with Protoscript® II RNA kit (New England Biolabs, Ipswich, MA, USA) according to manufacturer's instructions and used in follow-up qRT-PCR and droplet digital PCR (ddPCR) [105, 106].

For qRT-PCR, the TaqMan® Universal Master Mix II without UNG and predesigned TaqMan® Real-Time PCR assays Hs00184500_m1 *hABCB1* and Hs01053790_m1 *hABCG2* (all from Thermo Fisher Scientific, Waltham, MA, USA) were used. All samples were amplified in triplicates on 384-well plates (12.5 ng of each cDNA was used in a 5 µl reaction) using following thermal cycling conditions: 95 °C for 10 min, 40 cycles at 95 °C for 15 s and 60 °C for 60 s. Gene expression was analyzed by QuantStudio™ 6 system. *ABCB1* and *ABCG2* gene expression were normalized to *HPRT1* (Hs02800695_m1 *hHPRT1*; Thermo Fisher Scientific, Waltham, MA, USA), which was chosen as a reference gene based on a gene stability analysis performed by RefFinder (OmicX, Rouen, France) [107]. Target gene expression was evaluated by the comparative ΔΔCt method [108]. Data are reported as a target gene expression relative to a control sample run in all qPCR plates [105].

Prior to ddPCR, target-specific preamplification was conducted using PrimePCR™ probe assays qHsaCEP0058075 *hABCB1* and qHsaCEP0058168 *hABCG2*, SsoAdvanced PreAmp Supermix, and cDNA template (20 ng). Thermal cycling conditions consisted of activation (95 °C, 3 min), 12 cycles of denaturation (95 °C, 15 s), and annealing/extension (58 °C, 4 min). Reverse transcription and preamplification of tested miRNA were performed using TaqMan™ Advanced miRNA cDNA Synthesis Kit according to manufacturer's instructions (Thermo Fisher Scientific, Waltham, MA, USA). Afterwards, 10-times diluted preamplified cDNA with ddPCR™ Supermix for Probes and PrimePCR™ probe assays (qHsaCEP0058075 *hABCB1*, qHsaCEP0058168 *hABCG2*) or *hsa-478214_mir (miR-9-5p), hsa-478032_mir (miR-331-5p), hsa-477998_mir (miR-27a-5p)* assays (all miRNA probes purchased from Thermo Fisher Scientific, Waltham, MA, USA) were analyzed by the QX200™ Droplet Digital™ PCR system. Conditions for amplification were as follows: (I) 98 °C, 10 min, (II) 40 cycles at 94 °C for 30 s, (III) 55 °C, 1 min, and (IV) 98 °C, 10 min. Ramp rate was lowered by 2 °C in all steps.

Plates were run in the QX200™ Droplet Reader. The QuantaSoft™ Analysis Pro was used for the calculation of target gene concentrations, which was performed based on the positive and negative droplets and only in wells exceeding 13,000 droplets. Expression is presented as number of transcripts per 20 ng RNA 12-times preamplified. The QX200™ Droplet Digital™ PCR System and all consumables were obtained from Bio-Rad (Hercules, CA, USA) unless stated otherwise.

5.6 Accumulation assay and Annexin V/PI assay in PBMC

Accumulation assay was performed as described previously [105, 106]. Recovered PBMC in a density of 1×10^6 cells/mL were incubated for 15 min with 1 µM midostaurin, 0.5 µM abemaciclib, 0.5 µM palbociclib, or 7.5 µM ribociclib. Following preincubation, 1 µM mitoxantrone was added and incubated with mentioned inhibitors for additional 4 h at 37 °C, 5 % CO_2. Cells were then washed with cold PBS, resuspended in 2 % FBS/PBS (195 µL) and incubated for 30 min on ice with 5 µL anti-human CD34/PE antibody (4H11). Afterwards, cells were washed with 200 µL 1× annexin-binding buffer (ABB), resuspended in 195 µl 1× ABB and stained with 5 µL annexin V-FITC. Following 10 min incubation in the dark, 10 µL propidium iodide (PI) was added and samples were immediately measured by SONY SA3800 Spectral Cell Analyzer using excitation/emission (ex./em.) wavelengths of 488/530 nm for FITC, 488/620 nm for PI, and 638/680 nm for mitoxantrone.

5.7 Accumulation assay in HL-60

HL-60, HL-60 ABCB1 and HL-60 ABCG2 were incubated in a density of 5×10^5 cells/mL with a concentration range of tested inhibitors (midostaurin, abemaciclib, palbociclib, and ribociclib) or model inhibitors (1 µM LY335979 for ABCB1, 1 µM Ko143 for ABCG2). Following 15 min pre-incubation, 1 µM daunorubicin (ABCB1 substrate) or 1 µM mitoxantrone (ABCG2 substrate) were added and incubated for 1 h (37 °C, 5 % CO_2). Afterwards, cells were washed with cold PBS, resuspended in cold PBS, and measured. Experiments employing midostaurin were analyzed on SONY SA3800 Spectral Cell Analyzer with ex./em. wavelengths of 488/600 nm for daunorubicin and 638/680 nm for mitoxantrone. Experiments with abemaciclib, palbociclib, and ribociclib were measured by BD FACSCanto™ II flow cytometer using ex./em. wavelengths of 488/670 nm for daunorubicin and 633/660 nm for mitoxantrone [105, 106].

5.8   Caspases 3/7 activity in HL-60

HL-60 and HL-60 ABCB1 were seeded in a density of 5×10^5 cells/mL in 12-well plates. Cells were treated with a single agent (1 µM midostaurin or 1 µM daunorubicin) and a combination of both (1 µM midostaurin + 1 µM daunorubicin) and incubated in a humidified incubator for 24 h. Afterwards, 1×10^4 cells/mL were transferred from wells to a 96-well plate and incubated for 1 h at room temperature with 100 µL of RPMI medium and 100 µL of the Caspase-Glo® 3/7 reconstituted kit. Caspase activity was then measured as luminescence on the Hidex Sense Beta Plus 425-311 microplate reader. Caspase activity of treated samples was compared to activity of control samples [106].

5.9   SubG1 assessment in HL-60

1×10^5 cells/mL of HL-60, HL-60 ABCB1, HL-60 ABCG2 were incubated for 15 min in 1 µM abemaciclib, 10 µM palbociclib, 25 µM ribociclib, or 1 µM midostaurin-containing Opti-MEM solutions. Then, 0.2 µM daunorubicin or 1 µM mitoxantrone were added and incubated for additional 4 h (37 °C, 5 % CO_2). Afterwards, cells were washed with 2 % FBS/PBS and fixed with ice-cold 70 % ethanol for at least 30 min at -20 °C. Following fixation, cells were washed with 2 % FBS/PBS three times and incubated for 1 h (37 °C, 5 % CO_2) with addition of 50 µL of RNAse A (100 µg/mL) and 200 µL of PI (50 µg/mL). Samples were analyzed by SONY SA3800 Spectral Cell Analyzer (ex./em.: 488/620 nm for PI). Fractional DNA content in the late stage of apoptosis is presented as a percentage of subG1 fraction of a PI histogram [106].

5.10 Cell growth inhibitory assay

The MTT assay was used to determine *in vitro* drug sensitivity in gilteritinib-sensitive HL-60 WT and gilteritinib-resistant HL-60 G75 cells according to previously published protocol [109]. Prior to the experiments, cells were kept in gilteritinib-free RPMI medium for 24 h. For flat-bottom 96-well plates, a cell concentration of 7,500 cells/well was used for HL-60 WT, while 9,000 cells/well were used for HL-60 G75 and HL-60 G75 deprived of the drug (referred to as HL-60 G75-). Firstly, a concentration range of gilteritinib (12 drug dilutions ranging from 20 µM to 9 nM) was added to the wells in triplicates. Afterwards, a cell suspension was added to drug-containing wells as well as to non-treated wells to a final volume of 150 µL. After 96 h incubation, 15 µL of MTT (5 mg/mL) was added and incubated for additional 4 h (37 °C, 5 % CO_2). Formed formazan crystals reflecting the mitochondrial activity of cells were dissolved in acidified isopropanol (150 µL per well), thoroughly mixed and after 10 min, the optical

densities were measured at 540 nm by Hidex Sense Beta Plus 425-311 Microplate Reader. The IC_{50} value, which stands for the drug concentration that inhibits 50 % of the cell growth compared to untreated cells, was calculated. Resistance factors (RF) were calculated as ratios of gilteritinib-resistant or gilteritinib-deprived cells and gilteritinib-sensitive cells.

5.11 Apoptosis & cell cycle assays on gilteritinib-resistant HL-60

For apoptosis and cell cycle analysis on HL-60 WT and HL-60 G75, cells were cultured in gilteritinib-free RPMI medium for 24 h. Afterwards, cells were seeded in 12-well plates either in a density of 5×10^5 cells/mL for 24 h exposition or 2.5×10^5 cells/mL for 48 h exposition in a total volume of 1 mL. A concentration range of gilteritinib (1, 3, 5, 10 µM) was added and incubated for 24 h or 48 h. Volume of each well was split between apoptosis and cell cycle assay. In case of apoptosis, 200 µl of cell suspension was washed twice (first with PBS, then with 1× ABB), stained with annexin V-FITC (1:40 dilution) and incubated for 1 h at room temperature in the dark. Then, cells were washed with 1× ABB, resuspended in PBS and measured immediately after the addition of 10 µL PI (20 µg/mL) on SONY SA3800 Spectral Cell Analyzer (ex./em. wavelengths of 488/530 nm for FITC and 488/620 nm for PI). Remaining 800 µL of cell suspension was used for the cell cycle assay. Cells were washed once with PBS, fixed with 1 mL 70 % ice-cold ethanol, and kept at 4 °C overnight. The next day, cells were washed twice with PBS and incubated with 50 µL RNAse A (100 µg/mL) for 30 min at 37 °C, 5 % CO_2. Afterwards, 200 µL PI (50 µg/mL) was added and samples were measured on SONY SA3800 Spectral Cell Analyzer (ex./em.: 488/620 nm for PI).

5.12 Subcellular studies on gilteritinib-resistant HL-60

Microscopy study employing Lysotracker Deep Red & sunitinib

A cell concentration of 2×10^5 cells/mL was used for all tested cell lines: HL-60 WT, HL-60 G75, HL-60 G75- deprived of gilteritinib for 1 day (referred to as HL-60 G75- (1d)) and HL-60 G75- deprived of gilteritinib for 1 week (referred to as HL-60 G75- (1w)). Cells were stained with 300 nM Lysotracker Deep Red (referred to as Lysotracker), 1.25 µg/mL Hoechst 33342 (referred to as Hoechst), and 1 µM sunitinib in RPMI without (w/o) FBS for 15 min. After incubation, cells were spined down (150 × g, 5 min), resuspended in residual volume of cell culture medium (< 5 µL) and imaged with Nikon A1+ confocal laser scanning microscope equipped with Nikon CFI Plan Apochromat Lambda 100× Oil, N.A. 1.45 objective lens. For each sample, lasers with their respective emission filters were used (405 nm/DAPI for

Hoechst, 488 nm/FITC for sunitinib, and 638 nm/Cy5 for Lysotracker). Laser power was kept as low as possible to prevent photodamage and pinhole was set as 75.4 µm. Typically, 40 - 80 focal planes with 0.175 µm steps were taken to cover the whole volume of the samples.

Microscopy study employing Lysotracker Deep Red & dextran

For this study, same cell lines in the same cell concentrations as in the previous microscopy study were employed. Cells were incubated with 1 mg/mL FITC-dextran (MW 4000) for 24 h (37 °C, 5 % CO_2) in RPMI medium either with gilteritinib (in case of HL-60 G75) or without it (in case of HL-60 WT and gilteritinib-deprived HL-60 G75- (1d/1w)). Afterwards, cells were washed twice with PBS, resuspended in the respective medium and incubated for additional 4 h (37 °C, 5 % CO_2). Samples were washed again with PBS and stained similarly to previous study (300 nM Lysotracker and 1.25 µg/mL Hoechst in RPMI w/o FBS for 15 min). Cells were spined down (150 × g, 5 min), resuspended in residual volume of cell culture medium (< 5 µL) and imaged with Nikon A1+ confocal laser scanning microscope with 100× oil immersion objective lens as mentioned above.

Flow cytometry study employing Lysotracker Deep Red

A cell concentration of 5×10^5 cells/mL of all HL-60 cell lines (HL-60, HL-60 G75, HL-60 G75- (1d), HL-60 G75- (1w)) were incubated with 300 nM Lysotracker for 1 h (37 °C, 5 % CO_2). Afterwards, cells were washed twice with PBS, resuspended in PBS and after addition of 10 µL PI (20 µg/mL), immediately measured on SONY SA3800 Spectral Cell Analyzer (ex./em.: 638/670 nm for Lysotracker, 488/620 nm for PI). Only viable cells were considered in the analysis.

pH detection by Lysosensor Yellow/Blue DND-160

To determine pH in acidic organelles of HL-60 WT, HL-60 G75 and HL-60 G75- (1d), 5×10^4 cells/mL were seeded in 96-well plates (in triplicates) and incubated with 1 µM Lysosensor Yellow/Blue DND-160 (referred to as Lysosensor) for 0.5 h and 2 h (37 °C, 5 % CO_2). Cells were washed twice with PBS and measured by Hidex Sense Beta Plus 425-311 Microplate Reader in RPMI solution (ex./em.: 329/440 nm & 384/540 nm for Lysosensor). pH was established based on a standard curve determined from a series of RPMI solutions with adjusted pH (ranging from acidic to basic) and stained with 1 µM Lysosensor.

5.13 RNA-seq sample preparation and bioinformatic analysis

Sample preparation and total mRNA sequencing

RNA was isolated from samples by TRI Reagent® (Molecular Research Center, Cincinnati, OH, USA) according to manufacturer's instructions and the follow-up sample processing was outsourced to the Institute of Applied Biotechnologies (Prague, Czech Republic). RNA purity and quantity assessment was measured using the NanoDrop® ND-1000 and the Qubit™ RNA BR Assay Kit, respectively. Sample quality was assessed by the Agilent Bioanalyzer using the Agilent RNA 6000 Nano Chip. RNA Integrity Number (RIN) was calculated using the Agilent 2100 Expert software. A total RNA (330 - 700 ng, RIN > 6.5) was used for polyA mRNA isolation by the NEBNext Poly(A) mRNA Magnetic Isolation Module and subsequent preparation of mRNA-based library by the NEBNext Ultra II Directional RNA Library prep kit. The library quantification was performed using the Qubit™ DNA HS Assay Kit and its quality was assessed by the Agilent Bioanalyzer using the Agilent DNA High Sensitivity Chip. Libraries were pooled and sequenced using the NovaSeq 6000 (Illumina, CA, USA).

Data analysis

The quality of raw data produced by transcriptome sequencing was analyzed by the FastQC software [110]. Sequencing reads were aligned to the GRCh38 reference genome using STAR ver. 2.7.8a [111] with GENCODE project Reference Sequence transcript database [112]. Read counts for individual genes were obtained using featureCounts from the Subread package [113]. Read counts were normalized using edgeR and limma-voom [114, 115]. Lowly expressed genes were filtered by maintaining only genes with a count per million (CPM) value of 1 in at least one group (HL-60 G75 or HL-60 WT). Differentially expressed genes (DEGs) in HL-60 G75 compared to HL-60 WT were identified using limma-voom with the thresholds of false discovery rate (FDR) < 0.05 and fold change (FC) > 2. Three biological replicates were used for each sample. Gene Ontology (GO) and the Kyoto Encyclopedia of Genes and Genomes (KEGG) pathway enrichment analysis were evaluated based on FC values, performed using GSEA method [116] and visualized using iDEP [117] and ShinyGo [118]. Heatmaps were generated using Quickomics [119].

5.14 Proteomics sample preparation and bioinformatic analysis

Cell lysis, protein digestion and TMT peptide labeling

Cellular pellets responding to app. 5×10^6 cells were thawed, lysed in 0.5 mL of freshly prepared lysis buffer (3 % sodium deoxycholate (SDC) in 200 mM triethylammonium bicarbonate (TEAB)) and total protein concentration was determined using microBCA Protein Assay (Thermo Fisher Scientific, Waltham, MA, USA). Lysed samples (20 μg) were incubated with Tris(2-carboxyethyl)phosphine hydrochloride (TCEP) to reduce the reversibly oxidized cysteines at 60 °C for 15 min. Reduced cysteines were then alkylated by 10 mM methyl methanethiosulfonate (MMTS) labeled at RT for 10 min. Further, potential contaminants were removed by acetone precipitation, pellets were re-dissolved in 100 mM TEAB and proteins were digested by rLys-C/trypsin (Promega, Madison, WI, USA) at 37 °C overnight at 1:25 ratio (enzymes/substrate). After protein digestion, peptides were labeled by various TMT channels (TMT 10plex Label Reagent Set; Thermo Fisher Scientific, Waltham, MA, USA) at 25 °C for 1 h and the reaction was quenched by 5 % hydroxylamine. Subsequently, 3 biological replicates of gilteritinib-sensitive (HL-60 WT) and -resistant (HL-60 G75) cell lines were mixed in two different multiplexes in equal amount. Finally, both multiplexes were desalted and re-dissolved in 0.1 % TFA in 2 % AcN for LC-MS/MS.

Nano-Liquid chromatography coupled to tandem/mass spectrometry analysis

Two micrograms of each multiplex were injected onto UltiMate 3000 RSLCnano system (Thermo Fisher Scientific, Bremen, Germany) for the liquid chromatography separation. The analytical system consisted of PepMap100 C18, 3 μm, 100 Å, 75 μm × 20 mm trap column and Acclaim PepMap RSLC C18, 2 μm, 100 Å, 75 μm × 250 mm analytical column (both from Thermo Fisher Scientific, Bremen, Germany). The samples were loaded onto the trap column in 0.1 % TFA in 2 % AcN at 5 μL/min for 5 min. Tryptic peptides were separated by segment gradient running from 2 % to 34.5 % of mobile phase B (80 % AcN with 0.1 % FA) for 217 min, further to 45 % of B for 23 min at a flow rate of 250 nL/min and 40 °C. Eluted peptides were electrosprayed into Q-Exactive Plus using a Nanospray Flex ion source (both from Thermo Fisher Scientific, Bremen, Germany). Positive ion full scan MS spectra were acquired in the range of 350 – 1600 m/z using 3×10^6 AGC target in the Orbitrap at 70,000 resolution with a maximum ion injection time of 100 ms. Parameters of isolation window (IW) and normalized collision energy (NCE) were set at 1.6 m/z for IW and 33 for NCE. MS/MS spectra were acquired at resolution of 35,000 with a 1×10^5 AGC target and a maximum injection time

of 60 ms. Only 10 most intensive precursors with minimal AGC target of 2.4×10^4 and charge state ≥ 2 were fragmented. Dynamic exclusion window was 17 s. The fixed first mass was set to 100 m/z.

Data evaluation

Survey MS and MS/MS spectra were processed in MaxQuant 1.6.14. Enzyme specificity was set to trypsin/P and a maximum of two missed cleavages were allowed. Protein N-term acetylation and methionine oxidation were selected as variable modifications. The derived peak list was searched using the in-built Andromeda search engine in MaxQuant against human reference proteome (including contaminants) from UniProtKB database. Specified TMT10plex label has been set as quantification method. The minimum ratio count for label-based quantification was set to two quantified peptide pairs. Only unique or razor peptides were considered for calculating protein ratios. Remaining sample group-specific parameters were kept at default values. For data evaluation, output files from MaxQuant were processed in Perseus 2.0.6.0 [120].

Corrected reporter ion intensity values for labeled peptides were filtered to avoid potential contaminants including reverse peptides and valid values were log2 transformed and normalized to global internal standard intensity equally present in each multiplex. Technical replicates (n=3) were averaged for each TMT channel and peptides with valid value in each TMT channel were kept for further analysis. Comparative analysis of protein level changes related to cellular resistance was performed in Perseus. Differentially expressed proteins (DEPs) in HL-60 G75 vs HL-60 WT were analyzed using DEqMS [121] with thresholds of FC > 1.5 & FDR < 0.05. GO and KEGG pathway enrichment analysis were visualized using iDEP [117] and ShinyGo [118]. Heatmaps were generated using Quickomics [119].

5.15 Statistical analysis

Statistical analysis of all data, except for the RNA-seq and proteomics, was conducted using GraphPad Prism 9.4.1 software (GraphPad Software, Inc., San Diego, CA, USA). Statistics is enclosed within the description of all figures with p-value < 0.05 considered significant in all cases. Analysis of all flow cytometry data was performed in the FCS Express™ 6 software (De Novo Software, Pasadena, CA, USA).

6 RESULTS

6.1 Midostaurin & its role in AML

Data presented in the following subchapters provide information on midostaurin, FLT3 inhibitor approved in therapy of FLT3-mutated AML, and its association with ABCB1 and ABCG2 transporters in AML. Presented results were published in Biomedicine & Pharmacotherapy in 2022 (see Annex 1) [106].

6.1.1 Expression of *ABCB1* & *ABCG2* in our cohort of AML patients

Twenty-eight patients were included in this study and tested for *ABCB1* and *ABCG2* gene expression in their PBMC at diagnosis. An obvious relationship between *ABCB1* and *ABCG2* expression was found showing a clear co-expression of these genes within our collection of patient samples (Fig 9B). When comparing the two genes, *ABCB1* was expressed on a higher level compared to *ABCG2* (Fig 9A).
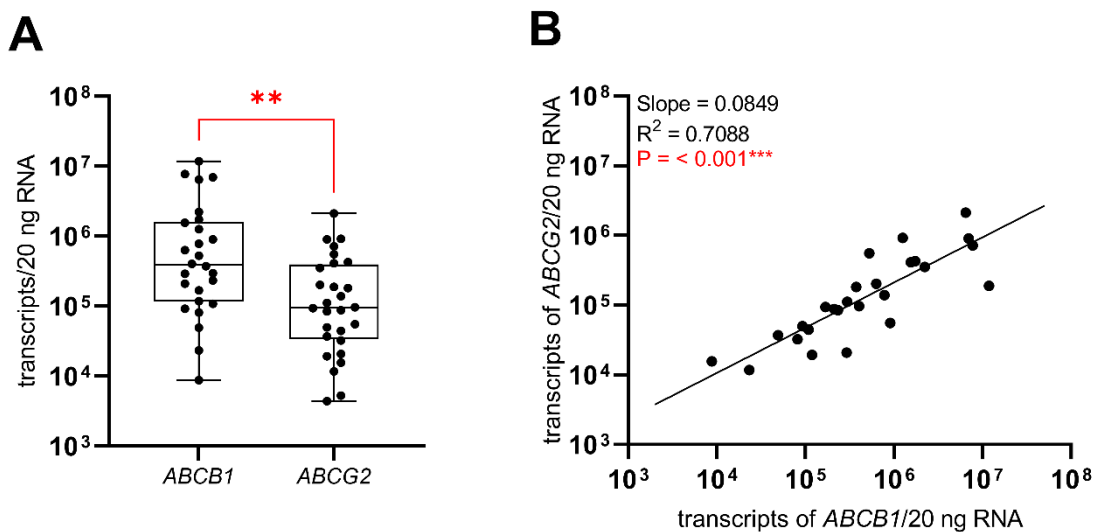
Fig 9. ABCB1 and ABCG2 gene expression in PBMC of de novo AML patients. (A) Higher ABCB1 expression was detected in tested samples compared to the expression of ABCG2. (B) A clear correlation of ABCB1 and ABCG2 expression was observed in these samples. The target genes' expression is reported as the number of transcripts per 20 ng RNA preamplified 12-times beforehand. Boxplot was evaluated by Mann-Whitney test and ABCB1/ABCG2 correlation was analyzed by linear regression; **p < 0.01, ***p < 0.001.

Closer evaluation of *ABCB1/ABCG2* gene expression in relationship to cell surface marker CD34 revealed a significantly higher *ABCB1* expression in CD34$^+$ group (equal to 36 % of all patients) compared to CD34$^-$ group (Fig 10A). In case of *ABCG2* expression, no significant difference was observed between these two groups (Fig 10D). Our patient cohort was further divided into groups based on the presence of *FLT3*-ITD (29 % *FLT3*-ITD$^+$ vs 71 % *FLT3*-ITD$^-$) or *NPM1* mutation (40 % *NPM1$^+$* vs 60 % *NPM1$^-$*). Expression levels of *ABCB1* and *ABCG2* did not differ between the positive and the negative group for either of these mutation (Fig 10B, C, E, F).

Patients' stratification according to ELN risk classification revealed that adverse risk group was associated with the highest *ABCB1* expression out of all three risk groups. As for *ABCG2,* no differences were observed among the risk groups (Fig 10G). When only patients treated with anthracycline-containing induction therapy were selected and divided into groups based on (un)achieved CR, those patients that did not achieve CR were the ones with the more pronounced *ABCB1* expression at diagnosis. No association of *ABCG2* and CR was observed in these samples (Fig 10H).
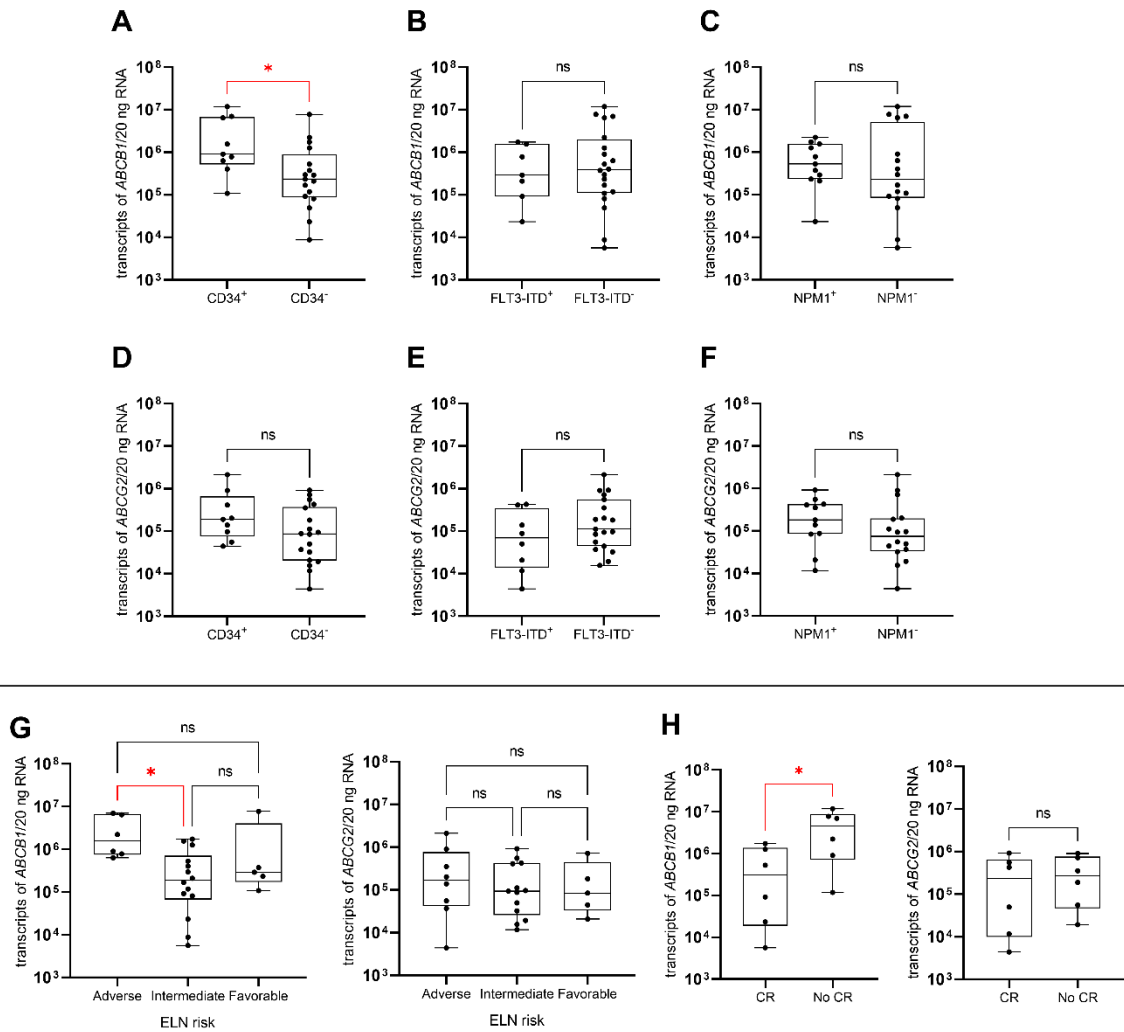
*Fig 10. ABCB1 and ABCG2 expression in de novo AML patients divided into subgroups based on their positivity for CD34 cell surface marker, FLT3-ITD and NPM1 mutations. (A) Expression of ABCB1 was significantly higher in CD34$^+$ AML patients compared to CD34$^-$ ones, (B, C) while no differences between the groups defined by either mutation were detected. (D, E, F) Similarly, no differences in ABCG2 expression levels were observed in either of the groups. (G) Adverse group of AML patients defined by the ELN risk stratification showed higher ABCB1 expression than intermediate or favorable group. (H) Unlike ABCG2 expression, lower expression of ABCB1 at diagnosis was associated with achievement of CR in patients who received anthracycline-containing induction therapy. Target genes' expression was evaluated using ddPCR and is presented as the number of transcripts per 20 ng RNA 12-times preamplified. Analysis of boxplots (A-F, H) was performed by Mann-Whitney test, while ELN-related boxplots (G) were evaluated by Kruskal-Wallis test; *p < 0.05.*

6.1.2 The effect of midostaurin on intracellular anthracycline accumulation in PBMC of AML patients

Knowing that our collection of patients has *ABCB1* and *ABCG2* expressed on mRNA level, we performed an accumulation study to test their involvement on a functional level. Mitoxantrone was selected as the anthracycline of choice because it presents a well-known substrate of both transporters. Midostaurin was chosen as the inhibitor since it has been implemented in therapy of FLT3-mutated AML [17], and has been also identified as ABCB1 inhibitor in previous studies [122, 123]. Therefore, midostaurin seemed like a perfect match for the study.

The effect of midostaurin on intracellular accumulation of mitoxantrone was examined in PBMC isolated from 20 *de novo* AML patients. Out of these, CD34$^+$ patients (50 % of all included samples) were able to reach higher intracellular levels of mitoxantrone *ex vivo* when co-administered with midostaurin (Fig 11A). Splitting of this PBMC collection into the ELN risk groups did not reveal any differences in mitoxantrone accumulation levels (Fig 11B). However, when only patients treated with anthracycline-containing induction therapy were selected, increased mitoxantrone accumulation in the presence of midostaurin was detected in those patients that did not achieve CR after the induction cycle (Fig 11C).
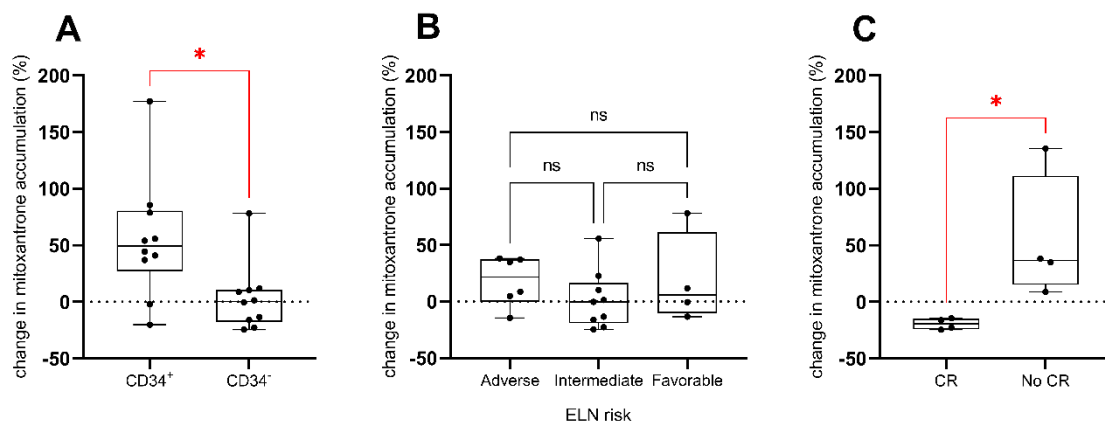
Fig 11. Mitoxantrone accumulation in the presence of midostaurin in PBMC isolated from AML patients at diagnosis. (A) Co-treatment (mitoxantrone and midostaurin) led to significantly higher intracellular levels of mitoxantrone in CD34$^+$ AML compared to CD34$^-$ AML. (B) Similar mitoxantrone levels were detected across all the ELN risk groups when treated with the combination of mitoxantrone and midostaurin. (C) Patients that were given anthracycline-based induction therapy, but did not eventually achieve CR, were able to reach higher intracellular levels of mitoxantrone in the presence of midostaurin. Changes in the mitoxantrone accumulation are presented as percentage difference

*between the effect caused by the combination of mitoxantrone and midostaurin vs mitoxantrone alone. Analysis of boxplots (A, C) was performed by Mann-Whitney test. Boxplot (B) was evaluated by Kruskal-Wallis test; *p < 0.05.*

6.1.3 Enhanced proapoptotic effect of daunorubicin resulting from midostaurin-mediated ABCB1 inhibition

To establish inhibitory properties of midostaurin specifically towards ABCB1 and ABCG2, HL-60 and its ABCB1/ABCG2-overexpressing variants were employed. Since HL-60 is a cell line without *FLT3*-ITD mutation, any effect of midostaurin on this mutation was eliminated. For this study, mitoxantrone and daunorubicin were selected as the anthracyclines of choice since they happen to be well-known cytotoxic substrates of ABC transporters of our interest - mitoxantrone of ABCG2 and daunorubicin of ABCB1.

Firstly, inhibitory effect of midostaurin was established in all HL-60 cell lines. In HL-60 ABCB1, daunorubicin accumulation increased in the presence of midostaurin with IC_{50} of 0.068 µM (Fig 12A). Similarly, intracellular mitoxantrone levels increased in HL-60 ABCG2 when midostaurin was present. In this case, IC_{50} equaled 4.436 µM (Fig 12B). No apparent increase in the accumulation of either anthracycline was detected in HL-60 showing that changes observed in PBMC (Fig 11) could have also resulted from ABCB1/ABCG2 inhibition.
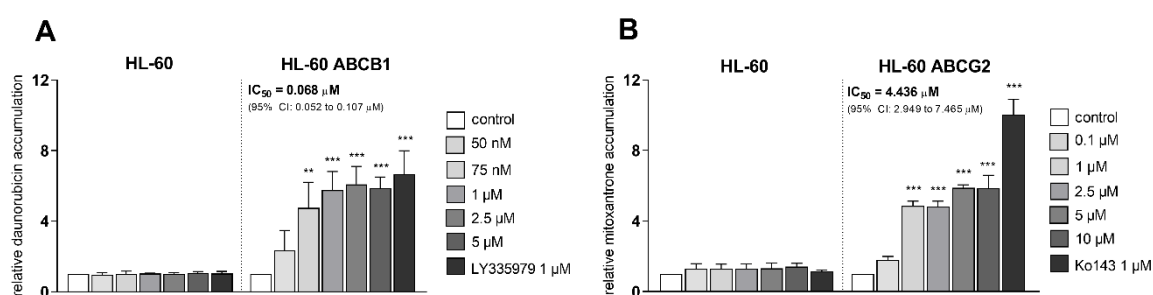
*Fig 12. Inhibitory effect of midostaurin on ABCB1- and ABCG2-mediated transport. Co-treatment of anthracycline (daunorubicin or mitoxantrone) and midostaurin on HL-60 ABCB1 and HL-60 ABCG2 revealed increased anthracycline accumulation in both cell lines confirming midostaurin as the ABCB1/ABCG2 inhibitor. No inhibitory effect of midostaurin was detected in control HL-60 which do not overexpress any of the transporters. Data were evaluated by one-way ANOVA with Dunnett's post hoc test (**p < 0.01, ***p < 0.001) and are presented as means ± SD of 3 independent experiments.*

Afterwards, midostaurin was subjected to apoptosis studies in which we tested whether it could enhance proapoptotic effects of daunorubicin. Unfortunately, insufficient material was obtained during PBMC isolation, therefore, these studies had to be performed on HL-60 cells. We proceeded with HL-60 ABCB1 and not HL-60 ABCG2 for two reasons: (I) in AML patients, *ABCB1* was more expressed than *ABCG2,* and (II) midostaurin appeared to be a stronger inhibitor of ABCB1 than ABCG2. Apoptosis was firstly evaluated based on the activity of caspases 3 and 7. A combination of daunorubicin and midostaurin revealed significantly elevated luminescence in HL-60 ABCB1 contrary to either drug alone (Fig 13A). This combination of drugs also increased subG1 fraction by 20 % when compared to daunorubicin as a single agent (Fig 13B). No changes in apoptosis were detected in control HL-60 not expressing ABCB1 suggesting that enhancement of apoptosis was a result of midostaurin-mediated inhibition of ABCB1.
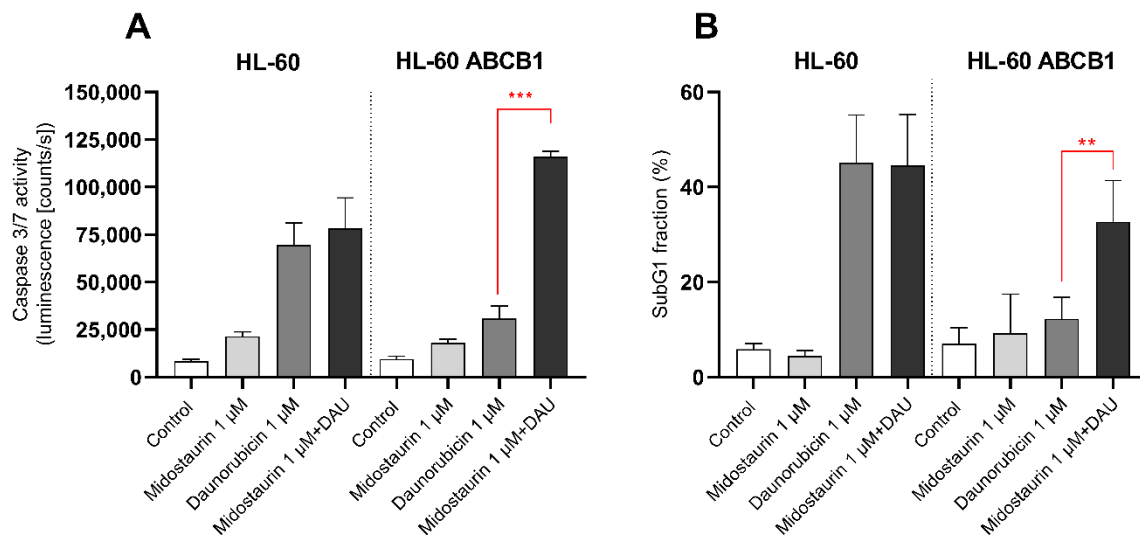
Fig 13. *Proapoptotic effect of daunorubicin as a consequence of ABCB1 inhibition mediated by midostaurin. (A) Exposure of HL-60 ABCB1 to the combination of daunorubicin (DAU) and midostaurin led to higher luminescence indicating higher activity of caspases 3 and 7. (B) Same treatment (daunorubicin + midostaurin) caused a 20 % increase of subG1 population in HL-60 ABCB1. (A, B) Neither daunorubicin, nor midostaurin as single agents exhibited such increase in apoptotic populations regardless of the method used. Moreover, no changes signifying enhanced apoptosis were observed in control HL-60 cells not overexpressing ABCB1. Data are reported as means ± SD of 3 independent experiments. Analysis was performed by unpaired t-test (**p < 0.01, ***p < 0.001).*

6.1.4 Regulation of ABCB1 expression by miR-9

To investigate epigenetic regulation of *ABCB1* expression in CD34$^+$ and CD34$^-$ patients, the expression of miR-9, miR-27a, and miR-331 were quantified (Fig 14A-C). Out of these, only miR-9 was revealed as differentially expressed in our cohort of AML patients. Downregulation of miR-9 was observed in CD34$^+$ patients, while in CD34$^-$ patients, expression level of miR-9 was elevated (Fig 14A). In CD34$^+$ group, high *ABCB1* expression as well as high mitoxantrone accumulation resulting from ABCB1 inhibition were detected, therefore, we wondered whether miR-9 could not predict this ABCB1-mediated efflux. We divided patient samples into two groups, low miR-9 & high miR-9, based on median miR-9 expression. The low miR-9 group was capable to accumulate mitoxantrone more than the high miR-9 group (Fig 14D). Moreover, a linear correlation between mitoxantrone accumulation and miR-9 expression was established (Fig 14G) suggesting that low miR-9 is related to high ABCB1 transcripts, and thus, higher efflux of chemotherapeutics. None of these relationships were observed for miR-27a or miR-331 (Fig 14E, F, H, I).
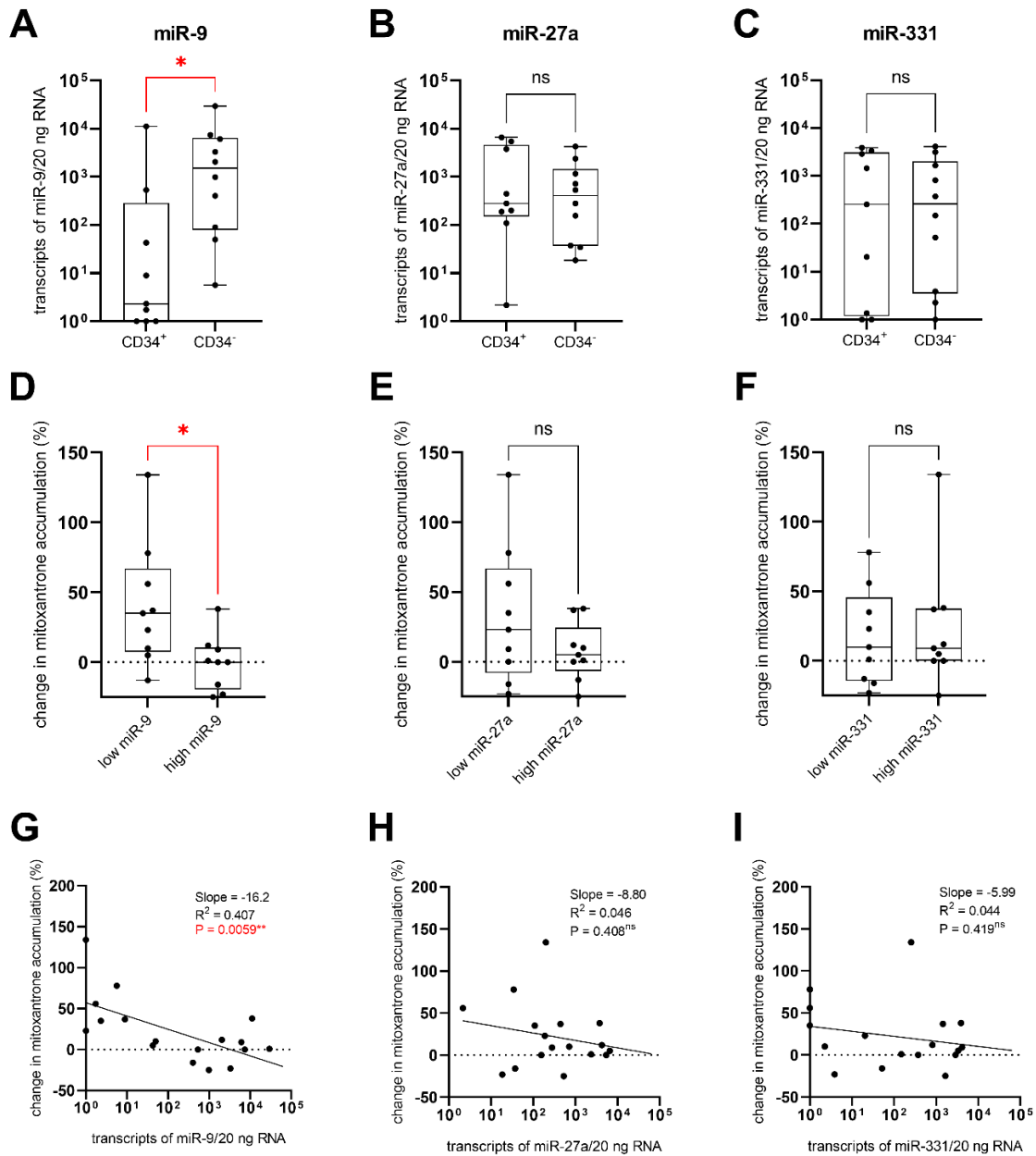
Fig 14. Association of selected miR with ABCB1 expression and function in AML cells. (A, B, C) Absolute expression of three miR (miR-9, miR-27a, miR-331) were evaluated and compared between CD34$^+$ and CD34$^-$ AML patients. Downregulation of miR-9 was found in CD34$^+$ patients, while no differences were detected for miR-27a or miR-331. (D, E, F) Division of AML patients based on median expression of each miR revealed low miR-9 group to be associated with higher midostaurin effect on mitoxantrone accumulation. No such relationship was detected for miR-27a or miR-331. (G, H, I) ABCB1-mediated efflux of mitoxantrone resulting from midostaurin inhibition correlated with miR-9 transcripts, but not with miR-27a or miR-331 transcripts. Boxplots (A-F) were analyzed by Mann-Whitney test and correlations (G-I) were examined using linear regression; *p < 0.05, **p < 0.01.

6.2 CDKi & their role in AML

Data presented in the following subchapters are dedicated to three inhibitors of CDK4/6 (abemaciclib, palbociclib, ribociclib) and their possible implementation in therapy of AML. Firstly, their inhibitory effects on ABC transporters were determined. Secondly, their effect on mitoxantrone accumulation and induction of apoptosis was investigated in AML cell lines as well as in PBMC isolated from AML patients. All presented results were published in Cancers in 2020 (see Annex 2) [105].

6.2.1 Enhanced daunorubicin and mitoxantrone accumulation by CDKi-mediated inhibition of ABC transporters

Selected CDKi (abemaciclib, palbociclib, ribociclib) were tested on HL-60 control cells and HL-60 overexpressing ABCB1 or ABCG2 transporters to determine their inhibitory properties. Daunorubicin accumulation in HL-60 ABCB1 as well as mitoxantrone accumulation in HL-60 ABCG2 were enhanced by all tested CDKi. Abemaciclib and palbociclib inhibited ABCB1 more effectively than ABCG2 with IC_{50} values of 0.354 μM for abemaciclib and 6.65 μM for palbociclib, respectively (Fig 15A, C). As for ABCG2, IC_{50} values equaled to 2.98 μM for abemaciclib and 45.5 μM for palbociclib (Fig 15B, D). Ribociclib showed similar inhibitory activity to both transporters (IC_{50} of 27.1 μM on ABCB1 & IC_{50} of 26.9 μM on ABCG2) (Fig 15E, F).
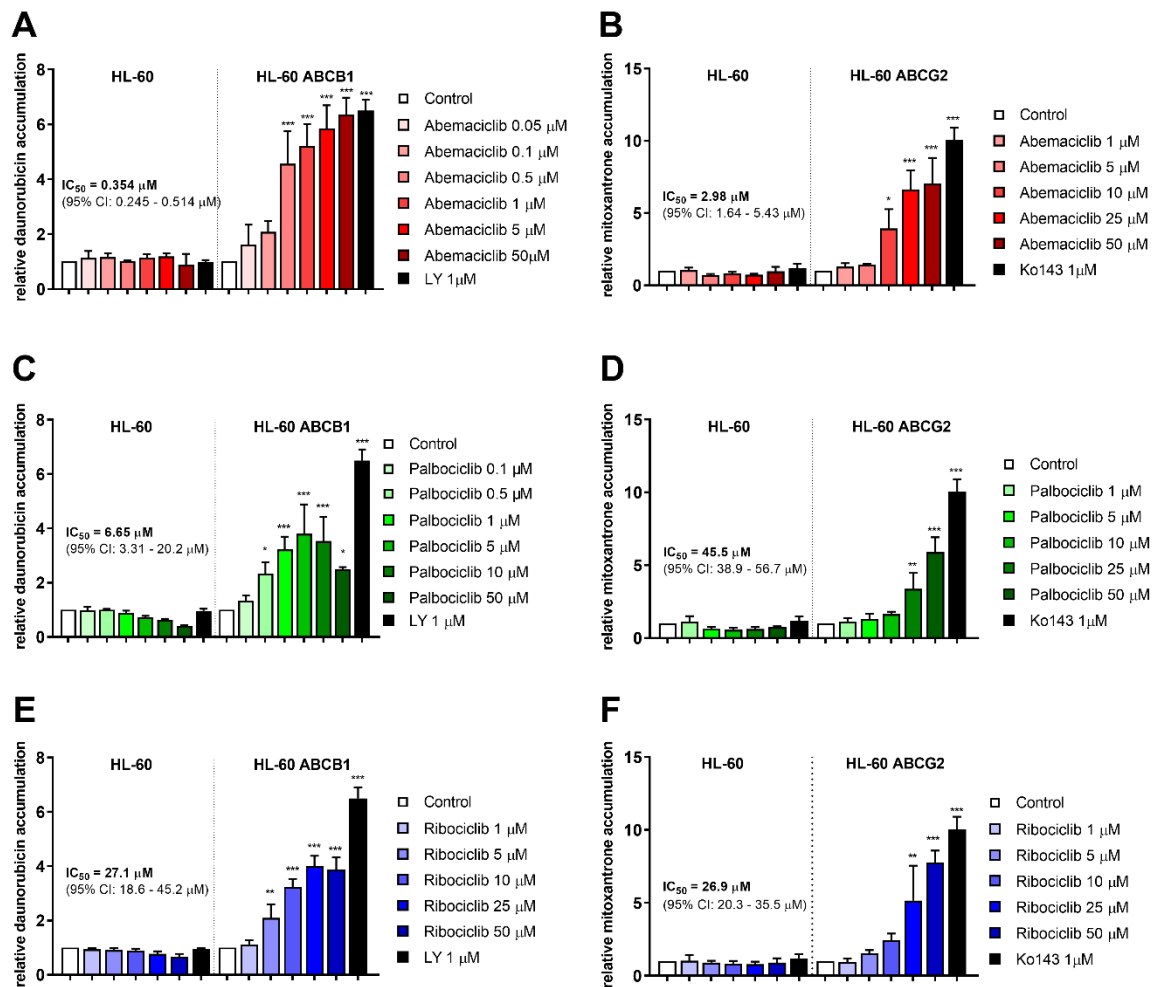
Fig 15. Effect of CDKi on daunorubicin and mitoxantrone accumulation in HL-60 cells. (A, C, E) Increased daunorubicin accumulation was observed in HL-60 ABCB1 as a result of ABCB1 inhibition mediated by all tested CDKi (abemaciclib, palbociclib, ribociclib). (B, D, F) Increase of mitoxantrone accumulation in HL-60 ABCG2 was detected when exposed to abemaciclib, palbociclib, or ribociclib. Data are presented as means ± SD of at least 3 independent experiments. All cell lines were exposed to a concentration range of selected CDKi and a specific ABC inhibitor (LY for ABCB1, Ko143 for ABCG2) together with the respective anthracycline as a substrate (daunorubicin for ABCB1, mitoxantrone for ABCG2) for 1 h. Results were compared to an untreated control and analyzed by one-way ANOVA (*p < 0.05, **p < 0.01, ***p < 0.001).

6.2.2 Induction of apoptosis by simultaneous exposure to anthracyclines and CDKi

To further determine whether tested CDKi can affect apoptosis in any way, cells were examined by double staining with annexin V/PI. HL-60, HL-60 ABCB1 and HL-60 ABCG2 were exposed to all tested drugs (abemaciclib, palbociclib, ribociclib) of which none affected the number of apoptotic cells. When exposed to mitoxantrone, roughly 70 % of HL-60 control cells

were sent to apoptosis, however, similar percentage of cells ended up in apoptosis even when exposed to a combination of mitoxantrone and all tested drugs (Fig 16A). In HL-60 ABCG2, the effect of mitoxantrone was not as pronounced since only 25.2 % cells were apoptotic. However, addition of abemaciclib and ribociclib, but not palbociclib, resulted in enhanced apoptosis of these cells (56.6 % for abemaciclib + mitoxantrone, 68.6 % for ribociclib + mitoxantrone) (Fig 16B). Interestingly, no proapoptotic effect of the selected combinations or mitoxantrone alone could be observed in HL-60 ABCB1 (Fig 16C). Additionally, subG1 fraction reflecting DNA fragmentation of HL-60 was determined. Similarly to results obtained by annexin V/PI staining, neither of CDKi alone, nor in combination with anthracyclines resulted in apoptosis (Fig 16D, F). Combination of mitoxantrone and abemaciclib increased the percentage of HL-60 ABCG2 apoptotic cells from 46.2 % to 64.6 %. An increase of 17.8 % was also observed after exposure of these cells to mitoxantrone and ribociclib, while no such effect was detected for simultaneous exposure to palbociclib and mitoxantrone (Fig 16E). As for HL-60 ABCB1, proapoptotic effect of daunorubicin was observed in combination with all tested CDKi since the number of apoptotic cells increased from 13.1 % to 47.5 % for abemaciclib, 35.6 % for ribociclib, and 30.7 % for palbociclib (Fig 16G).
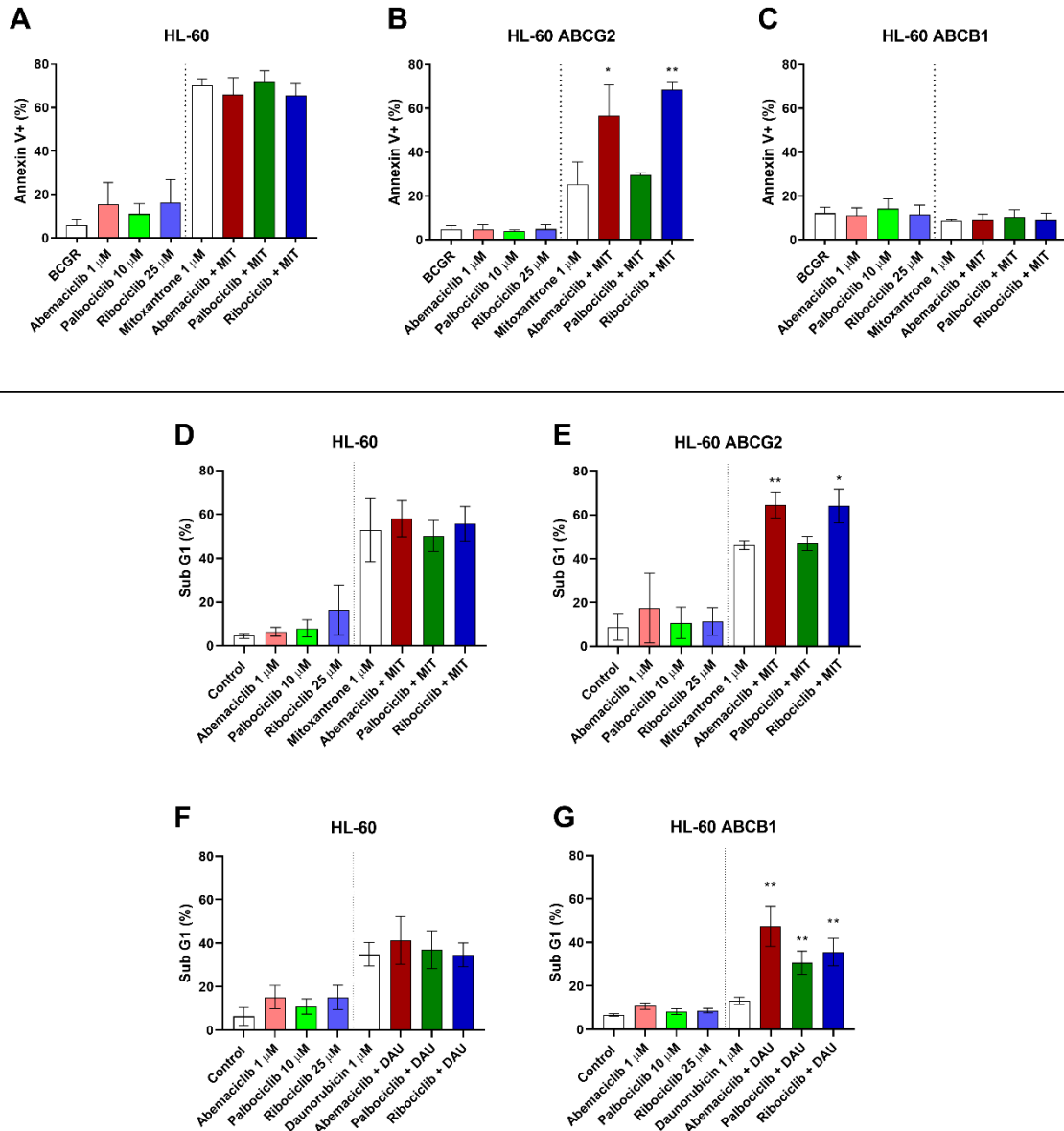
Fig 16. The effect of tested CDKi on apoptosis in HL-60, HL-60 ABCB1 and HL-60 ABCG2. (B, E) Combinations of abemaciclib and ribociclib, but not palbociclib, with mitoxantrone (MIT) enhanced the percentage of HL-60 ABCG2 apoptotic cells when compared to mitoxantrone alone. The enhancement of apoptosis was observed by both methods, annexin V/PI staining and subG1 assessment. (C, G) All tested combinations (abemaciclib/palbociclib/ribociclib + daunorubicin (DAU)) resulted in significant increase of subG1 fraction in HL-60 ABCB1 cells. However, no changes in apoptosis were detected when HL-60 ABCB1 were exposed to the combinations of CDKi and mitoxantrone. (A, D, F) None of these drug combinations resulted in increased apoptotic populations of HL-60 control cells. No effect of CDKi as single agents was observed in HL-60 control cells or transporter-overexpressing HL-60 ABCB1/HL-60 ABCG2. Apoptosis in cells treated with the combinations of CDKi and anthracyclines was compared to anthracycline-treated controls, while apoptosis in cells treated with CDKi as single

agents was compared to an untreated control. Data were analyzed by unpaired t-test and are presented as means ± SD of at least 3 independent experiments (*p < 0.05, **p < 0.01).

6.2.3 CDKi increases mitoxantrone accumulation in CD34$^+$ and *FLT3*-ITD$^-$ AML cells

The effects of CDKi on anthracycline accumulation were further investigated directly in PBMC isolated from *de novo* AML patients. Altogether, 15 patient samples were included in this study. All samples were exposed to dual ABCB1/ABCG2 substrate mitoxantrone either alone or in combination with abemaciclib, palbociclib, or ribociclib. Patients were split into CD34$^+$/CD34$^-$ and *FLT3*-ITD$^+$/*FLT3*-ITD$^-$ groups and accumulation levels of mitoxantrone were compared between them. All three tested drugs combined with mitoxantrone revealed an increase of mitoxantrone accumulation in CD34$^+$ patients as well as in *FLT3*-ITD$^-$ patients. Accumulation level of mitoxantrone remained similar to untreated cells in CD34$^-$ and *FLT3*-ITD$^+$ groups (Fig 17).
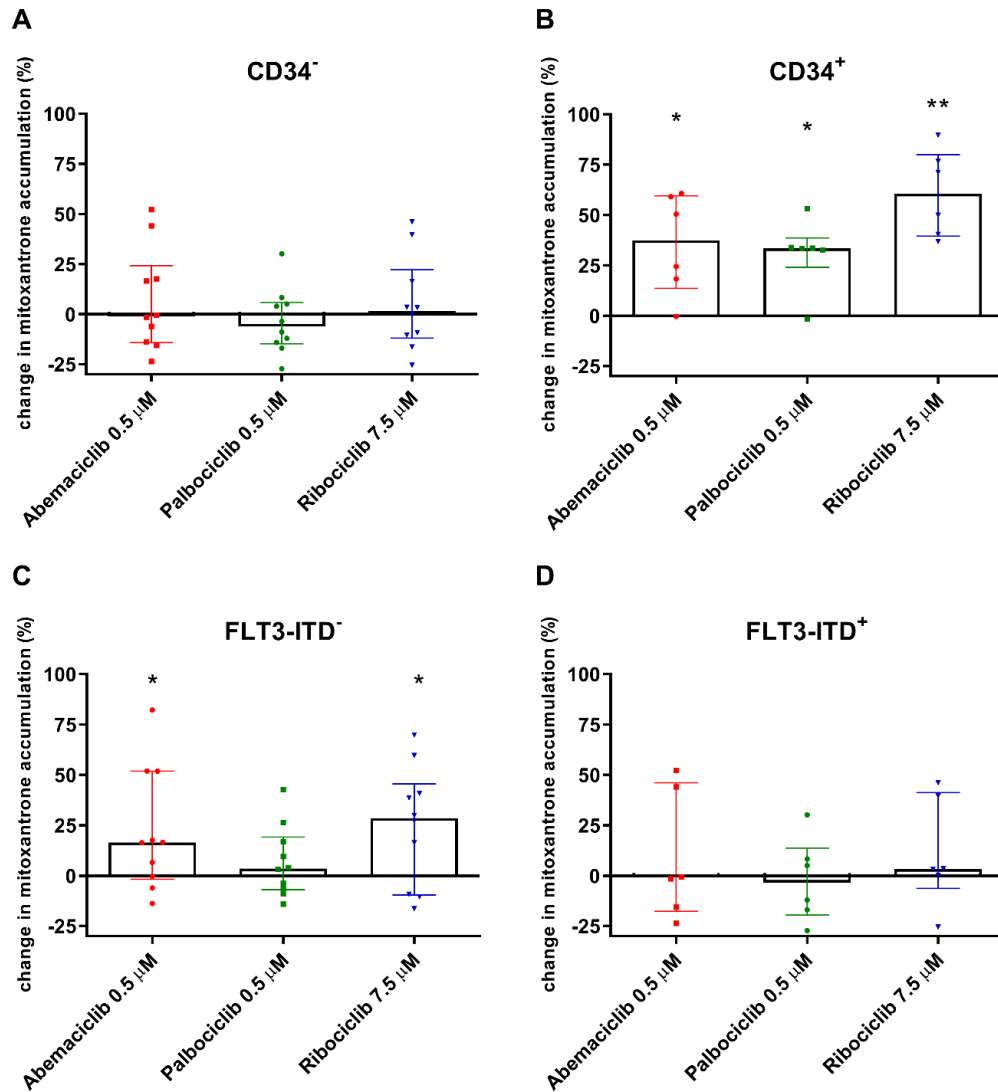
Fig 17. Effects of CDKi on mitoxantrone accumulation in PBMC isolated from de novo AML patients. (A, B) Exposure of AML samples to the combination of mitoxantrone and tested CDKi revealed higher mitoxantrone accumulation in CD34$^+$, but not CD34$^-$ patients, for all CDKi (abemaciclib, palbociclib, and ribociclib). (C, D) Same combination of drugs resulted in increased mitoxantrone accumulation in patients negative for FLT3-ITD, but not those positive for FLT3-ITD. The treated samples were compared to the untreated controls and analyzed by Mann-Whitney test (*p < 0.05, **p < 0.01). Data are presented as medians ± interquartile range.

6.2.4   CDKi enhance apoptosis in CD34$^+$ AML patients

Following accumulation studies, we performed annexin V/PI double staining of PBMC to determine whether selected CDKi can enhance apoptosis in these samples. All PBMC isolated from AML patients were exposed to either each CDKi alone or in combination with mitoxantrone. Similarly to accumulation studies, samples were split into groups based on the

CD34 phenotype and presence of *FLT3*-ITD mutation. Single agent treatment (abemaciclib, palbociclib, or ribociclib alone) did not show any changes in apoptosis regardless of the group (CD34$^{+/-}$ or FLT3-ITD$^{+/-}$). Cells exposed to CDKi and mitoxantrone revealed higher percentage of cells in apoptosis compared to apoptosis caused by mitoxantrone alone, specifically in CD34^{+} samples (Fig 18C). When comparing apoptosis in *FLT3*-ITD^{+} and *FLT3*-ITD^{-} groups, no changes were observed (Fig 18C, D).
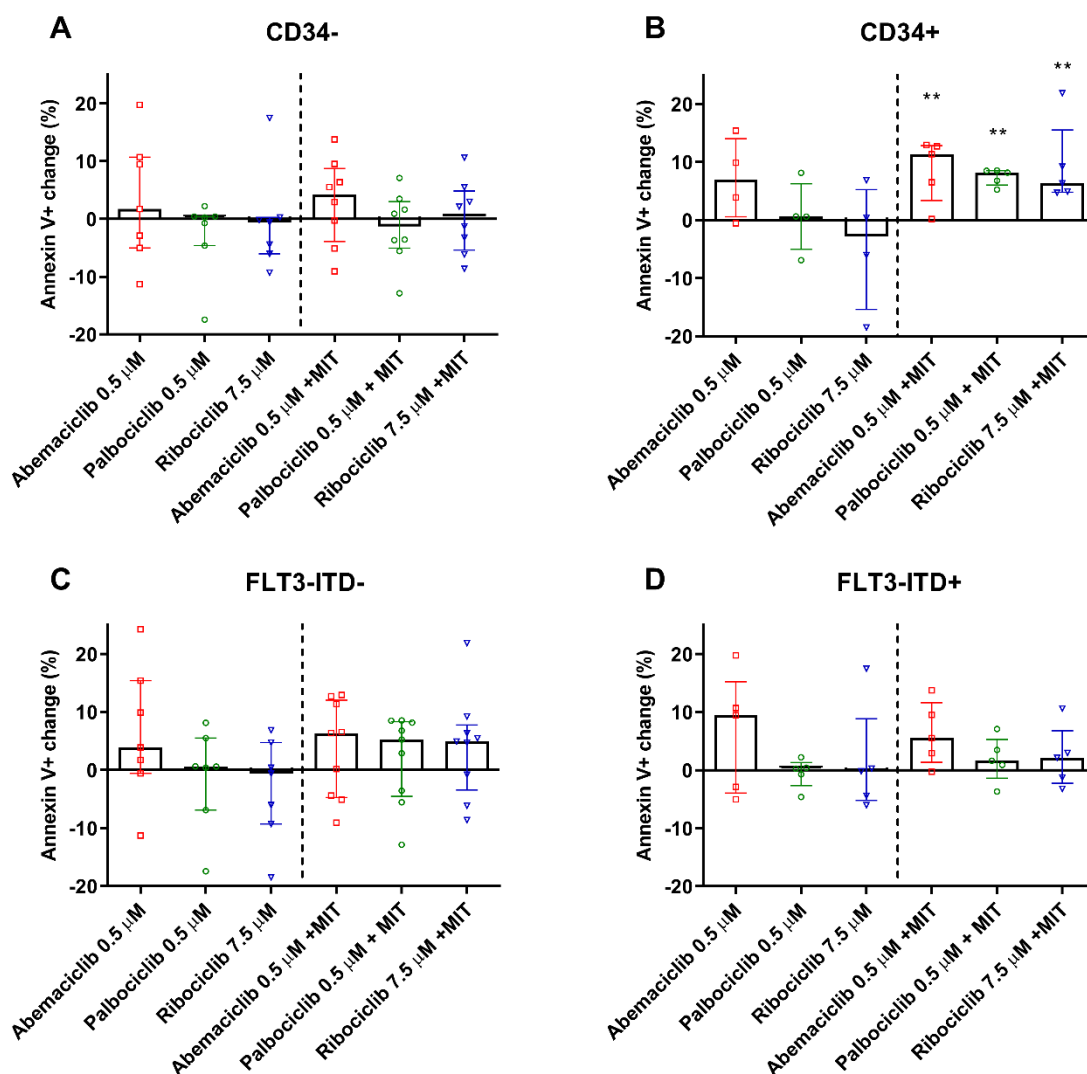
Fig 18. Apoptotic changes in groups of AML patients divided based on their CD34 phenotype and the presence of FLT3-ITD mutation. Left side of each graph depicts the change in apoptotic population of PBMC exposed to CDKi alone (abemaciclib, palbociclib, ribociclib), which was compared to the untreated control cells. Right side of each graph represents apoptotic changes in PBMC treated with the combination of CDKi + mitoxantrone (MIT) compared to the treatment by mitoxantrone only. (A) No apoptosis was detected in CD34^{-} patients, (B) while apoptotic percentage increased in CD34^{+} patients when simultaneously exposed to each CDKi and mitoxantrone. (C, D) No CDKi effect was

observed in AML samples when comparing FLT3-ITD⁺ and FLT3-ITD⁻ groups. Data are presented as medians ± interquartile range. Results were analyzed by Mann-Whitney test (**p < 0.01).

6.2.5 Correlation of *ABCB1/ABCG2* expression and CDKi effect on mitoxantrone accumulation in AML samples

Based on our findings that I) all CDKi inhibit ABCB1 and ABCG2 transporters and II) the fact that their combination with mitoxantrone increases its accumulation as well as apoptosis in patient samples, we wondered about the level of *ABCB1/ABCG2* expression in these samples. For this study, *ABCB1/ABCG2* mRNA expression was determined by qRT-PCR and normalized to *HPRT1* selected as the reference gene. The expression of *ABCB1*, but not *ABCG2*, differed significantly between patient groups defined by the CD34 phenotype. Higher expression of *ABCB1* was detected in CD34⁺ patients, while similar levels of *ABCG2* expression were observed in both CD34$^{+/-}$ groups (Fig 19A). Comparison of *FLT3*-ITD⁺ and *FLT3*-ITD⁻ patients revealed no significant differences in the expression of either gene (Fig 19B). To evaluate the relationship between *ABCB1/ABCG2* mRNA expression and mitoxantrone accumulation resulting from exposure to mitoxantrone and CDKi, linear regression analysis was performed. The analysis showed a correlation of *ABCB1* expression with the functional effect of abemaciclib and ribociclib on the tested patient cohort, while the effect of palbociclib on mitoxantrone accumulation appeared to be increasing yet fell short of statistical significance (Fig 19C). As for *ABCG2* expression, no relationship was observed with either CDKi (Fig 19D).
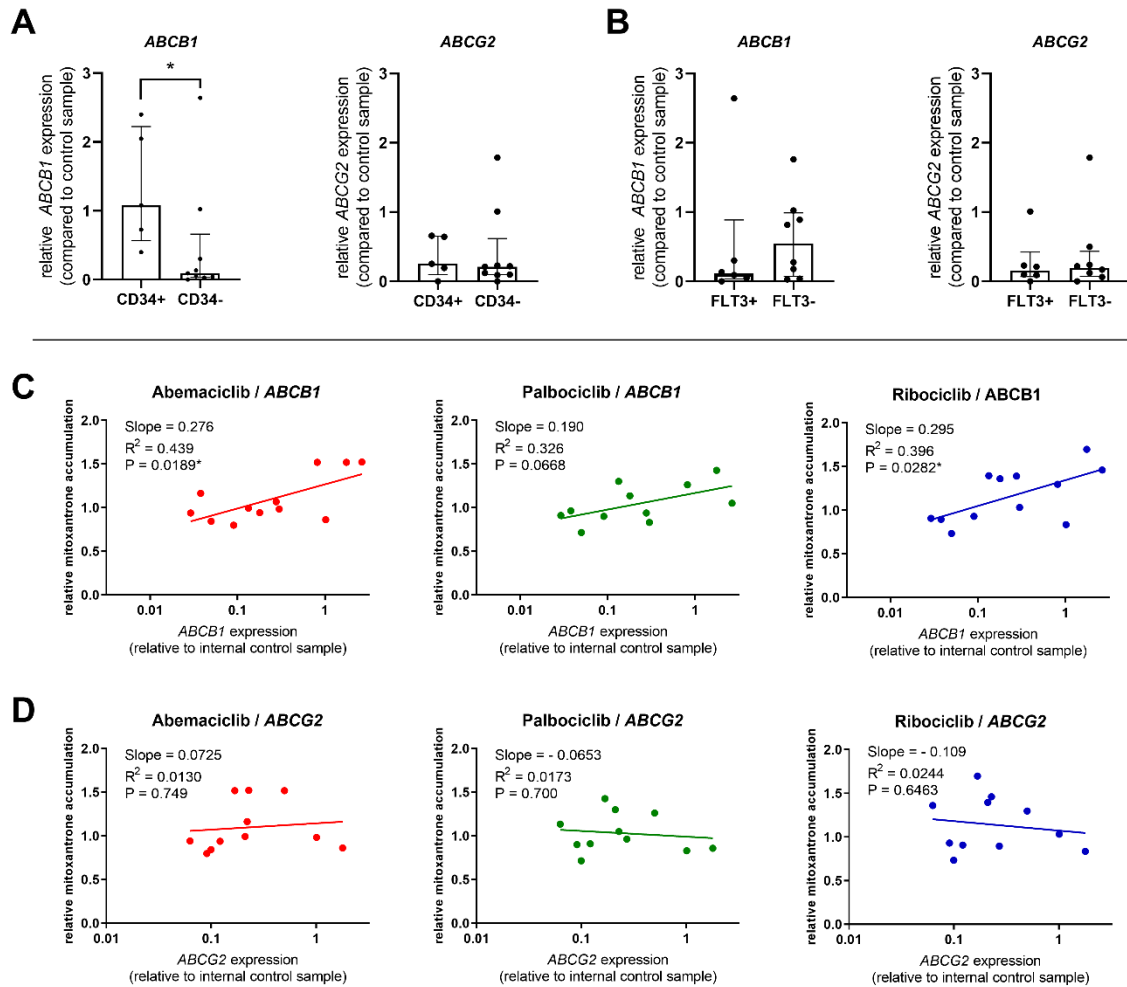
Fig 19. ABCB1/ABCG2 mRNA expression in AML samples & their relationship to functional effect of CDKi on mitoxantrone accumulation. (A, B) Target gene expression was evaluated and compared between CD34^{+/-} patients and FLT3-ITD^{+/-} patients. Significant difference was observed only for ABCB1 in CD34-defined groups when CD34^{+} patients showed higher expression of ABCB1 than CD34^{-} patients. (C) Correlation of ABCB1 expression and CDKi effect on mitoxantrone accumulation was detected only in case of abemaciclib and ribociclib, but not palbociclib. (D) No such correlation was observed for any of the CDKi and ABCG2 gene expression. The expression of ABCB1/ABCG2 was determined by qRT-PCR and normalized to HPRT1 reference gene. Target gene expression is presented as relative to the control sample included in every qPCR plate. Data are reported as medians ± interquartile range and were analyzed by Mann-Whitney test (*p < 0.05). Correlations were evaluated by linear regression, p < 0.05 was considered significant.

6.3 Gilteritinib & its role in AML

Following subchapters comprise data obtained on gilteritinib-sensitive & gilteritinib-resistant HL-60 cell lines generated in our lab and describe the differences in their transcriptomic and proteomic profiles. General gene and protein characteristics are followed by the elaboration of lysosomes and their role in the gilteritinib-resistant cells. At the moment, manuscripts comprising these data are in preparation and will be submitted to journals with IF once finalized.

6.3.1 Sensitivity of gilteritinib-sensitive HL-60 WT and gilteritinib-resistant HL-60 G75 cells

Gilteritinib-sensitive HL-60 WT and gilteritinib-resistant HL-60 G75 cells were tested for their sensitivity towards gilteritinib. Dose-response curves revealed HL-60 G75 to be less responsive to gilteritinib (IC_{50} of 1.087 µM) than HL-60 WT (IC_{50} of 0.500 µM) with the RF of 2.2 (Fig 20A). To determine the stability of acquired resistance to gilteritinib in HL-60 G75, these cells were cultured in gilteritinib-free culture medium and tested for the sensitivity to gilteritinib on weekly basis. Gradual decrease of RF was observed reaching RF of 1.1 after 4 weeks of gilteritinib-deprived cell culture (Fig 20B). These results suggest that HL-60 G75 acquired transient resistance to gilteritinib.

HL-60 WT	IC_{50} = 0.500 µM (95% CI: 0.449 - 0.555 µM)
HL-60 G75	IC_{50} = 1.087 µM (95% CI: 0.890 - 1.343 µM) RF = 2.2

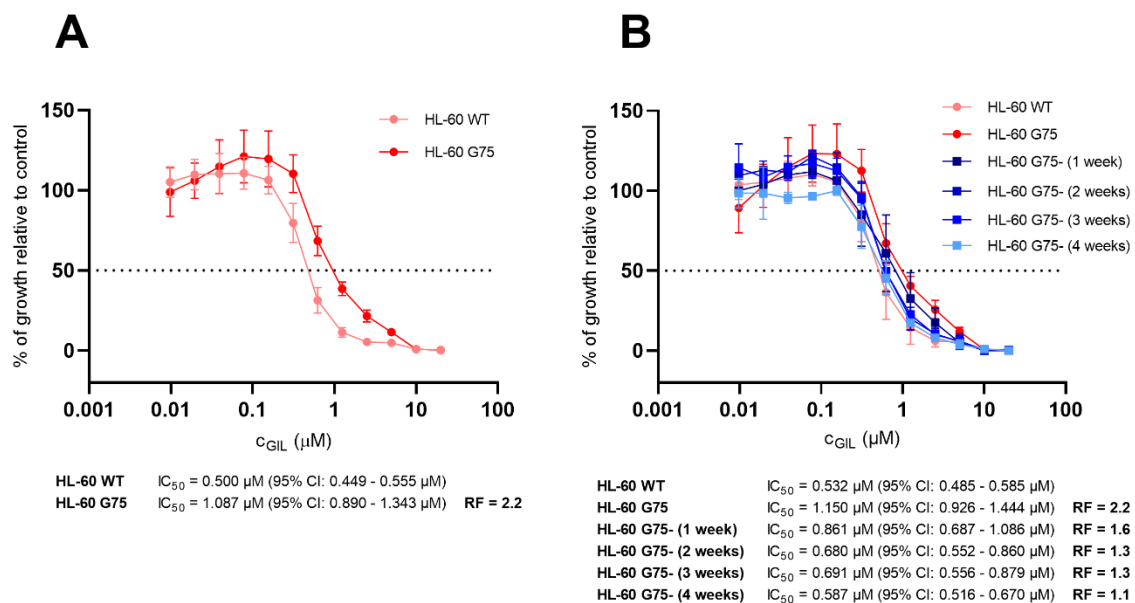|		
HL-60 WT	IC_{50} = 0.532 µM (95% CI: 0.485 - 0.585 µM)	
HL-60 G75	IC_{50} = 1.150 µM (95% CI: 0.926 - 1.444 µM)	RF = 2.2
HL-60 G75- (1 week)	IC_{50} = 0.861 µM (95% CI: 0.687 - 1.086 µM)	RF = 1.6
HL-60 G75- (2 weeks)	IC_{50} = 0.680 µM (95% CI: 0.552 - 0.860 µM)	RF = 1.3
HL-60 G75- (3 weeks)	IC_{50} = 0.691 µM (95% CI: 0.556 - 0.879 µM)	RF = 1.3
HL-60 G75- (4 weeks)	IC_{50} = 0.587 µM (95% CI: 0.516 - 0.670 µM)	RF = 1.1

Fig 20. Drug sensitivity of gilteritinib-sensitive HL-60 WT and gilteritinib-resistant HL-60 G75 cells evaluated after 96 h exposure to gilteritinib by MTT assay. (A) HL-60 G75 showed resistance to gilteritinib with RF of 2.2 compared to HL-60 WT. (B) HL-60 G75 acquired transient resistance to gilteritinib. Cells cultured in gilteritinib-free culture medium (referred to as HL-60 G75- with

corresponding number of weeks in gilteritinib-free culture medium) for 4 weeks responded to gilteritinib similarly as HL-60 WT with its RF dropping to 1.1. Results are presented as the cell growth of the treated cells relative to the untreated cells. Means ± SD of at least 3 independent experiments are presented and were evaluated by non-linear fit. In the figure, IC₅₀ (half maximal inhibitory concentration) values and confidence intervals (CI) are reported.

6.3.2 Identification of DEGs and enriched pathways

To investigate changes in gene expression between both cell lines (HL-60 WT and HL-60 G75), RNA-seq was performed and transcriptomic signatures of cell lines were compared. Using limma-voom, we identified 3,372 DEGs between gilteritinib-sensitive and -resistant cells. Of those, 2,199 DEGs were downregulated and 1,173 DEGs were upregulated in HL-60 G75 (Fig 21).
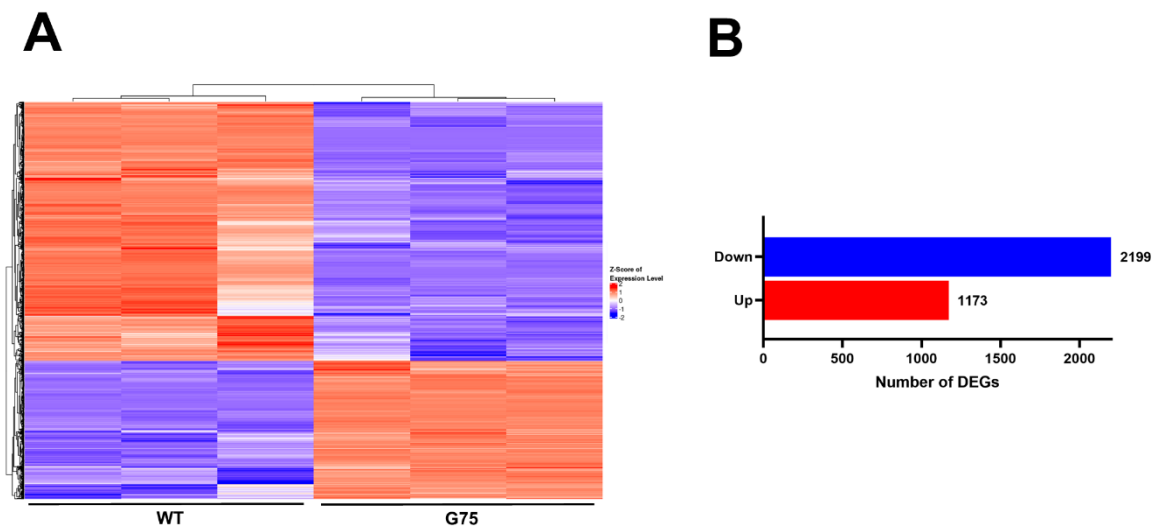

Fig 21. RNA-seq analysis of gilteritinib-sensitive HL-60 WT and gilteritinib-resistant HL-60 G75 cells. (A) Heatmap and (B) barplot show a total of 3,372 DEGs between HL-60 WT and HL-60 G75; 2,199 downregulated (blue on barplot) and 1,173 upregulated (red on barplot) DEGs in HL-60 G75. Blue color on the heatmap indicates downregulated DEGs for the respective cell line, while red color indicates upregulated DEGs for the respective cell line. Analysis was performed on 3 biological replicates using limma-voom with the thresholds: FC > 2 & FDR < 0.05.

GO and KEGG pathway enrichment analysis of both upregulated and downregulated genes in HL-60 G75 were performed. Most of the significantly upregulated GO terms were associated with ribosomes and their subunits, endoplasmic reticulum (ER) and protein localization, and DNA binding suggesting an enhanced transcription activity and protein synthesis. KEGG pathway enrichment analysis studying gene interactions in the organism identified "ribosome"

as the most affected pathway. Interestingly, transcriptomic profile of gilteritinib-resistant cells resembled viral diseases such as herpes simplex virus 1 (HSV-1) or coronavirus disease, which were among the most impacted KEGG pathways. Gilteritinib has been recently associated with viral diseases, mostly SARS-CoV-2, due to its newly identified antiviral properties [124, 125]. Therefore, it is not surprising that genes involved in viral infections were upregulated in the gilteritinib-resistant cells (Fig 22A). In comparison to upregulated genes, RNA-seq analysis identified almost twice as many downregulated DEGs. These were related to GTPase activity and kinase activity, which could be associated with suppressed cell signaling and signal transduction. Many downregulated genes were also linked to biological processes such as cell adhesion, cell migration, cell motility or regulation of actin cytoskeleton. Additionally, export from cell, secretion and extracellular matrix were among downregulated processes too, suggesting that gilteritinib-resistant cells avoid intercellular communication and cell-to-cell contact (Fig 22B).
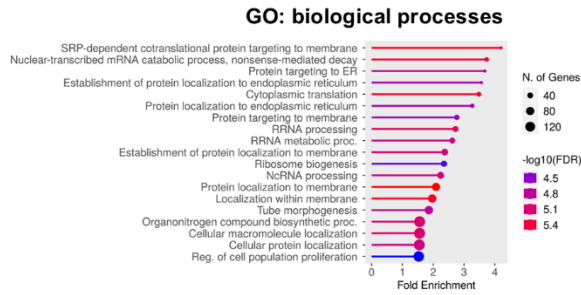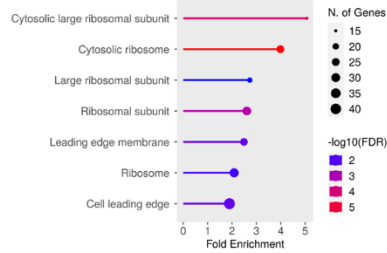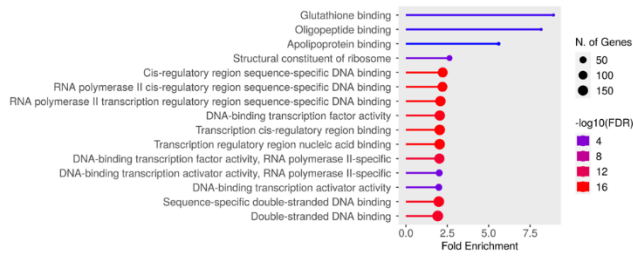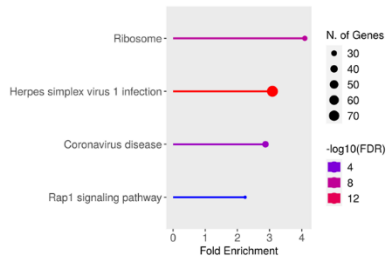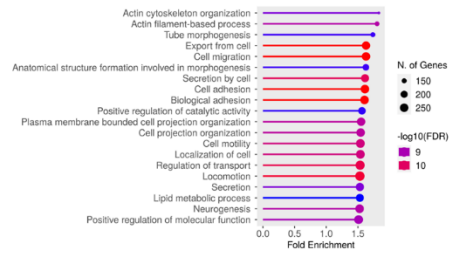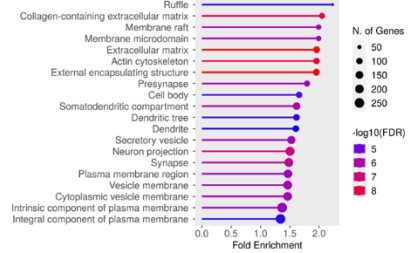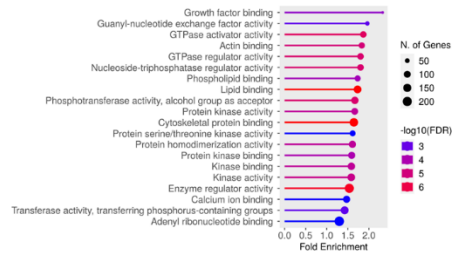
Fig 22. GO and KEGG pathway enrichment analysis of upregulated and downregulated DEGs in gilteritinib-resistant HL-60 G75. Top enriched pathways are listed by the fold change of HL-60 G75 vs HL-60 WT. Colors indicate -log10(FDR) and the size of the points indicate the number of genes in the pathway.

6.3.3 Identification of DEPs and enriched pathways

Protein signatures of HL-60 WT and HL-60 G75 were determined by DEqMS, which revealed a total of 174 DEPs between these cell lines. Similarly to RNA-seq, a higher number of proteins was identified as downregulated than upregulated (97 vs 77, respectively) (Fig 23).
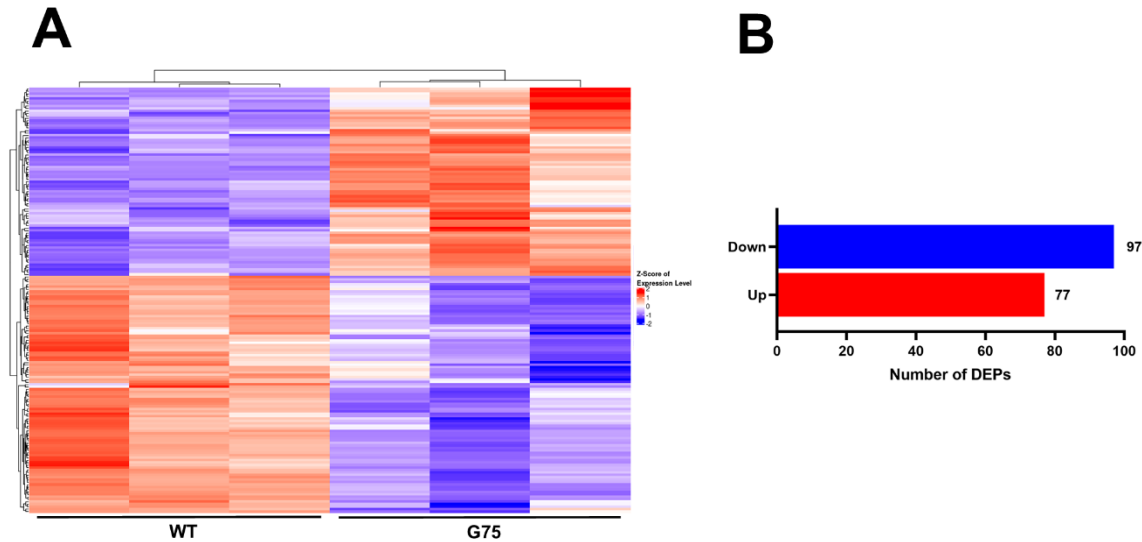
Fig 23. Proteomics analysis of gilteritinib-sensitive HL-60 WT and gilteritinib-resistant HL-60 G75 cells. (A) Heatmap and (B) barplot show a total of 174 DEPs between HL-60 WT and HL-60 G75; 97 downregulated (blue on barplot) and 77 upregulated (red on barplot) DEPs in HL-60 G75. Blue color on the heatmap indicates downregulated DEPs for the respective cell line, while red color indicates upregulated DEPs for the respective cell line. Analysis was performed on 3 biological replicates using DEqMS with the thresholds: FC > 1.5 & FDR < 0.05.

Just as for DEGs, GO and KEGG pathway enrichment analysis were conducted for DEPs as well. While DEGs showed a clear distinction between gene expression profiles of gilteritinib-resistant and -sensitive cells, DEPs belonging to similar pathways were identified among the most downregulated, but also upregulated terms. Considering that every pathway is a set of strictly regulated proteins with various functions, downregulation of some proteins might be complementary to upregulation of other proteins within that specific pathway. In the case of gilteritinib-resistant HL-60 G75, immune response carried out by myeloid leukocytes and neutrophils was one of the top biological processes affected alongside secretion, exocytosis, and export from cell. Under the category of cellular components, DEPs were associated with vacuoles and their lumens as well as lumens of other secretory membrane organelles, such as vesicles or secretory granules. "Azurophil granule lumen" together with "azurophil granule", "primary lysosome", and "lysosome", all related to lysosomes, were found among the most

downregulated pathways although some of them could be found among the top upregulated pathways too. As for molecular functions, specific enzymatic activities were suppressed (e.g., desaturases or sulfotransferases) in HL-60 G75 as well as binding associated with calcium. Downregulation of "cadherin binding", "cell adhesion molecule binding" and "actin binding" coincide with the downregulated DEGs supporting the theory of suppressed cell-cell communication. On the other hand, molecular functions related to inflammation were revealed among the most upregulated terms (e.g., "Toll-like receptor 4 binding", "arachidonic acid binding", "icosanoid binding", "icosatetraenoic acid binding", or "RAGE receptor binding") suggesting that immunoresponsiveness of HL-60 G75 was impacted (Fig 24).
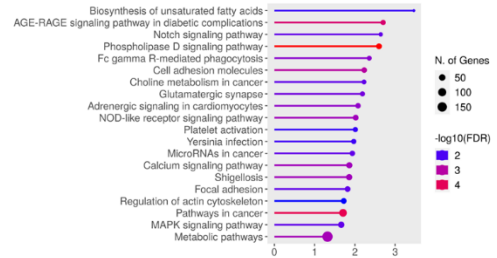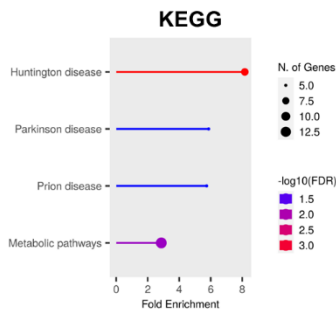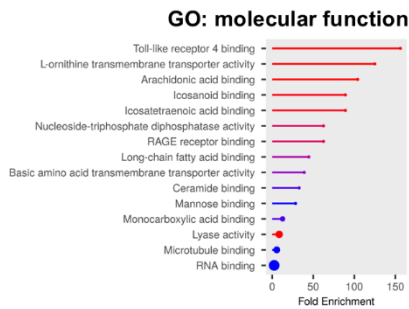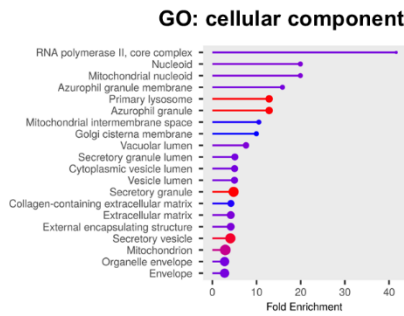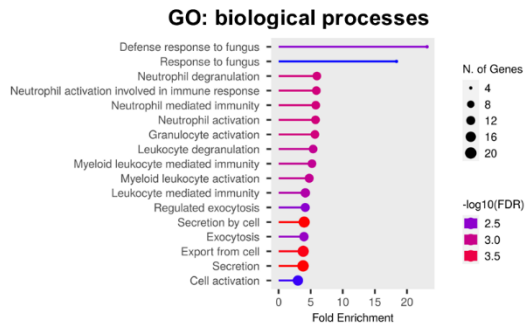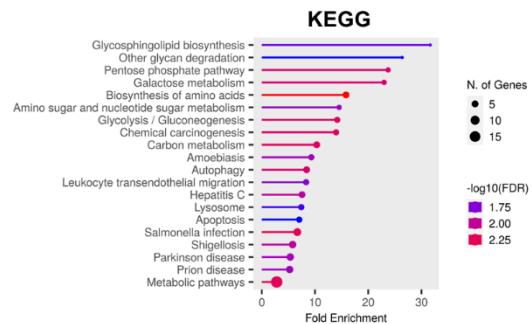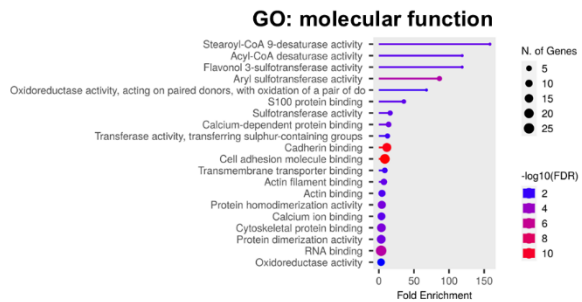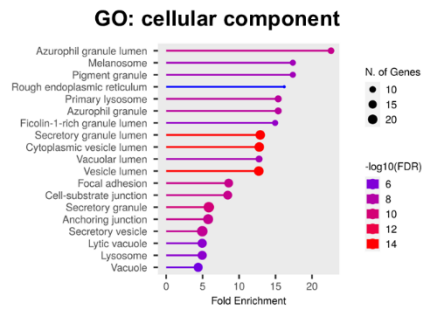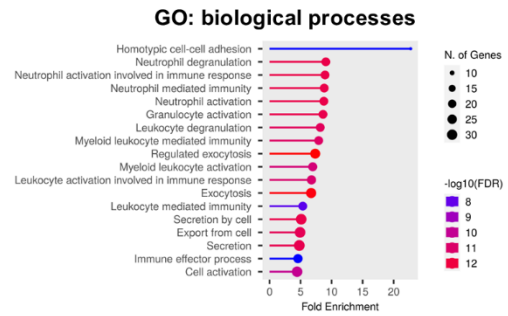
Fig 24. GO and KEGG pathway enrichment analysis of upregulated and downregulated DEPs in HL-60 G75. Top enriched pathways are listed by the fold change of HL-60 G75 vs HL-60 WT. Colors indicate -log10(FDR) and the size of the points indicate the number of genes in the pathway.

6.3.4 Transcriptome and proteome correlation analysis

Combined analysis of 2,199 DEGs identified by RNA-seq and 174 DEPs identified by proteomics revealed exactly 100 genes which were translated to their corresponding proteins

(Fig 25A). Three of them were negatively correlated meaning two upregulated genes (*NEFH, MBNL3*) were downregulated on a protein level and one downregulated gene (*NFKB2*) was upregulated on a protein level. Out of remaining 97 DEGs/DEPs, 59 were downregulated on both mRNA and protein level, while 38 were upregulated on both levels (Fig 25B).
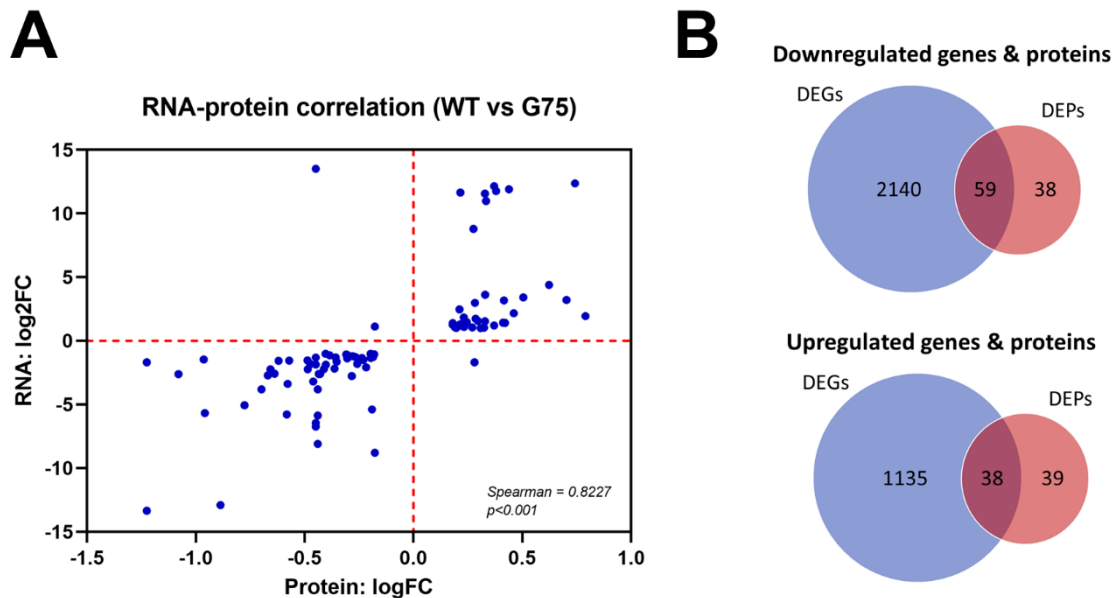
Fig 25. Correlation analysis of DEGs identified by RNA-seq and DEPs identified by proteomics in HL-60 G75 vs HL-60 WT. (A) Scatter plot of 100 DEGs, that were also detected on a protein level, and calculated Spearman correlation. (B) Venn diagrams showing positively correlated DEGs and DEPs either downregulated or upregulated. Thresholds: FC > 2 & FDR < 0.05 for RNA-seq and FC > 1.5 & FDR < 0.05 for proteomics.

GO and KEGG pathway enrichment analysis were performed on down- and upregulated genes/proteins excluding the three negatively correlated genes. Most of the enriched pathways in proteomics matched enriched pathways in correlated DEGs/DEPs. Immune response mediated by myeloid leukocytes and neutrophils and other immune system associated terms were identified among the top deregulated biological processes. Processes related to transmembrane transport of amino acids L-arginine, L-lysine, and L-ornithine emerged to be the top upregulated ones. These amino acids, L-arginine especially, participate in the immune response of a cell, which further underlines the importance of immune system in the resistant cells. In accordance with pathway enrichment of DEPs, "exocytosis", "export from cell", and "secretion" were among the most downregulated processes. Similarly to proteomics enrichment, cellular components such as "vacuoles", "secretory vesicles", "lysosomes" and their lumens were greatly deregulated in HL-60 G75. As for molecular functions, terms related

to inflammation were primarily upregulated just like in the proteomics enrichment (e.g., "Toll-like receptor 4 binding", "arachidonic acid binding", "icosanoid binding", "icosatetraenoic acid binding", "RAGE receptor binding"), while enzymatic activity was downregulated (especially desaturases and sulfotransferases). Additionally, genes and proteins belonging to cytoskeleton related groups were vastly downregulated (e.g., "filamin binding", "cadherin binding", or "actin binding"). KEGG pathway enrichment analysis revealed majority of correlated genes and proteins to be downregulated. Most of these pathways included biosynthesis, metabolism, and degradation of lipids, amino acids, or carbohydrates, which can be involved in multiple cellular processes. For example, downregulated glycosphingolipid biosynthesis might play a role in suppressed transmembrane signaling and cell-cell communication, while glycosaminoglycan degradation might be involved in impaired cell adhesion or cell growth and proliferation. Unsaturated fatty acids function as precursors of lipid mediators including pro- and anti-inflammatory eicosanoids, which might be complementary to upregulated inflammatory processes detected in HL-60 G75. Several enriched pathways detected in resistant cells are generally involved in providing energy in a form of glucose; therefore, their deregulation might indicate changes in energy availability or suppression of energy requirements. These pathways include galactose and pyruvate metabolism, pentose phosphate pathway or glycolysis/gluconeogenesis (Fig 26).
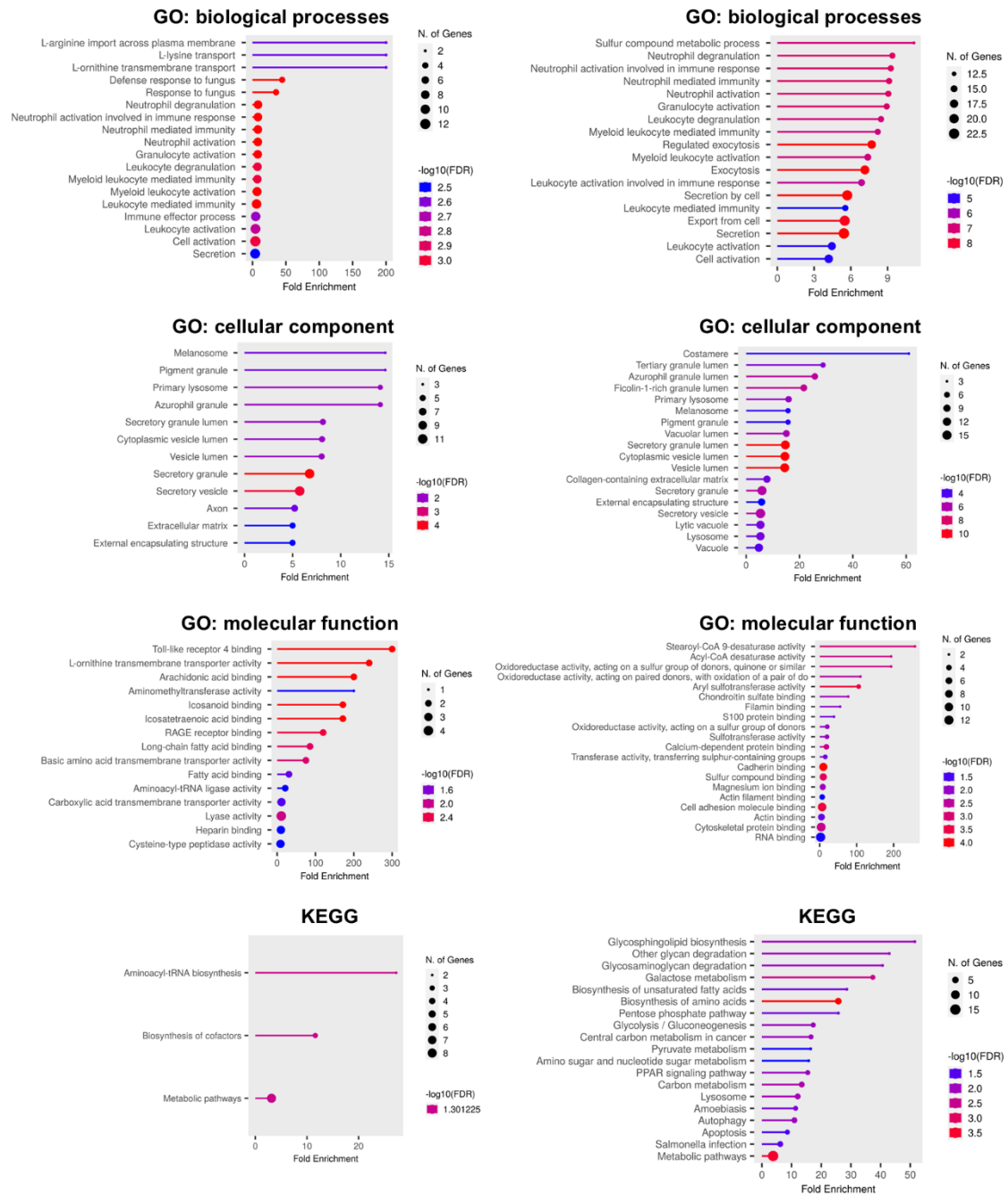
Fig 26. GO and KEGG pathway enrichment analysis of upregulated and downregulated DEGs/DEPs in HL-60 G75. Top enriched pathways are listed by the fold change of HL-60 G75 vs HL-60 WT. Colors indicate -log10(FDR) and the size of the points indicate the number of genes in the pathway.

6.3.5 RNA-seq & proteomics profiling indicate involvement of lysosomes in gilteritinib resistance

RNA-seq and proteomics analysis showed a great distinction of HL-60 WT and HL-60 G75 profiles. Lysosome-associated terms and pathways were included among the most deregulated ones in both transcriptome and proteome of HL-60 G75. In transcriptome, 167 DEGs (53 upregulated & 114 downregulated) were identified, while in proteome, 24 DEPs (7 upregulated & 17 downregulated) were detected for lysosome (GO: 0005764) (Fig 27B, C). Of those, 15 DEGs were translated to their respective proteins - 4 were upregulated (MPO, GGH, VAPA, STX7) and 11 were downregulated (CTSG, CTSD, LYZ, AHNAK, HEXB, CST7, PRTN3, ANXA6, GLB1, ATP6V1A, MNDA) (Fig 27A).
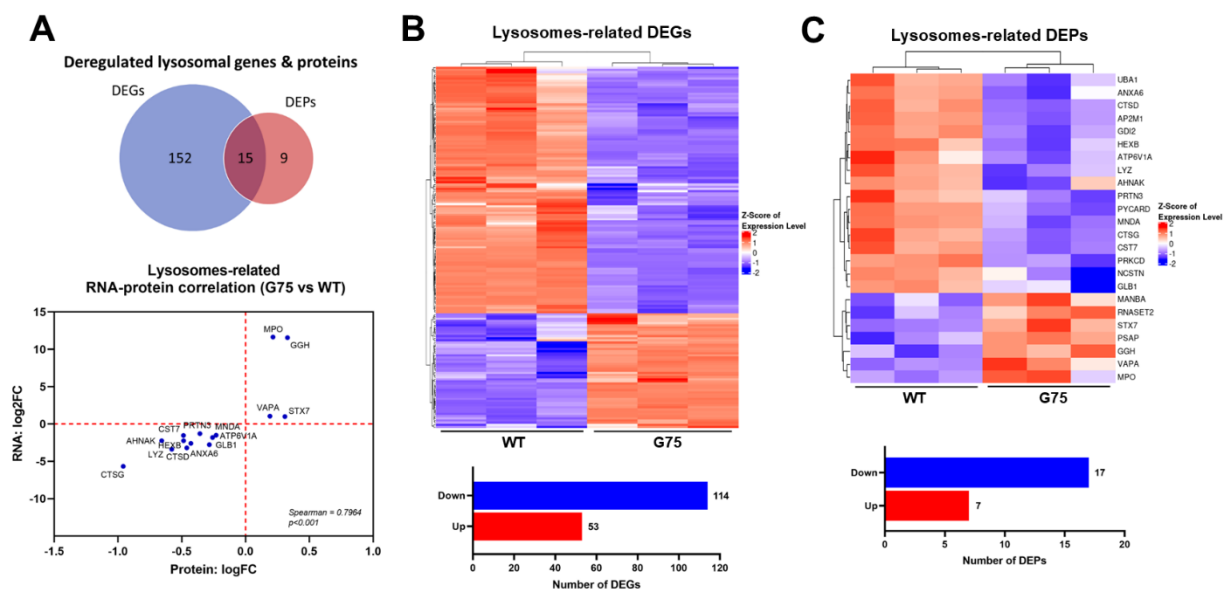
Fig 27. RNA-seq & proteomics analysis focusing on lysosomes-associated genes and proteins (GO: 0005764). (A) Venn diagram of DEGs and DEPs in HL-60 G75 vs HL-60 WT. Scatter plot showing 15 DEGs that correlated with their expression on a protein level. (B) Heatmap and barplot depicting 167 DEGs identified by RNA-seq. (C) Heatmap and barplot showing 24 DEPs identified by proteomics. Blue color on the heatmaps indicates downregulated genes or proteins for the respective cell line, while red color indicates upregulated genes or proteins for the respective cell line. In barplots, downregulated genes/proteins are blue-colored, while upregulated ones are red-colored. Analysis was performed on 3 biological replicates using limma-voom and the thresholds of FDR < 0.05 & FC > 2 for RNA-seq, while DEqMS and the thresholds of FDR < 0.05 & FC > 1.5 were used for proteomics.

6.3.6 HL-60 G75 showed cross-resistance to sunitinib, but not midostaurin

Based on the so far presented data, we suspected lysosomes to be involved in the resistance of HL-60 G75. Not only did transcriptome and proteome profiling revealed lysosome-related pathways to be highly deregulated in HL-60 G75, but also its low RF of 2.2 implicated lysosomal involvement. Lysosome-mediated resistance is generally associated with only 2- to 3-fold increase of RF, which was also the case of our gilteritinib-resistant cells. Moreover, it has been previously implied that gilteritinib affects endolysosomal compartment [103]. Therefore, we decided to dive into the lysosomal sequestration a bit deeper. Lysosomal sequestration is a well-described reversible mechanism of resistance with one major limitation - only weak base drugs can be trapped by lysosomes. That is another reason why gilteritinib resistance could be mediated via lysosomes as gilteritinib meets the criterium of a weak base drug with its pKa of 8.47 and logP of 4.35 [126]. For another FLT3 inhibitor, sunitinib, resistance mediated by lysosomal sequestration has been well-described [127-129], hence, HL-60 G75 were tested for its cross-resistance to sunitinib. Similar level of resistance to sunitinib was detected in these cells as was to gilteritinib ($RF_{gilteritinib}$ = 2.2 vs $RF_{sunitinib}$ = 3.2; Fig 28A). Cross-resistance of HL-60 G75 to midostaurin, another FLT3 inhibitor with similar mechanism of action as gilteritinib, was examined as well, yet not detected since RF equaled to 1.0 (Fig 28B).

HL-60 WT	IC$_{50}$ = 0.980 μM (95% CI: 0.828 - 1.159 μM)
HL-60 G75	IC$_{50}$ = 3.120 μM (95% CI: 2.651 - 3.687 μM) **RF = 3.2**

HL-60 WT	IC$_{50}$ = 0.300 μM (95% CI: 0.230 - 0.394 μM)
HL-60 G75	IC$_{50}$ = 0.288 μM (95% CI: 0.254 - 0.327μM) **RF = 1.0**
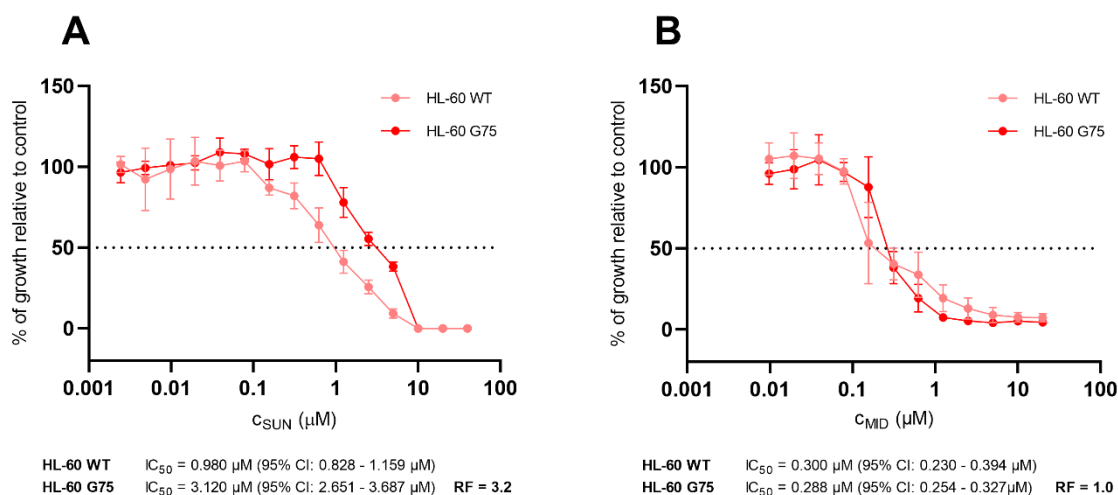
Fig 28. Cross-resistance of HL-60 G75 to sunitinib & midostaurin. (A) HL-60 G75 showed cross-resistance to sunitinib (RF of 3.2), (B) but not to midostaurin (RF of 1.0) after 96 h exposure to sunitinib or midostaurin and subsequent evaluation by the MTT assay. Data were analyzed by non-linear fit and are presented as means ± SD of at least 3 independent experiments. Results are shown

6.3.7 Increased number and fluorescent signal of lysosomes in gilteritinib-resistant HL-60 G75 cells

To further investigate the role of lysosomes in gilteritinib resistance, cells were stained with a lysosome-specific dye (Lysotracker) and imaged on a confocal microscope. HL-60 G75, which had been constantly exposed to gilteritinib, showed a higher signal of Lysotracker and a slight increase in the number of lysosomes compared to HL-60 WT. HL-60 G75 kept in gilteritinib-free medium for 1 day (referred to as HL-60 G75- (1d)) and for 1 week (referred to as HL-60 G75- (1w)) seemed to resemble the lysosomal staining in HL-60 WT more than in HL-60 G75 (Fig 29A). The same pattern was observed when analyzed by flow cytometry. HL-60 G75 showed higher AUC of Lysotracker (reflecting the lysosomal mass) as well as higher MFI of Lysotracker (reflecting intensity of the lysosomal signal) when compared to the other cell lines (Fig 29B, C).

Since Lysotracker enters lysosomes based on their pH, we wanted to eliminate the possibility that the observed differences were caused by altered pH in cells. Therefore, we stained three of the investigated cell lines - HL-60 WT, HL-60 G75, HL-60 G75- (1d) - with Lysotracker and dextran, which enters acidic organelles such as lysosomes independently of pH. Imaged lysosomes showed a similar Lysotracker staining as in Fig 29A. Dextran, however, appeared to stain lysosomes similarly in all three cell lines (Fig 29D). The number of organelles stained with dextran is apparently greater than with Lysotracker. That is due to dextran not being lysosome-specific. Dextran enters all acidic organelles including endosomes in this case. Even though cell lines were kept in dextran-free culture medium for 4 h to allow the transfer of dextran from endosomes to lysosomes, dextran was partially retained in endosomes, and as a result, stained both lysosomes and endosomes. To confirm that pH changes do not cause the differences in Lysotracker staining, we incubated all three cell lines with Lysosensor to detect their exact lysosomal pH. Averaged pH $\pm$ SD (of at least three independent experiments) obtained after 0.5 h incubation with Lysosensor were as follows: 5.7 $\pm$ 0.5 for HL-60 WT, 5.8 $\pm$ 0.5 for HL-60 G75, and 5.7 $\pm$ 0.5 for HL-60 G75- (1d). After 2 h incubation, similar pH values were detected: 5.8 $\pm$ 0.5 for HL-60 WT, 5.8 $\pm$ 0.4 for HL-60 G75, and 5.8 $\pm$ 0.5 for HL-60 G75- (1d). Thereby, pH changes across cell lines were eliminated.
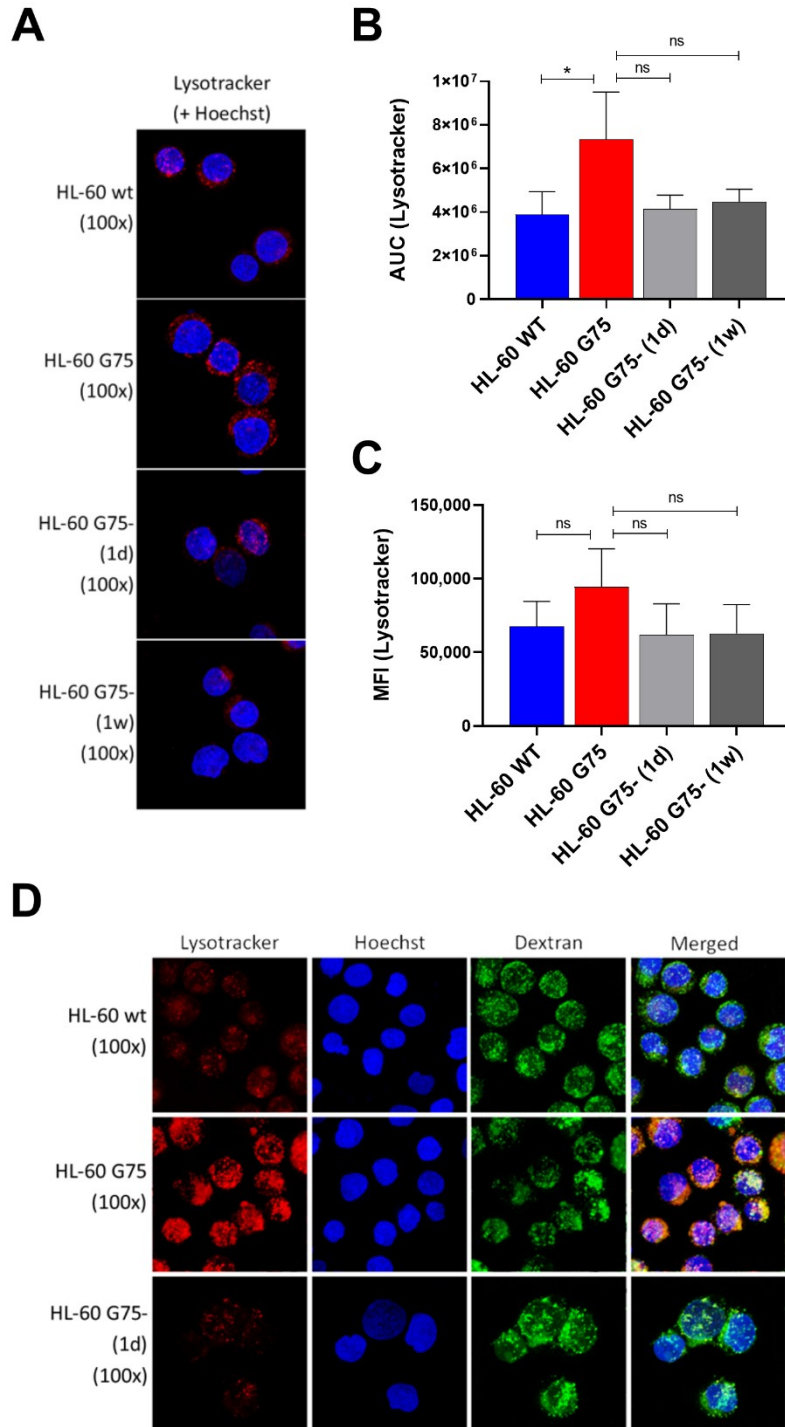
Fig 29. Lysosomal staining in HL-60 WT, HL-60 G75, HL-60 G75- (1d), and HL-60 G75- (1w).
(A) HL-60 G75 constantly exposed to gilteritinib showed higher signal of Lysotracker (red) as well as increased number of lysosomes compared to HL-60 WT or any of the cells deprived of gilteritinib. (B, C) Flow cytometry analysis revealed higher AUC (reflecting the number of lysosomes) and MFI (reflecting intensity of the lysosomal signal) of Lysotracker in HL-60 G75 compared to HL-60 WT or gilteritinib-deprived cells. (D) Staining with Lysotracker showed the same distinct pattern as in A with HL-60 G75 having the strongest signal and the highest number of lysosomes. However, pH-independent

dextran conjugated with FITC (green) stained all three cell lines similarly and did not differ in the intensity of FITC-dextran signal. All confocal images were also stained with Hoechst (blue) to distinguish cell nuclei. Representative images of at least 3 independent experiments are presented. For all images, 100× magnification and scale bars of 20 μm were used. Flow cytometry data (B, C) are presented as means ± SD of at least 3 independent experiments. Only viable (PI-negative) cells were considered. Data were analyzed by unpaired t-test; *p < 0.05.

6.3.8 Sunitinib sequestered in lysosomes of gilteritinib-resistant HL-60 G75, but appeared to spread into cytosol upon gilteritinib withdrawal

To further investigate the changes in Lysotracker staining, we decided to examine our cells using sunitinib, which, unlike gilteritinib, is fluorescent. Sunitinib, a FLT3 inhibitor just like gilteritinib, is known for its lysosomal sequestering by which cells acquire temporary resistance to it. Simultaneous staining of HL-60 G75 with Lysotracker and sunitinib revealed an obvious colocalization of their fluorescence signals within the cells. Recorded fluorescence intensity profiles of both Lysotracker and sunitinib confirmed their colocalization. In contrast, little to no colocalization was detected in HL-60 WT. Confocal images of HL-60 G75- (1d) and HL-60 G75- (1w) revealed Lysotracker signal to be barely visible and sunitinib to be predominantly spread within the cytosol, but also accumulated in the very few lysosomes present in these cells. On the contrary, fluorescence intensity profiles indicated an apparent colocalization of sunitinib and Lysotracker in both gilteritinib-deprived cell lines. These results suggest either a direct interaction of Lysotracker and gilteritinib or acute effect of gilteritinib, which is pronounced only in continual gilteritinib presence yet diminished once gilteritinib is withdrawn (Fig 30).
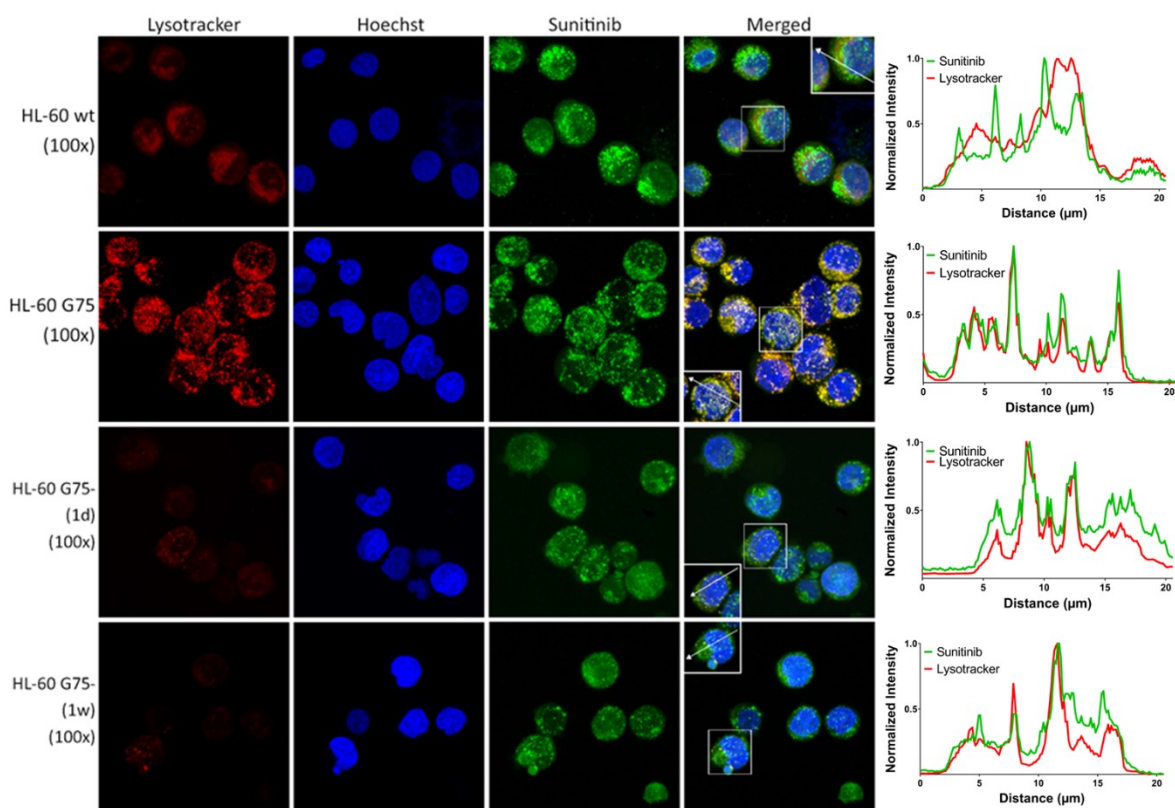
Fig 30. Intracellular sublocalization of sunitinib within HL-60 WT, HL-60 G75, HL-60 G75- (1d), HL-60 G75- (1w) and its colocalization with Lysotracker. Lysotracker (red) showed the highest signal and the highest lysosomal mass in HL-60 G75, while in the other three cell lines, it was less or barely visible. Sunitinib (green) seemed to colocalize with Lysotracker in HL-60 G75. Although sunitinib and Lysotracker colocalized to a certain level in HL-60 G75- (1d) and HL-60 G75- (1w), sunitinib was also identified within the cytosol. Little to no colocalization was observed in HL-60 WT. All confocal images were stained with Hoechst (blue) to distinguish cell nuclei. Representative images of at least 3 independent experiments are presented. For all images, 100× magnification and scale bars of 20 µm were used. Intensity profiles of the fluorescence signals are shown on the right side of the figure for the respective cells. Bars indicate measured area and represent 14.7 µm.

6.3.9 Apoptosis induction by gilteritinib and its effect on cell cycle

To evaluate functional consequences of potential gilteritinib sequestration, apoptosis and cell cycle analyses were conducted. HL-60 WT and HL-60 G75 were exposed to multiple concentrations of gilteritinib for 24 h and 48 h. Shorter incubation time (24 h) seemed insufficient to induce apoptosis in either of the cell lines (Fig 31B). Longer exposure (48 h) to higher concentrations of gilteritinib (10 µM) led cells to apoptosis, however, it appeared to be induced similarly in both HL-60 WT (gilteritinib-sensitive) and HL-60 G75 (gilteritinib-resistant) cells. Significance in apoptosis of HL-60 WT and HL-60 G75 was

detected only in case of the untreated cells and the cells treated with 1 µM gilteritinib. Nevertheless, less than 10 % of apoptotic cells were detected in all cases, which was considered negligible (Fig 31C). Cell cycle analyses revealed an overall higher responsiveness of HL-60 WT than HL-60 G75 to gilteritinib. Most of HL-60 WT cells were in G1 phase of the cell cycle when exposed to lower gilteritinib concentration (1 µM) for 24 h, while higher concentrations (5 µM, 10 µM) sent the cells to G2/M (Fig 31D). Cell distribution across the cell cycle phases was, however, not so pronounced after 48 h exposure to gilteritinib (Fig 31E). On the other hand, HL-60 G75 did not react to gilteritinib exposure by alterations of the cell cycle phases. No apparent changes in the number of cells in S or G2/M phases were observed, suggesting an overall decrease in progression of the cell cycle (Fig 31F, G).
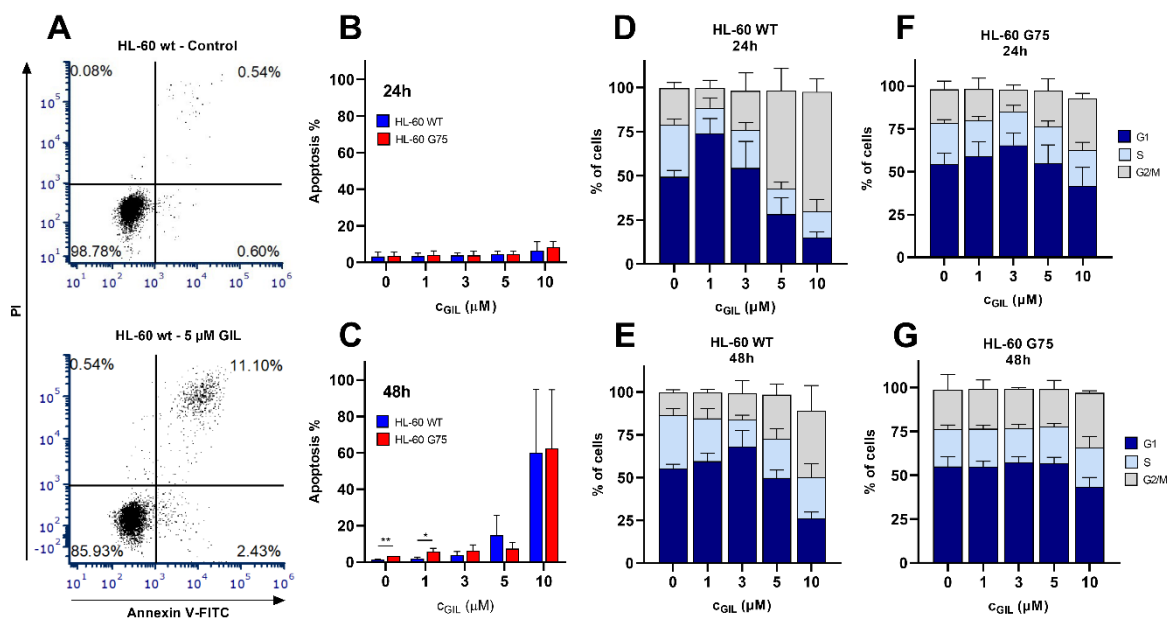
Fig 31. Effect of gilteritinib on apoptosis and cell cycle. (A) Representative flow cytometry dot plots of induced apoptosis by 48 h exposure to gilteritinib. Apoptosis was analyzed by annexin V/PI double staining of which annexin V indicates early and late apoptotic cells and PI necrotic cells. Control HL-60 WT cells (upper dot plot) remained viable, while HL-60 WT exposed to 5 µM gilteritinib (GIL) resulted in ca. 11 % increase of late apoptotic cells (annexin V+/PI+). (B, C) No induction of apoptosis was observed in HL-60 WT or HL-60 G75 after 24 h exposure to gilteritinib. Longer exposure (48 h) to higher gilteritinib concentrations (10 µM) induced apoptosis, but similarly in both cell lines. Significant differences in apoptosis were observed in the untreated cells and cells exposed to 1 µM gilteritinib, however, the apoptotic populations were < 10 % in all cases; therefore, these changes were considered negligible. (D, E) Cell cycle analyses evaluated by PI staining revealed HL-60 WT as responsive to gilteritinib. Distribution of the cells shifted from G1 phase when exposed to lower gilteritinib

concentrations (1 µM) to G2/M when exposed to higher gilteritinib concentrations (5 µM, 10 µM). A more distinct distribution of cells was observed after 24 h than 48 h. (F, G) Cell cycle phases of HL-60 G75 after gilteritinib exposure (24 h or 48 h) remained relatively unchanged, indicating lower responsiveness of the resistant cells to the drug. Data (B - G) are presented as means ± SD of at least 3 independent experiments. For apoptosis, HL-60 WT was compared to HL-60 G75 in each incubation time point and each drug concentration. Statistical analysis was performed by unpaired t-test; *p < 0.05, **p < 0.01.

7   DISCUSSION

AML is a blood cancer that has been treated with a combination of cytarabine and anthracycline in all eligible cases for several decades [8]. Since the search for a replacement therapy with better outcome rate has not been successful, optimization of the current treatment regimens is crucial. That means finding new combinations of drugs from which patients would benefit even more than they do from the current standard treatment. Such treatment, however, might not be universal for all patients suffering from AML. Therefore, identification of prognostic and predictive markers is critical in order to tailor the therapy in a right way [130, 131]. Nevertheless, high adaptability of cancer cells to their surroundings presents one of the major obstacles in the therapy. When exposed to the drugs, cancer cells activate survival mode and are altered in a way that helps them escape the treatment. Even patients that were responsive to the therapy upon its initiation might develop a certain form of resistance during the treatment [132, 133].

This thesis elaborated on anthracycline resistance and possible improvement of anthracycline-based therapy by the addition of targeted agents. Drugs with different mechanisms of actions were selected. First, midostaurin as a member of FLT3-targeting agents and second, abemaciclib, palbociclib, and ribociclib from the group of CDK4/6-targeting drugs. Their effect was tested primarily in relation to ABC transporters, which were also evaluated from the point of prognosis and predictivity of therapy response. This work was followed by the investigation of resistance acquired to one of the FLT3-targeting agents - gilteritinib. Transcriptome and proteome of gilteritinib-resistant and -sensitive AML cells were compared to uncover changes leading to resistance acquirement. Role of one particular mechanism of resistance, lysosomal sequestration, was investigated deeper. Discussion and interpretation of the data presented in this thesis is divided into three separate blocks. Each of them closely elaborates on specific topics: (I) role of midostaurin in therapy of AML and prognostic impact of ABC transporters in AML patients, (II) role of CDK4/6 inhibitors (abemaciclib, palbociclib, ribociclib) in therapy of AML, and (III) mechanisms of acquired resistance to gilteritinib.

MIDOSTAURIN & ITS ROLE IN AML

In the study involving midostaurin, we first looked at the expression of two ABC transporters highly associated with drug resistance, *ABCB1* and *ABCG2*. Patient blood samples used in this study were collected prior to any treatment. Median age of these patients was 63.5 years.

Employing ddPCR, absolute number of transcripts was quantified revealing a strong coexpression of *ABCB1* and *ABCG2*. Coexpression of these transporters had been observed before and had been associated with chemoresistance in AML [71, 93]. Although their expression correlated in our patient cohort, *ABCB1* appeared to be present on a higher level than *ABCG2*. Due to its tight link with chemoresistance, we wanted to see whether *ABCB1* expression had any effect on the outcome of induction cycles consisting of anthracycline and cytarabine. Indeed, patients with high *ABCB1* expression did not respond sufficiently to the induction therapy, which prevented them from achieving CR. Similarly to our study, association of CR and *ABCB1* expression had been observed previously, but in younger patients suffering from AML [85, 134-136]. The role of *ABCB1* in therapy failure was further underlined by patient division based on the ELN risk classification. Adverse risk group, that typically displays the worst prognosis, was the one that overexpressed *ABCB1* the most. Furthermore, high *ABCB1* expression was related to CD34+ phenotype, which had been confirmed as a negative predictor of clinical outcome [84, 137, 138]. All these data suggested negative impact of *ABCB1* on therapy outcomes. Therefore, we wondered whether suppression of ABCB1 activity could improve outcomes of the induction therapy and whether it could be enabled by introducing new targeted agents, such as midostaurin, into the AML treatment schedule.

Since midostaurin has become a key element in therapy of FLT3-mutated AML, we decided to include this drug in the following studies. Moreover, midostaurin has shown inhibitory effects on ABCB1 [122, 123], which was crucial for our studies. Its effect was first tested in PBMC of patients with *de novo* AML. Samples were exposed to midostaurin and mitoxantrone (ABCB1 substrate), which resulted in enhanced mitoxantrone accumulation mainly in CD34+ patients and led to induction of apoptosis in ABCB1-overexpressing cells. These observations indicated that ABCB1 could be an off-target of midostaurin as expected and that abolishment of its function could play in favor of better response to the induction therapy. Currently, midostaurin is administered after the anthracycline-based induction cycle, however, based on our observations, midostaurin appears to positively impact intracellular accumulation of anthracyclines when administered simultaneously with them. Therefore, AML patients, in particular CD34+ ABCB1-overexpressing patients, might benefit from such combination. Nevertheless, concomitant administration of midostaurin and daunorubicin was a subject of a clinical trial, that ended up being terminated [139]. The clinical trial was terminated due to the cytotoxicity of the combined therapy, which might be associated with the hypothesized ABCB1 impact on their pharmacokinetic interaction. Due to midostaurin inhibiting ABCB1,

intracellular daunorubicin accumulation was enhanced and its side effects were most likely amplified too. Since midostaurin as a single drug treatment was well tolerated even in higher doses, we suspected daunorubicin to be responsible for the cytotoxicity rather than midostaurin [17, 139]. Therefore, we hypothesize that lower daunorubicin concentration could be sufficient to treat AML patients if combined with midostaurin. Moreover, their concomitant administration might prevent adverse effects of daunorubicin. Such adjustments in the induction therapy could make it available even to the patients otherwise ineligible for the intensive chemotherapy. Therefore, daunorubicin dosage as well as midostaurin placement in the induction treatment protocol should be reevaluated. Furthermore, *FLT3*-ITD mutation appeared not to have a distinct impact on the cell response to the combination of midostaurin and daunorubicin. Although our study suggested possible midostaurin benefits in *FLT3*-ITD⁻ patients at the time, recent observations indicated the opposite as no benefits were seen in *FLT3*-ITD⁻ AML patients [140].

Not only adjustments of the treatment protocols, but also identification of prognostic markers is vital in the cancer therapy. In this study, we looked at miRNA in more detail, specifically those involved in the regulation of ABCB1 such as miR-9, whose involvement has been described in myeloid cells before [82, 141]. In this study, we showed a direct linkage between miR-9 expression and ABCB1 efflux activity in primary AML cells, and its suppression mediated by midostaurin. Low or no expression of miR-9 was detected specifically in CD34⁺ patients known for their weak response to the chemotherapy, which supported the suspected impact of miR-9 on therapy response. MiR-9 expression could, therefore, serve as a valuable prognostic marker in drug-resistant AML. Moreover, similar miR-9 expression was detected in plasma of these AML patients as was on cellular level (data not shown), which would be of great diagnostic value for patients considering the accessibility of plasma.

To conclude, ABCB1 was most pronounced in AML patients poorly responding to the induction treatment and unable to achieve CR. It was highly associated with CD34⁺ phenotype, while *FLT3*-ITD mutation seemed to have no impact on ABCB1 expression. ABCB1 was identified as an off-target of midostaurin, a drug primarily targeting FLT3 in AML. Its inhibitory effect was observed also in leukemic cells negative for *FLT3*-ITD suggesting that ABCB1 inhibition is not necessarily dependent on *FLT3*-ITD mutation. Moreover, miR-9, which post-transcriptionally regulates ABCB1, was identified in therapy-resistant AML patients as lowly expressed proposing its predicting value in therapy outcome. Nevertheless, AML patients

are very heterogenous on a molecular level and their response to therapy often vary too. Therefore, tailoring therapy to each individual patient is crucial in AML and emphasized greatly in the recent years.

CDK4/6 INHIBITORS & THEIR ROLE IN AML

In the next study, we focused on drugs with different mechanism of action compared to midostaurin, i.e., CDK4/6-targeting agents. We specifically looked at three inhibitors of CDK4/6 - abemaciclib, palbociclib, ribociclib - and investigated their effect on ABC-mediated drug resistance in AML. First, we had to determine whether selected drugs exhibit any inhibitory effects on ABC transporters of interest, ABCB1 and ABCG2. For that, transporters-overexpressing leukemic cell lines were used. Abemaciclib was identified as a dual inhibitor of ABCB1 and ABCG2, which was supported by the results obtained by Wu et al. on cancer cell lines other than leukemic [142]. Similar inhibitory properties were observed for palbociclib and ribociclib, which inhibited both ABCB1 and ABCG2 in leukemic cells. Inhibitory effect of ribociclib was observed also in non-leukemic cells, which was published in our previous study [143]. Resulting IC_{50} values were evaluated with respect to the guidelines provided by regulatory authorities for preclinical drug evaluation [63, 144] and maximum drug concentrations in plasma after standard dosing in clinical settings [145-147]. Considering these, both abemaciclib and ribociclib inhibited ABCB1 and ABCG2 in clinically relevant concentrations. While palbociclib-mediated inhibition of ABCB1 met these criteria as well, the concentration required for successful ABCG2 inhibition exceeded its c_{max} approximately 100 times.

Inhibitory effects of CDKi on ABC transporters were further utilized in follow-up studies determining their impact on apoptosis induction. In combined treatment with mitoxantrone, abemaciclib and ribociclib, but not palbociclib, increased the intracellular mitoxantrone accumulation by inhibiting ABCG2 transporter in HL-60 ABCG2 cells and led to induction of apoptosis. Interestingly, dual staining with annexin V-FITC & PI showed no apoptosis in HL-60 ABCB1, even though proapoptotic morphological changes were clearly visible. There is no clear explanation for this phenomenon, however, we suppose that other mitoxantrone-specific mechanisms might be involved. One of them might be altered expression of Bcl-2 or Bcl-xL, which Belhoussine et al. observed in their study conducted on anthracycline-resistant HL-60 cells [148]. Furthermore, anthracycline concentration and length of exposure have been found

crucial in apoptotic studies especially when distinguishing between immediate necrosis and apoptosis [149, 150]. Therefore, we employed an additional method to detect apoptotic and/or necrotic cell populations. The method is less specific than annexin V/PI staining. It identifies apoptotic cells based on their reduced DNA content and nuclear condensation and is commonly referred to as subG1 fraction. These results confirmed that abemaciclib and ribociclib in combination with anthracyclines successfully led both ABCB1- and ABCG2-overexpressing leukemic cells to apoptosis, whereas palbociclib enhanced only daunorubicin-mediated apoptosis in ABCB1-overexpressing cells.

Given the promising *in vitro* data, we proceeded to *ex vivo* investigation of CDKi using PBMC isolated from patients with *de novo* diagnosed AML. As already mentioned in the midostaurin part of the discussion, coexpression of ABC transporters is tightly linked to chemoresistance in AML, especially to CD34$^+$ phenotype [71, 84, 93, 151]. Looking at the intracellular accumulation of mitoxantrone, another dual ABCB1/ABCG2 substrate, in the presence of either CDKi, we could see that its increase was more pronounced in CD34$^+$ than in CD34$^-$ patients. Moreover, change in the intracellular accumulation of mitoxantrone was observed even in the presence of palbociclib. Since its ABCG2 inhibition appeared to be ineffective, we suppose that the effect in CD34$^+$ cells was predominantly driven by ABCB1 activity. Therefore, we compared gene expression of both ABC transporters in CD34$^{+/-}$ patients and detected significantly higher *ABCB1* expression in CD34$^+$ group, while similar *ABCG2* levels were revealed in CD34$^+$ and CD34$^-$ patients. These results are in accordance with previous studies [84, 151] as well as our midostaurin study [106] in which additional patients were included and *ABCB1/ABCG2* expression was absolutely quantified. The predominant role of ABCB1 was further supported by significant correlation between *ABCB1* expression and CDKi-mediated ABCB1 inhibition.

Just like in the midostaurin study, we divided our patient cohort into two groups based on the presence of *FLT3*-ITD mutation, which is known to give rise to the most adverse AML cases. Unlike in midostaurin study, here we detected slightly higher *ABCB1* expression in *FLT3*-ITD$^-$ patients although below the significance threshold. This could have occurred due to the smaller number of patients included in this study, while in cohort twice as big, differences between groups evened out. Evaluation of functional studies revealed the potency of two CDKi (abemaciclib and ribociclib) to inhibit ABC transporters in *FLT3*-ITD$^-$ patients, and thereby increase the accumulation of mitoxantrone within these cells. Considering only patient samples

involved in the CDKi study and the fact that no CDKi effect on mitoxantrone accumulation was seen in *FLT3*-ITD[+] patients, we hypothesized that the presence of *FLT3*-ITD mutation could be linked to low ABCB1 activity and possibly to low CD34 expression. Such association would coincide with previous studies [71, 72], where similar linkage was observed. Nevertheless, in this small sample group, four out of eight *FLT3*-ITD^{-} patients were CD34^{+}, which was most likely the reason for higher ABCB1 expression and activity detected in *FLT3*-ITD^{-} patients. Based on these observations as well as those from the midostaurin study, we assume that ABCB1 expression and activity is predominantly associated with CD34 phenotype of leukemic cells and not with *FLT3*-ITD mutation.

To conclude, all three tested CDKi (abemaciclib, ribociclib, palbociclib) were capable of inhibiting ABCB1 in clinically relevant concentrations and enhanced anthracycline-mediated apoptosis in ABCB1-overexpressing leukemic cells. As for ABCG2-overexpressing cells, effective ABCG2 inhibition and apoptosis enhancement were provided only by abemaciclib and ribociclib. In primary cells, ABCB1 activity and expression appeared to be more pronounced in patients positive for CD34.

GILTERITINIB & ITS ROLE IN AML

Gilteritinib is a drug, that has been used to treat AML for only a few years (approved by the FDA in 2018 [44] and by the EMA in 2019 [45]). Currently, it is indicated as monotherapy for refractory AML patients and those that have relapsed after receiving the induction therapy. At the moment, gilteritinib is indicated only for patients positive for FLT3 mutation [21]. It has been described as a potent and more selective FLT3 inhibitor than other agents targeting FLT3 (e.g., midostaurin). Despite having multiple targets, *FLT3*-ITD mutation is the primary target of both midostaurin and gilteritinib, and their efficacy in AML is tightly associated with this mutation. *FLT3*-ITD provides leukemic cells with proliferative advantage due to the constitutive activation of FLT3 signaling. Nevertheless, gilteritinib also inhibits FLT3-WT, which in non-mutated state controls cell proliferation and cell differentiation too. Although currently gilteritinib appears to be efficient in majority of AML cases, cells will eventually most likely develop some form of resistance that will help them avoid the drug.

Therefore, we exposed HL-60, leukemic cell line with FLT3-WT, to gilteritinib to uncover mechanisms leading to gilteritinib resistance that are, however, not dependent on FLT3

mutation. Long exposure to step-wise increasing concentration of gilteritinib led to eventual acquirement of resistance. Upon gilteritinib withdrawal, resistance started to slowly fade away and was entirely lost after 4 weeks of gilteritinib-free cell culture. So far, gilteritinib resistance has been associated mostly with mutations that emerged after gilteritinib treatment. Either additional mutations in *FLT3* (e.g., D835, Y842, F691L) or FLT3-unrelated mutations (e.g., *NRAS, KRAS, PTPN11, CBL*) were detected [152-155]. That was not the case in our gilteritinib-resistant HL-60 cells since mutations generally cause permanent changes in a cell and our cells became sensitive to gilteritinib after just several weeks. Nevertheless, a rather permanent resistance seems to be developing in a cell line currently being made resistant to gilteritinib in our lab. That is MV4-11, which carries *FLT3*-ITD mutation and so far, even after five weeks in gilteritinib-free cell culture, it appears to retain its original resistance (our not yet published data).

Gene and protein analysis of gilteritinib-sensitive HL-60 WT and gilteritinib-resistant HL-60 G75 revealed distinct profiles in both cell lines. Correlation analysis identified several deregulated genes and proteins involved in numerous pathways (immune response, cell-cell communication, metabolism, lysosomes) suggesting a complex cell adaptation to the presence of the drug. Gilteritinib-resistant cells had vastly deregulated immune response mediated by neutrophils. Many proteins involved in neutrophil degranulation were downregulated as well as those related to different granules. Neutrophils play a crucial role in regulation of immune and inflammatory responses during infectious and non-infectious diseases. In resting cells, different granules such as azurophil/primary, secondary, tertiary, or secretory vesicles store specific molecules (e.g., myeloperoxidase, cathepsins, lysozyme) responsible for the cell defense. Upon activation, content of the granules is released in a process called degranulation, which appears to be suppressed in gilteritinib-resistant cells [156, 157] as well as secretory granules, tertiary and azurophil granules, or more specifically their lumens. Besides, biological processes involved in secretion, regulated exocytosis and exocytosis were among the most downregulated ones proposing that resistant cells retain their contents, which can eventually lead to suppressed cell-cell communication and signal transduction.

Cell communication with other cells and extracellular matrix can be also associated with cell adhesion molecules, whose binding was downregulated in the resistant cells too. Adhesion molecules play a pivotal role not only in cell communication, but in many other cellular processes, including morphogenesis, differentiation, or signal transduction. In the generated

gilteritinib-resistant cells, predominantly binding of cadherins was detected as downregulated. Deregulation of cadherin-mediated cell-cell adhesion is typically observed in hematological cancers and its low expression has been found to promote cell growth [158]. E-cadherin is a well-known tumor suppressor and has been found reduced in leukemia due to abnormal hypermethylation [159]. Levels of cadherins, however, did not seem to be affected by long-term exposure to gilteritinib except for cadherin 24 (*CDH24*), which was upregulated on mRNA level. The *CDH24* gene did not translate to protein, which might implicate involvement of post-transcriptional regulatory units. Nevertheless, impairment of cadherins would favor the growth of resistant cells. Downregulation of calcium-dependent protein binding further supported this theory as cadherin binding is highly dependent on Ca^{2+}. Adhesion molecules typically bind to the actin cytoskeleton. More specifically, cadherins on the cell surface bind to catenins and actin filaments in cytosol. This process, however, appeared to be suppressed since a few catenins (*CTNNA1, CTNNAL1, CTNNBIP1*) were downregulated on mRNA level and actin filament binding was downregulated on both mRNA and protein level. Since actin filaments are essential for cellular movement and processes such as vesicle formation or organelle communication, the loss of cell communication appeared to be one of the most prominent features of the gilteritinib-resistant cells [160].

On the contrary, inflammation seemed to be enhanced, especially when it came to binding of pro-inflammatory eicosatetraenoic acid and eicosanoids, which can have pro- and anti-inflammatory roles. The precursor of these molecules is arachidonic acid, which together with eicosanoids belong to fatty acids [161, 162]. Binding of these fatty acids happened to be upregulated in cells resistant to gilteritinib. Similarly, S100A8 and S100A9 proteins, which participate in metabolism of arachidonic acid, were among the most upregulated ones. Highly expressed S100A8 and S100A9 proteins trigger RAGE- and TLR4-mediated inflammatory signaling [163, 164]. These calcium-binding proteins are usually constitutively expressed in myeloid cells and play roles not only in inflammatory response, but also differentiation, autophagy, or apoptosis [164, 165]. Altered expression of S100A8/S100A9 has been previously associated with drug resistance in AML [166, 167] and recently, it has been linked to gilteritinib resistance as well. In a study by Zavorka Thomas et al. [168], *FLT3*-ITD^{+} AML cells responded to gilteritinib by increased expression of S100A8/S100A9 and decreased Ca^{2+} levels. In this case, overexpression of S100A9 led to decreased cell sensitivity to gilteritinib, which we observed in our gilteritinib-resistant cells too. Moreover, this paper showed that increase of S100A9 expression directly resulted from the loss of BCL6, a transcriptional regulator, which

happened to be decreased on mRNA in our cells too [168]. These results in combination with ours suggest that BCL6-S100A9 regulation occurs not only in FLT3-mutated cells, but also in FLT3-WT cells, and therefore, do not strictly depend on the FLT3 mutation.

All these changes in the profile of gilteritinib-resistant cells propose a multifactorial mechanism of cellular adaptation to a stress stimulus in a form of exogenous drug. Cells are prevented from contacting their surroundings or other cells by suppressing any kind of binding or release of vesicles. Their movement seems to be impaired, while translational and ribosomal activity remain massively upregulated on mRNA level. All these processes have been previously observed in dedifferentiating *Dictyostelium* cells, which can reverse their development in only 24 h unlike mammalian cells [169]. Dedifferentiation is a transient process in which cells return to their earlier developmental stages, stem cells in our case. In earlier stages of development, cells have higher plasticity, rapidly regenerate, and adapt to various stress-induced stimuli or changes happening within a cell. Once all necessary adaptive mechanisms have been activated, cells can restart their differentiation but this time with lesser responsiveness to the present stimuli.

Although the resistance that HL-60 acquired to gilteritinib seemed to be a very complex set of molecular changes, we focused on the one that was detected among the most deregulated ones, yet not mentioned in the discussion so far - lysosomes. Not only has increase of lysosomal mass been observed in dedifferentiating cells before [170], it has been also widely associated with drug resistance [100]. As mentioned before, Zdzalik-Bielecka et al. recently implicated that gilteritinib might impair the endolysosomal system [103]. Therefore, we investigated whether long-term exposure to gilteritinib had any effect on lysosomal system in AML cells. Staining with lysosome-specific dye Lysotracker revealed increased fluorescence intensity and number of lysosomes in HL-60 G75 cells that were continuously cultured in gilteritinib-containing culture medium. Once the cells were deprived of gilteritinib, lysosomal number as well as intensity of their fluorescence decreased and resembled Lysotracker staining of gilteritinib-sensitive HL-60 WT. Moreover, it did not matter whether the cells were deprived of gilteritinib for just a day or for a week. Therefore, the observed changes in lysosomes had to be quick and most likely happening within 24 h. Firstly, we looked more into Lysotracker itself, since it is a pH-dependent dye meaning its accumulation within lysosomes is greatly reliant on pH. Lysotracker enters lysosomes, and thereby exhibits fluorescence only when lysosomes are acidic. To verify that lysosomal pH did not cause the changes in Lysotracker staining, we

stained cells with FITC-dextran, which enters acidic organelles independently of pH. Dextran colocalized with Lysotracker in lysosomes and while Lysotracker fluorescence differed among cell lines, dextran appeared to exhibit similar level of fluorescence in all of them. Direct detection of lysosomal pH confirmed that pH was not affected by gilteritinib presence or its withdrawal. Thereby, pH alteration was excluded. Another rapid mechanism that could lead to altered accumulation of Lysotracker is pharmacokinetic interaction with ABCB1 transporter, which is expressed on the lysosomal membrane [171, 172]. Lysotracker has been described as ABCB1 substrate [173], and thereby could be actively pumped out of the cell. Moreover, gilteritinib as identified ABCB1 inhibitor (data not shown) could contribute to higher Lysotracker accumulation in gilteritinib-resistant cells. However, HL-60 typically do not express ABCB1, and its mRNA expression was not detected in our gilteritinib-sensitive or gilteritinib-resistant cells either (data not shown).

Lysosomes are acidic organelles which can contribute to drug resistance through a process called lysosomal sequestration. They are capable of accumulating weak base drugs, hence, prevent them from reaching their targets. Gilteritinib meets the criteria of such drug, and therefore, might be susceptible to lysosomal sequestration. Since gilteritinib is not fluorescent, it could not be used in the microscopy study. Instead, sunitinib was selected to investigate sequestering capacity of lysosomes. Sunitinib is a TKi and FLT3i just like gilteritinib and the resistance to sunitinib is known to be mediated by lysosomes. Moreover, the gilteritinib-resistant cells revealed similar level of resistance to sunitinib as to gilteritinib proposing possible involvement of lysosomes. Gilteritinib-resistant cells were capable of sequestering all sunitinib within their lysosomes, which multiplied in number. Once cultured in gilteritinib-free culture medium for a day or a week, lysosomal mass decreased. Sunitinib could be found in residual lysosomes present in these cells, but most of it was spread in cytosol. This indicated insufficient number of lysosomes in the cells, which seemed to be directly correlated to the presence of gilteritinib. We can speculate that lysosomal biogenesis might be affected by gilteritinib since the more lysosomes, the higher intrinsic resistance to the drug. However, activation of lysosomal biogenesis is dependent on phosphorylation and dephosphorylation of two key elements, transcription factor EB (TFEB) and mammalian target of rapamycin complex 1 (mTORC1). Whether activated or inactivated forms of these proteins are present would have to be tested using phosphoproteomics or western blotting. Nonetheless, phosphorylation can be a very quick process, which would coincide with the rapidly occurring changes in our cells. TFEB is translocated into nucleus upon its dephosphorylation by mTORC1

[174]. Gilteritinib could be potentially blocking phosphorylation of TFEB or affect mTORC1 directly. Moreover, mTORC1 responds to stress stimuli such as deprivation of amino acids or alteration of energy availability [175], both processes observed in transcriptome and proteome analysis. Furthermore, overexpression of TFEB has been found to upregulate the genes encoding lysosomal enzymes [176, 177]. We, however, observed a completely opposite regulation with TFEB and lysosomal enzymes such as CTSD, CTSG, or HEXB being downregulated. Release of cathepsins, mainly CTSD, generally leads to cell death. When examining apoptosis after cell exposure to gilteritinib, gilteritinib-sensitive and gilteritinib-resistant cells responded similarly and induced apoptosis only in high gilteritinib concentrations (10 µM) after longer drug exposure (48 h). In the study by Qiao et al. [178], it has been described that gilteritinib concentration relies greatly on the presence of *FLT3*-ITD mutation. Gilteritinib has been developed to target mainly *FLT3*-ITD$^+$ cells, therefore, as low as 12.5 nM concentration was sufficient to induce apoptosis in these cells after 24 h exposure. On the other hand, 24 h exposure of FLT3-WT to 4 µM gilteritinib was not high enough to induce apoptosis. Another study conducted by Hu et al. [179] detected higher sensibility of *FLT3*-ITD$^+$ AML cells to gilteritinib than FLT3-WT, when gilteritinib concentrations up to 20 nM led to significant decrease in cell viability. Same concentrations, however, had no effect on viability of FLT3-WT cells.

In summary, resistance of HL-60 cells to gilteritinib was mediated by modulation of multiple cellular processes. The resistance was only temporary and completely reversed upon gilteritinib withdrawal. Lysosomes appeared to be a key component involved in the gilteritinib resistance. Whether gilteritinib sequestered in lysosomes was not determined, however, its presence seemed to significantly upregulate biogenesis and/or activity of lysosomes. The exact mechanism leading to this upregulation will have to be further investigated.

8 CONCLUSIONS

AML is a malignant blood cancer known for its substantial inter- and intra-patient heterogeneity, poor therapy outcomes and high rate of relapses. The main reason for therapy failure is the presence of highly resistant leukemic clones at diagnosis and rapid cell adaptation when encountering a threat, which is chemotherapy in this case. Resistant leukemic clones evade the induction therapy and continue to drive the disease. One way to identify these clones is characterization of their cellular features and respective regulatory units. Here, we report that ABCB1 transporter contributes to the resistance via disabling the transport of chemotherapy into target cells and is directly regulated by miR-9 on post-transcriptional level. Extensive ABCB1 presence and lowly expressed miR-9 at diagnosis were associated with resistant CD34 phenotype and inability of patients to achieve CR. Blockage of ABCB1, however, exposed cells to elevated anthracyclines concentrations. Factors such as these are crucial in treatment decision-making and can help to tailor the therapy based on individual patient needs. The heterogeneity of AML patients is the reason why personalized medicine has come to the forefront in the recent years and is believed to tip the scales in favor of improved treatment outcomes.

Leukemic cells can, however, develop resistance even during the ongoing treatment. Therefore, it is important to track these cells and uncover the mechanisms they utilize to change their behavior. Here, we studied leukemic cells with acquired resistance to gilteritinib, one of the targeted agents used in AML. Transcriptomic and proteomic changes revealed a multifactorial adaptation of cells with some processes more deregulated than others, lysosomal activity being one of them. Due to the well-known rapid evolution of resistance in AML, identification of resistance-driving mechanisms is vital to either prevent it from happening or to provide a lead for future drug development. Collectively, our findings provide new insights into the mechanisms contributing to drug resistance in AML and potential therapeutic ways to counteract it.

9 LIST OF PUBLICATIONS RELATED TO THE DOCTORAL THESIS TOPIC

- **Sucha, S.**, V. Palande, M. Vajrychova, J. Skoda, M. Svoren, F. Ahmed, B. Visek and M. Ceckova (2023). "Transcriptome and proteome profile of gilteritinib-resistant HL-60 cells." - in preparation

  Candidate's contribution:
  - Performing experiments, specifically:
    - Cell culture of HL-60 cells
    - Proliferation assays (MTT)
    - Isolation of PBMC from AML patients
    - RNA isolation
    - Expression analysis by qRT-PCR
  - Partly involved in RNA-seq and proteomics analysis
  - Visualization of RNA-seq and proteomics data
  - Interpretation of results, writing of the manuscript and revising the publication

- **Sucha, S.**, V. Palande, M. Vajrychova, M. Machacek, J. Skoda, M. Svoren, J. Cloos, G. Jansen, B. Visek and M. Ceckova (2023). "Gilteritinib-resistant HL-60 show impaired lysosomal enzymatic function but high sequestering capacity." - in preparation

  Candidate's contribution:
  - Performing experiments, specifically:
    - Cell culture of HL-60 cells
    - Proliferation assays (MTT)
    - Flow cytometry analysis
    - Microscopy studies
    - Isolation of PBMC from AML patients
    - RNA isolation
    - Expression analysis by qRT-PCR
  - Partly involved in RNA-seq and proteomics analysis
  - Visualization of RNA-seq and proteomics data
  - Interpretation of results, writing of the manuscript and revising the publication

- **Sucha, S.**, A. Sorf, M. Svoren, D. Vagiannis, F. Ahmed, B. Visek and M. Ceckova (2022). "ABCB1 as a potential beneficial target of midostaurin in acute myeloid leukemia." *Biomed Pharmacother* 150: 112962. **(IF 2021 = 7.419, Q1; AIS 2021 = 0.906, Q2)**

  Candidate's contribution:
  - Performing experiments, specifically:
    - Isolation of PBMC from AML patients
    - RNA isolation
    - Expression analysis by ddPCR
    - Cell culture of HL-60 cells
    - Accumulation assays in PBMC & HL-60
    - Assessment of subG1 fraction in HL-60
  - Data analysis, interpretation of results, visualization
  - Writing of the manuscript and revising the publication

- Sorf, A., **S. Sucha**, A. Morell, E. Novotna, F. Staud, A. Zavrelova, B. Visek, V. Wsol and M. Ceckova (2020). "Targeting Pharmacokinetic Drug Resistance in Acute Myeloid Leukemia Cells with CDK4/6 Inhibitors." *Cancers (Basel)* 12(6). **(IF 2020 = 6.639, Q1; AIS 2020 = 1.323, Q1)**

  Candidate's contribution:
  - Performing experiments, specifically:
    - Cell culture of HL-60 cells
    - Contributed to annexin V/PI apoptosis assays in HL-60
    - Assessment of subG1 fraction in HL-60
    - Isolation of PBMC from AML patients
    - Contributed to RNA isolation & expression analysis by qRT-PCR
    - Contributed to accumulation assays & annexin V/PI apoptosis assays in PBMC
  - Data analysis, visualization, writing respective parts of the manuscript and revising the publication

10 LIST OF OTHER INPUTS OF THE CANDIDATE

10.1 Other publications not related to the doctoral thesis topic

- Sorf, A., K. Nalevkova, S. Dudicova, **S. Sucha**, B. Visek and M. Ceckova (2022). "FLT3-mutated AML is linked to decreased expression and function of cytarabine carrier OCTN1." - in preparation

- Tupova, L., B. Hirschmugl, **S. Sucha**, V. Pilarova, V. Szekely, E. Bakos, L. Novakova, C. Ozvegy-Laczka, C. Wadsack and M. Ceckova (2020). "Interplay of drug transporters P-glycoprotein (MDR1), MRP1, OATP1A2 and OATP1B3 in passage of maraviroc across human placenta." *Biomed Pharmacother* 129: 110506. **(IF 2020 = 6.530, Q1; AIS 2020 = 0.936, Q2)**

- Hofman, J., A. Sorf, D. Vagiannis, **S. Sucha**, S. Kammerer, J. H. Kupper, S. Chen, L. Guo, M. Ceckova and F. Staud (2019). "Brivanib Exhibits Potential for Pharmacokinetic Drug-Drug Interactions and the Modulation of Multidrug Resistance through the Inhibition of Human ABCG2 Drug Efflux Transporter and CYP450 Biotransformation Enzymes." *Mol Pharm* 16(11): 4436-4450. **(IF 2019 = 3.664, Q1; AIS 2019 = 1.126, Q1)**

- Hofman, J., A. Sorf, D. Vagiannis, **S. Sucha**, E. Novotna, S. Kammerer, J. H. Kupper, M. Ceckova and F. Staud (2019). "Interactions of Alectinib with Human ATP-Binding Cassette Drug Efflux Transporters and Cytochrome P450 Biotransformation Enzymes: Effect on Pharmacokinetic Multidrug Resistance." *Drug Metab Dispos* 47(7): 699-709. **(IF 2019 = 3.231, Q1; AIS 2019 = 0.866, Q2)**

10.2 Oral presentations

- 13th Postgraduate and Postdoc Conference, Hradec Kralove, Czech Republic: „Gilteritinib resistance in acute myeloid leukemia" (Feb 2023)
- 26th Interdisciplinary Toxicology Conference, Stara Lesna, Slovakia: "ABCB1-resistant phenotype in acute myeloid leukemia" (Sep 2021)
- 11th Postgraduate and Postdoc Conference, Hradec Kralove, Czech Republic: "Role of ABCB1 transporter in drug sensitivity of acute myeloid leukemia" (Jan 2021)

- 10th Postgraduate and Postdoc Conference, Hradec Kralove, Czech Republic**:** "Midostaurin as a novel modulator of ABC transporters in acute myeloid leukemia" (Jan 2020)

10.3 Poster presentations

- ESCCA 2022, Belfast, Northern Ireland: "ABCB1 as a target of midostaurin in acute myeloid leukemia" (Sep 2022)
- 69th Pharmacological days, Prague, Czech Republic: "Midostaurin inhibits ABCB1 and ABCG2 and enhances daunorubicin and mitoxantrone induced apoptosis of AML cells" (Sep 2019)

11 LIST OF ABBREVIATIONS

ABB   annexin-binding buffer

ABC   ATP-binding cassette

AML   acute myeloid leukemia

AUC   area under the curve

CDK   cyclin-dependent kinase

CDKi   cyclin-dependent kinase inhibitors

CI   confidence interval

CPM   count per million

CR   complete remission

DAU   daunorubicin

ddPCR   droplet digital PCR

DEG   differentially expressed gene

DEP   differentially expressed protein

DMSO   dimethylsulfoxide

ELN   the European LeukemiaNet classification

ER   endoplasmic reticulum

ex./em.   excitation/emission

FAB   the French-American-British classification

FBS   fetal bovine serum

FC   fold change

FDR   false discovery rate

FLT3   fms-like tyrosine kinase 3

FLT3i   fms-like tyrosine kinase 3 inhibitors

GIL	gilteritinib
GO	Gene Ontology
HCT	hematopoietic cell transplantation
IDAC	intermediate-dose cytarabine
IDH1/2	isocitrate dehydrogenase 1/2
ITD	internal tandem duplication
IW	isolation window
KEGG	Kyoto Encyclopedia of Genes and Genomes
LSC	leukemic stem cells
LY	LY335979
MFI	mean fluorescence intensity
miR/miRNA	microRNA
MIT	mitoxantrone
MMTS	methyl methanethiosulfonate
MRD	measurable (minimal) residual disease
mTORC1	mammalian target of rapamycin complex 1
MTT	3-(4,5-dimethylthiazol-2-yl)-2,5-diphenyltetrazolium bromide
NCE	normalized collision energy
NPM1	nucleophosmin 1
PBMC	peripheral blood mononuclear cells
PBS	phosphate-buffered saline
PI	propidium iodide
RF	resistance factor
RIN	RNA Integrity Number

RPMI	Roswell Park Memorial Institute culture medium
R/R	relapsed/refractory
SDC	sodium deoxycholate
TCEP	tris(2-carboxyethyl)phosphine hydrochloride
TEAB	triethylamonium bicarbonate
TFEB	transcription factor EB
TKD	tyrosine kinase domain
TKi	tyrosine kinase inhibitor
w/o	without
WT	wild-type

12 REFERENCES

1.	Jagannathan-Bogdan, M. and L.I. Zon, *Hematopoiesis*. Development, 2013. **140**(12): p. 2463-7.

2.	Laurenti, E. and B. Gottgens, *From haematopoietic stem cells to complex differentiation landscapes*. Nature, 2018. **553**(7689): p. 418-426.

3.	Vakiti, A. and P. Mewawalla, *Acute Myeloid Leukemia*, in *StatPearls*. 2022: Treasure Island (FL).

4.	Siegel, R.L., et al., *Cancer statistics, 2022*. CA Cancer J Clin, 2022. **72**(1): p. 7-33.

5.	SEER, N.C.I. *Cancer Stat Facts: Leukemia - Acute Myeloid Leukemia (AML)*. Nov 16, 2022]; Available from: https://seer.cancer.gov/statfacts/html/amyl.html.

6.	Schiffer, C.A. and S. Gurbuxani, *Clinical manifestations, pathologic features, and diagnosis of acute myeloid leukemia*, ed. R.A. Larson and A.G. Rosmarin. 2022: UpToDate, Waltham, MA.

7.	Arber, D.A., et al., *The 2016 revision to the World Health Organization classification of myeloid neoplasms and acute leukemia*. Blood, 2016. **127**(20): p. 2391-405.

8.	Dohner, H., et al., *Diagnosis and management of AML in adults: 2022 recommendations from an international expert panel on behalf of the ELN*. Blood, 2022. **140**(12): p. 1345-1377.

9.	Dix, C., et al., *Measurable Residual Disease in Acute Myeloid Leukemia Using Flow Cytometry: A Review of Where We Are and Where We Are Going*. J Clin Med, 2020. **9**(6).

10.	Zeijlemaker, W., et al., *CD34(+)CD38(-) leukemic stem cell frequency to predict outcome in acute myeloid leukemia*. Leukemia, 2019. **33**(5): p. 1102-1112.

11.	Zeijlemaker, W. and G.J. Schuurhuis, *Minimal Residual Disease and Leukemic Stem Cells in Acute Myeloid Leukemia*. 2013: IntechOpen.

12.	Mrózek, K. and C.D. Bloomfield, *Chromosome Abnormalities in Acute Myeloid Leukaemia and Their Clinical Importance*. Chromosomal Translocations and Genome Rearrangements in Cancer, ed. J. Rowley, M. Le Beau, and T. Rabbitts. 2015: Springer.

13.	Padmakumar, D., et al., *A concise review on the molecular genetics of acute myeloid leukemia*. Leuk Res, 2021. **111**: p. 106727.

14.	DiNardo, C.D. and J.E. Cortes, *Mutations in AML: prognostic and therapeutic implications*. Hematology Am Soc Hematol Educ Program, 2016. **2016**(1): p. 348-355.

15. Grimwade, D., A. Ivey, and B.J. Huntly, *Molecular landscape of acute myeloid leukemia in younger adults and its clinical relevance.* Blood, 2016. **127**(1): p. 29-41.

16. Dombret, H. and C. Gardin, *An update of current treatments for adult acute myeloid leukemia.* Blood, 2016. **127**(1): p. 53-61.

17. Stone, R.M., et al., *Midostaurin plus Chemotherapy for Acute Myeloid Leukemia with a FLT3 Mutation.* N Engl J Med, 2017. **377**(5): p. 454-464.

18. Castaigne, S., et al., *Effect of gemtuzumab ozogamicin on survival of adult patients with de-novo acute myeloid leukaemia (ALFA-0701): a randomised, open-label, phase 3 study.* Lancet, 2012. **379**(9825): p. 1508-16.

19. Jen, E.Y., et al., *FDA Approval: Gemtuzumab Ozogamicin for the Treatment of Adults with Newly Diagnosed CD33-Positive Acute Myeloid Leukemia.* Clin Cancer Res, 2018. **24**(14): p. 3242-3246.

20. Society, T.A.C. *Typical Treatment of Acute Myeloid Leukemia (Except APL).* Nov 29, 2022]; Available from: https://www.cancer.org/cancer/acute-myeloid-leukemia/treating/typical-treatment-of-aml.html.

21. Perl, A.E., et al., *Gilteritinib or Chemotherapy for Relapsed or Refractory FLT3-Mutated AML.* N Engl J Med, 2019. **381**(18): p. 1728-1740.

22. Montesinos, P., et al., *Ivosidenib and Azacitidine in IDH1-Mutated Acute Myeloid Leukemia.* N Engl J Med, 2022. **386**(16): p. 1519-1531.

23. Stein, E.M., et al., *Enasidenib in mutant IDH2 relapsed or refractory acute myeloid leukemia.* Blood, 2017. **130**(6): p. 722-731.

24. Niederwieser, D., et al., *One and a half million hematopoietic stem cell transplants: continuous and differential improvement in worldwide access with the use of non-identical family donors.* Haematologica, 2022. **107**(5): p. 1045-1053.

25. Society, T.A.C. *If Acute Myeloid Leukemia (AML) Doesn't Respond or Comes Back After Treatment.* Nov 29, 2022]; Available from: https://www.cancer.org/cancer/acute-myeloid-leukemia/treating/recurrence.html.

26. Baudino, T.A., *Targeted Cancer Therapy: The Next Generation of Cancer Treatment.* Curr Drug Discov Technol, 2015. **12**(1): p. 3-20.

27. Kazi, J.U. and L. Ronnstrand, *FMS-like Tyrosine Kinase 3/FLT3: From Basic Science to Clinical Implications.* Physiol Rev, 2019. **99**(3): p. 1433-1466.

28. Gilliland, D.G. and J.D. Griffin, *The roles of FLT3 in hematopoiesis and leukemia.* Blood, 2002. **100**(5): p. 1532-42.

29. Grafone, T., et al., *An overview on the role of FLT3-tyrosine kinase receptor in acute myeloid leukemia: biology and treatment.* Oncol Rev, 2012. **6**(1): p. e8.

30. Kottaridis, P.D., R.E. Gale, and D.C. Linch, *Flt3 mutations and leukaemia.* Br J Haematol, 2003. **122**(4): p. 523-38.

31. Daver, N., et al., *Targeting FLT3 mutations in AML: review of current knowledge and evidence.* Leukemia, 2019. **33**(2): p. 299-312.

32. Kennedy, V.E. and C.C. Smith, *FLT3 Mutations in Acute Myeloid Leukemia: Key Concepts and Emerging Controversies.* Front Oncol, 2020. **10**: p. 612880.

33. Tao, S., et al., *Prognosis and outcome of patients with acute myeloid leukemia based on FLT3-ITD mutation with or without additional abnormal cytogenetics.* Oncol Lett, 2019. **18**(6): p. 6766-6774.

34. Borlenghi, E., et al., *Prognostic Relevance of NPM1 and FLT3 Mutations in Acute Myeloid Leukaemia, Longterm Follow-Up-A Single Center Experience.* Cancers (Basel), 2022. **14**(19).

35. Sakaguchi, M., et al., *Significance of FLT3-tyrosine kinase domain mutation as a prognostic factor for acute myeloid leukemia.* Int J Hematol, 2019. **110**(5): p. 566-574.

36. Boddu, P., et al., *Co-occurrence of FLT3-TKD and NPM1 mutations defines a highly favorable prognostic AML group.* Blood Adv, 2017. **1**(19): p. 1546-1550.

37. Juliusson, G., et al., *The prognostic impact of FLT3-ITD and NPM1 mutation in adult AML is age-dependent in the population-based setting.* Blood Adv, 2020. **4**(6): p. 1094-1101.

38. Wagner, K., et al., *FLT3-internal tandem duplication and age are the major prognostic factors in patients with relapsed acute myeloid leukemia with normal karyotype.* Haematologica, 2011. **96**(5): p. 681-6.

39. Dohner, K., et al., *Impact of NPM1/FLT3-ITD genotypes defined by the 2017 European LeukemiaNet in patients with acute myeloid leukemia.* Blood, 2020. **135**(5): p. 371-380.

40. Daver, N., S. Venugopal, and F. Ravandi, *FLT3 mutated acute myeloid leukemia: 2021 treatment algorithm.* Blood Cancer J, 2021. **11**(5): p. 104.

41. Stein, E.M. and M.S. Tallman, *Emerging therapeutic drugs for AML.* Blood, 2016. **127**(1): p. 71-8.

42. Yu, J., et al., *Advances in targeted therapy for acute myeloid leukemia.* Biomark Res, 2020. **8**: p. 17.

43.   Stone, R.M., et al., *Midostaurin: its odyssey from discovery to approval for treating acute myeloid leukemia and advanced systemic mastocytosis.* Blood Adv, 2018. **2**(4): p. 444-453.

44.   FDA. *FDA approves gilteritinib for relapsed or refractory acute myeloid leukemia (AML) with a FLT3 mutatation.* 2018   Jan 10, 2023]; Available from: https://www.fda.gov/drugs/fda-approves-gilteritinib-relapsed-or-refractory-acute-myeloid-leukemia-aml-flt3-mutatation.

45.   EMA.   *Xospata.*   Jan   10,   2023];   Available   from: https://www.ema.europa.eu/en/medicines/human/EPAR/xospata.

46.   Ding, L., et al., *The Roles of Cyclin-Dependent Kinases in Cell-Cycle Progression and Therapeutic Strategies in Human Breast Cancer.* Int J Mol Sci, 2020. **21**(6).

47.   Malumbres, M. and M. Barbacid, *Cell cycle, CDKs and cancer: a changing paradigm.* Nat Rev Cancer, 2009. **9**(3): p. 153-66.

48.   Nanolive. *High-resolution time-lapse imaging of cell response to CDK2-inhibition.* Dec 19, 2022]; Available from: https://www.nanolive.ch/high-resolution-cdk2-inhibition/.

49.   Vermeulen, K., D.R. Van Bockstaele, and Z.N. Berneman, *The cell cycle: a review of regulation, deregulation and therapeutic targets in cancer.* Cell Prolif, 2003. **36**(3): p. 131-49.

50.   Baker, S.J., et al., *CDK4: a master regulator of the cell cycle and its role in cancer.* Genes Cancer, 2022. **13**: p. 21-45.

51.   Beaver, J.A., et al., *FDA Approval: Palbociclib for the Treatment of Postmenopausal Patients with Estrogen Receptor-Positive, HER2-Negative Metastatic Breast Cancer.* Clin Cancer Res, 2015. **21**(21): p. 4760-6.

52.   Dhillon, S., *Palbociclib: first global approval.* Drugs, 2015. **75**(5): p. 543-51.

53.   Kim, E.S., *Abemaciclib: First Global Approval.* Drugs, 2017. **77**(18): p. 2063-2070.

54.   Syed, Y.Y., *Ribociclib: First Global Approval.* Drugs, 2017. **77**(7): p. 799-807.

55.   Richter, A., et al., *Cyclin-Dependent Kinase Inhibitors in Hematological Malignancies-Current Understanding, (Pre-)Clinical Application and Promising Approaches.* Cancers (Basel), 2021. **13**(10).

56.   Lopez, S., et al., *An essential pathway links FLT3-ITD, HCK and CDK6 in acute myeloid leukemia.* Oncotarget, 2016. **7**(32): p. 51163-51173.

57.   Uras, I.Z., V. Sexl, and K. Kollmann, *CDK6 Inhibition: A Novel Approach in AML Management.* Int J Mol Sci, 2020. **21**(7).

58. Wang, L., et al., *Pharmacologic inhibition of CDK4/6: mechanistic evidence for selective activity or acquired resistance in acute myeloid leukemia.* Blood, 2007. **110**(6): p. 2075-83.

59. Lee, D.J. and J.F. Zeidner, *Cyclin-dependent kinase (CDK) 9 and 4/6 inhibitors in acute myeloid leukemia (AML): a promising therapeutic approach.* Expert Opin Investig Drugs, 2019. **28**(11): p. 989-1001.

60. Rees, D.C., E. Johnson, and O. Lewinson, *ABC transporters: the power to change.* Nat Rev Mol Cell Biol, 2009. **10**(3): p. 218-27.

61. Chai, S., K.K. To, and G. Lin, *Circumvention of multi-drug resistance of cancer cells by Chinese herbal medicines.* Chin Med, 2010. **5**: p. 26.

62. Dietrich, C.G., A. Geier, and R.P. Oude Elferink, *ABC of oral bioavailability: transporters as gatekeepers in the gut.* Gut, 2003. **52**(12): p. 1788-95.

63. International Transporter, C., et al., *Membrane transporters in drug development.* Nat Rev Drug Discov, 2010. **9**(3): p. 215-36.

64. Vasiliou, V., K. Vasiliou, and D.W. Nebert, *Human ATP-binding cassette (ABC) transporter family.* Hum Genomics, 2009. **3**(3): p. 281-90.

65. Pilotto Heming, C., et al., *P-glycoprotein and cancer: what do we currently know?* Heliyon, 2022. **8**(10): p. e11171.

66. Vasconcelos, F.C., et al., *Update on drug transporter proteins in acute myeloid leukemia: Pathological implication and clinical setting.* Crit Rev Oncol Hematol, 2021. **160**: p. 103281.

67. Leonard, G.D., T. Fojo, and S.E. Bates, *The role of ABC transporters in clinical practice.* Oncologist, 2003. **8**(5): p. 411-24.

68. Hirsch, P., et al., *Prognostic impact of high ABC transporter activity in 111 adult acute myeloid leukemia patients with normal cytogenetics when compared to FLT3, NPM1, CEBPA and BAALC.* Haematologica, 2012. **97**(2): p. 241-5.

69. Legrand, O., et al., *Pgp and MRP activities using calcein-AM are prognostic factors in adult acute myeloid leukemia patients.* Blood, 1998. **91**(12): p. 4480-8.

70. Leith, C.P., et al., *Acute myeloid leukemia in the elderly: assessment of multidrug resistance (MDR1) and cytogenetics distinguishes biologic subgroups with remarkably distinct responses to standard chemotherapy. A Southwest Oncology Group study.* Blood, 1997. **89**(9): p. 3323-9.

71.	Marzac, C., et al., *ATP Binding Cassette transporters associated with chemoresistance: transcriptional profiling in extreme cohorts and their prognostic impact in a cohort of 281 acute myeloid leukemia patients.* Haematologica, 2011. **96**(9): p. 1293-301.

72.	Boyer, T., et al., *Clinical Significance of ABCB1 in Acute Myeloid Leukemia: A Comprehensive Study.* Cancers (Basel), 2019. **11**(9).

73.	da Silveira Junior, L.S., et al., *P-glycoprotein and multidrug resistance-associated protein-1 expression in acute myeloid leukemia: Biological and prognosis implications.* Int J Lab Hematol, 2020. **42**(5): p. 594-603.

74.	Sourdeau, E., et al., *Clinical and biological impact of ATP-binding cassette transporter activity in adult acute myeloid leukemia.* Haematologica, 2022.

75.	Buhagiar, A., J. Borg, and D. Ayers, *Overview of current microRNA biomarker signatures as potential diagnostic tools for leukaemic conditions.* Noncoding RNA Res, 2020. **5**(1): p. 22-26.

76.	To, K.K., *MicroRNA: a prognostic biomarker and a possible druggable target for circumventing multidrug resistance in cancer chemotherapy.* J Biomed Sci, 2013. **20**(1): p. 99.

77.	Toscano-Garibay, J.D. and G. Aquino-Jarquin, *Regulation exerted by miRNAs in the promoter and UTR sequences: MDR1/P-gp expression as a particular case.* DNA Cell Biol, 2012. **31**(8): p. 1358-64.

78.	Bartel, D.P., *MicroRNAs: target recognition and regulatory functions.* Cell, 2009. **136**(2): p. 215-33.

79.	Ling, H., M. Fabbri, and G.A. Calin, *MicroRNAs and other non-coding RNAs as targets for anticancer drug development.* Nat Rev Drug Discov, 2013. **12**(11): p. 847-65.

80.	Feng, D.D., et al., *Down-regulated miR-331-5p and miR-27a are associated with chemotherapy resistance and relapse in leukaemia.* J Cell Mol Med, 2011. **15**(10): p. 2164-75.

81.	Li, Y., et al., *miR-9 regulates the multidrug resistance of chronic myelogenous leukemia by targeting ABCB1.* Oncol Rep, 2017. **37**(4): p. 2193-2200.

82.	Liu, Y., et al., *miR-9 Enhances the Chemosensitivity of AML Cells to Daunorubicin by Targeting the EIF5A2/MCL-1 Axis.* Int J Biol Sci, 2019. **15**(3): p. 579-586.

83.	Haenisch, S., A.N. Werk, and I. Cascorbi, *MicroRNAs and their relevance to ABC transporters.* Br J Clin Pharmacol, 2014. **77**(4): p. 587-96.

84.   van den Heuvel-Eibrink, M.M., et al., *CD34-related coexpression of MDR1 and BCRP indicates a clinically resistant phenotype in patients with acute myeloid leukemia (AML) of older age.* Ann Hematol, 2007. **86**(5): p. 329-37.

85.   Chauhan, P.S., et al., *Expression of genes related to multiple drug resistance and apoptosis in acute leukemia: response to induction chemotherapy.* Exp Mol Pathol, 2012. **92**(1): p. 44-9.

86.   Damiani, D., et al., *The prognostic value of P-glycoprotein (ABCB) and breast cancer resistance protein (ABCG2) in adults with de novo acute myeloid leukemia with normal karyotype.* Haematologica, 2006. **91**(6): p. 825-8.

87.   Steinbach, D., et al., *BCRP gene expression is associated with a poor response to remission induction therapy in childhood acute myeloid leukemia.* Leukemia, 2002. **16**(8): p. 1443-7.

88.   Bartholomae, S., et al., *Coexpression of Multiple ABC-Transporters is Strongly Associated with Treatment Response in Childhood Acute Myeloid Leukemia.* Pediatr Blood Cancer, 2016. **63**(2): p. 242-7.

89.   Raaijmakers, M.H., et al., *Breast cancer resistance protein in drug resistance of primitive CD34+38- cells in acute myeloid leukemia.* Clin Cancer Res, 2005. **11**(6): p. 2436-44.

90.   Ho, M.M., D.E. Hogge, and V. Ling, *MDR1 and BCRP1 expression in leukemic progenitors correlates with chemotherapy response in acute myeloid leukemia.* Exp Hematol, 2008. **36**(4): p. 433-42.

91.   Paprocka, M., et al., *MRP1 protein expression in leukemic stem cells as a negative prognostic marker in acute myeloid leukemia patients.* Eur J Haematol, 2017. **99**(5): p. 415-422.

92.   Benderra, Z., et al., *Breast cancer resistance protein and P-glycoprotein in 149 adult acute myeloid leukemias.* Clin Cancer Res, 2004. **10**(23): p. 7896-902.

93.   Liu, B., et al., *Co-expression of ATP binding cassette transporters is associated with poor prognosis in acute myeloid leukemia.* Oncol Lett, 2018. **15**(5): p. 6671-6677.

94.   Xu, H. and D. Ren, *Lysosomal physiology.* Annu Rev Physiol, 2015. **77**: p. 57-80.

95.   Yang, C. and X. Wang, *Lysosome biogenesis: Regulation and functions.* J Cell Biol, 2021. **220**(6).

96.   Cuesta-Casanovas, L., et al., *Lysosome-mediated chemoresistance in acute myeloid leukemia.* Cancer Drug Resist, 2022. **5**(1): p. 233-244.

97. Rafiq, S., et al., *Lysosomes in acute myeloid leukemia: potential therapeutic targets?* Leukemia, 2021. **35**(10): p. 2759-2770.

98. ZerialLab. *Biogenesis of Early Endosomes*. Dec 19, 2022]; Available from: https://zeriallab.org/biogenesis-of-early-endosomes/.

99. Halaby, R., *Influence of lysosomal sequestration on multidrug resistance in cancer cells.* Cancer Drug Resist, 2019. **2**(1): p. 31-42.

100. Zhitomirsky, B. and Y.G. Assaraf, *Lysosomes as mediators of drug resistance in cancer.* Drug Resist Updat, 2016. **24**: p. 23-33.

101. Zhai, X. and Y. El Hiani, *Getting Lost in the Cell-Lysosomal Entrapment of Chemotherapeutics.* Cancers (Basel), 2020. **12**(12).

102. Zhitomirsky, B. and Y.G. Assaraf, *Lysosomal sequestration of hydrophobic weak base chemotherapeutics triggers lysosomal biogenesis and lysosome-dependent cancer multidrug resistance.* Oncotarget, 2015. **6**(2): p. 1143-56.

103. Zdzalik-Bielecka, D., et al., *Bemcentinib and Gilteritinib Inhibit Cell Growth and Impair the Endo-Lysosomal and Autophagy Systems in an AXL-Independent Manner.* Mol Cancer Res, 2022. **20**(3): p. 446-455.

104. Schmitt, M.V., et al., *Quantitation of Lysosomal Trapping of Basic Lipophilic Compounds Using In Vitro Assays and In Silico Predictions Based on the Determination of the Full pH Profile of the Endo-/Lysosomal System in Rat Hepatocytes.* Drug Metab Dispos, 2019. **47**(1): p. 49-57.

105. Sorf, A., et al., *Targeting Pharmacokinetic Drug Resistance in Acute Myeloid Leukemia Cells with CDK4/6 Inhibitors.* Cancers (Basel), 2020. **12**(6).

106. Sucha, S., et al., *ABCB1 as a potential beneficial target of midostaurin in acute myeloid leukemia.* Biomed Pharmacother, 2022. **150**: p. 112962.

107. Xie, F., et al., *miRDeepFinder: a miRNA analysis tool for deep sequencing of plant small RNAs.* Plant Mol Biol, 2012.

108. Vandesompele, J., et al., *Accurate normalization of real-time quantitative RT-PCR data by geometric averaging of multiple internal control genes.* Genome Biol, 2002. **3**(7): p. RESEARCH0034.

109. van Meerloo, J., G.J. Kaspers, and J. Cloos, *Cell sensitivity assays: the MTT assay.* Methods Mol Biol, 2011. **731**: p. 237-45.

110. Bioinformatics, B. *FastQC*. Dec 27, 2022]; Available from: https://www.bioinformatics.babraham.ac.uk/projects/fastqc/.

111. Dobin, A., et al., *STAR: ultrafast universal RNA-seq aligner.* Bioinformatics, 2013. **29**(1): p. 15-21.

112. Frankish, A., et al., *Gencode 2021.* Nucleic Acids Res, 2021. **49**(D1): p. D916-D923.

113. Liao, Y., G.K. Smyth, and W. Shi, *featureCounts: an efficient general purpose program for assigning sequence reads to genomic features.* Bioinformatics, 2014. **30**(7): p. 923-30.

114. Ritchie, M.E., et al., *limma powers differential expression analyses for RNA-sequencing and microarray studies.* Nucleic Acids Res, 2015. **43**(7): p. e47.

115. Robinson, M.D., D.J. McCarthy, and G.K. Smyth, *edgeR: a Bioconductor package for differential expression analysis of digital gene expression data.* Bioinformatics, 2010. **26**(1): p. 139-40.

116. Subramanian, A., et al., *Gene set enrichment analysis: a knowledge-based approach for interpreting genome-wide expression profiles.* Proc Natl Acad Sci U S A, 2005. **102**(43): p. 15545-50.

117. Ge, S.X., E.W. Son, and R. Yao, *iDEP: an integrated web application for differential expression and pathway analysis of RNA-Seq data.* BMC Bioinformatics, 2018. **19**(1): p. 534.

118. Ge, S.X., D. Jung, and R. Yao, *ShinyGO: a graphical gene-set enrichment tool for animals and plants.* Bioinformatics, 2020. **36**(8): p. 2628-2629.

119. Gao, B., et al., *Quickomics: exploring omics data in an intuitive, interactive and informative manner.* Bioinformatics, 2021.

120. Tyanova, S., et al., *The Perseus computational platform for comprehensive analysis of (prote)omics data.* Nat Methods, 2016. **13**(9): p. 731-40.

121. Zhu, Y., et al., *DEqMS: A Method for Accurate Variance Estimation in Differential Protein Expression Analysis.* Mol Cell Proteomics, 2020. **19**(6): p. 1047-1057.

122. Hsiao, S.H., et al., *The FLT3 inhibitor midostaurin selectively resensitizes ABCB1-overexpressing multidrug-resistant cancer cells to conventional chemotherapeutic agents.* Cancer Lett, 2019. **445**: p. 34-44.

123. Ji, N., et al., *Midostaurin Reverses ABCB1-Mediated Multidrug Resistance, an in vitro Study.* Front Oncol, 2019. **9**: p. 514.

124. Boytz, R., et al., *Anti-SARS-CoV-2 activity of targeted kinase inhibitors: Repurposing clinically available drugs for COVID-19 therapy.* J Med Virol, 2022.

125.   Maarifi, G., et al., *Identifying enhancers of innate immune signaling as broad-spectrum antivirals active against emerging viruses.* Cell Chem Biol, 2022. **29**(7): p. 1113-1125 e6.

126.   DrugBank. *Gilteritinib.* [cited Dec 16, 2022; Available from: https://go.drugbank.com/drugs/DB12141.

127.   Gotink, K.J., et al., *Lysosomal sequestration of sunitinib: a novel mechanism of drug resistance.* Clin Cancer Res, 2011. **17**(23): p. 7337-46.

128.   Wu, S., et al., *Drug resistance-related sunitinib sequestration in autophagolysosomes of endothelial cells.* Int J Oncol, 2020. **56**(1): p. 113-122.

129.   Giuliano, S., et al., *Resistance to sunitinib in renal clear cell carcinoma results from sequestration in lysosomes and inhibition of the autophagic flux.* Autophagy, 2015. **11**(10): p. 1891-904.

130.   Kantarjian, H., et al., *Acute myeloid leukemia: current progress and future directions.* Blood Cancer J, 2021. **11**(2): p. 41.

131.   Kadia, T.M., et al., *Toward Individualized Therapy in Acute Myeloid Leukemia: A Contemporary Review.* JAMA Oncol, 2015. **1**(6): p. 820-8.

132.   Fodale, V., et al., *Mechanism of cell adaptation: when and how do cancer cells develop chemoresistance?* Cancer J, 2011. **17**(2): p. 89-95.

133.   Hanahan, D., *Hallmarks of Cancer: New Dimensions.* Cancer Discov, 2022. **12**(1): p. 31-46.

134.   Gupta, R., et al., *Multi-drug resistance protein 1 as prognostic biomarker in clinical practice for acute myeloid leukemia.* Int J Lab Hematol, 2016. **38**(5): p. e93-e97.

135.   Marie, J.P., R. Zittoun, and B.I. Sikic, *Multidrug resistance (mdr1) gene expression in adult acute leukemias: correlations with treatment outcome and in vitro drug sensitivity.* Blood, 1991. **78**(3): p. 586-92.

136.   Pirker, R., et al., *MDR1 gene expression and treatment outcome in acute myeloid leukemia.* J Natl Cancer Inst, 1991. **83**(10): p. 708-12.

137.   de Grouw, E.P., et al., *Preferential expression of a high number of ATP binding cassette transporters in both normal and leukemic CD34+CD38- cells.* Leukemia, 2006. **20**(4): p. 750-4.

138.   Zeijlemaker, W., et al., *Absence of leukaemic CD34(+) cells in acute myeloid leukaemia is of high prognostic value: a longstanding controversy deciphered.* Br J Haematol, 2015. **171**(2): p. 227-238.

139. Stone, R.M., et al., *Phase IB study of the FLT3 kinase inhibitor midostaurin with chemotherapy in younger newly diagnosed adult patients with acute myeloid leukemia.* Leukemia, 2012. **26**(9): p. 2061-8.

140. Cloos, J. and et al., *Midostaurin in Patients (Pts) with Newly Diagnosed FLT3-Mutation Negative Acute Myeloid Leukemia (AML): Final Results and Measurable Residual Disease (MRD) Analyses from the Unify Trial.* Blood, 2021. **138**: p. 1303.

141. Chen, Y., et al., *Oestrogen-related receptor alpha mediates chemotherapy resistance of osteosarcoma cells via regulation of ABCB1.* J Cell Mol Med, 2019. **23**(3): p. 2115-2124.

142. Wu, T., et al., *Effect of abemaciclib (LY2835219) on enhancement of chemotherapeutic agents in ABCB1 and ABCG2 overexpressing cells in vitro and in vivo.* Biochem Pharmacol, 2017. **124**: p. 29-42.

143. Sorf, A., et al., *Ribociclib shows potential for pharmacokinetic drug-drug interactions being a substrate of ABCB1 and potent inhibitor of ABCB1, ABCG2 and CYP450 isoforms in vitro.* Biochem Pharmacol, 2018. **154**: p. 10-17.

144. FDA. *In Vitro Metabolism and Transporter Mediated Drug-Drug Interaction Studies Guidance for Industry.* 2017 Jan 09, 2023]; Available from: https://www.fda.gov/files/drugs/published/In-Vitro-Metabolism--and-Transporter--Mediated-Drug-Drug-Interaction-Studies-Guidance-for-Industry.pdf.

145. Infante, J.R., et al., *A Phase I Study of the Cyclin-Dependent Kinase 4/6 Inhibitor Ribociclib (LEE011) in Patients with Advanced Solid Tumors and Lymphomas.* Clin Cancer Res, 2016. **22**(23): p. 5696-5705.

146. Patnaik, A., et al., *Efficacy and Safety of Abemaciclib, an Inhibitor of CDK4 and CDK6, for Patients with Breast Cancer, Non-Small Cell Lung Cancer, and Other Solid Tumors.* Cancer Discov, 2016. **6**(7): p. 740-53.

147. Tamura, K., et al., *Phase I study of palbociclib, a cyclin-dependent kinase 4/6 inhibitor, in Japanese patients.* Cancer Sci, 2016. **107**(6): p. 755-63.

148. Belhoussine, R., et al., *Two distinct modes of oncoprotein expression during apoptosis resistance in vincristine and daunorubicin multidrug-resistant HL60 cells.* Adv Exp Med Biol, 1999. **457**: p. 365-81.

149. Efferth, T., U. Fabry, and R. Osieka, *Apoptosis and resistance to daunorubicin in human leukemic cells.* Leukemia, 1997. **11**(7): p. 1180-6.

150. Masquelier, M., et al., *Relationship between daunorubicin concentration and apoptosis induction in leukemic cells.* Biochem Pharmacol, 2004. **67**(6): p. 1047-56.

151. Shman, T.V., et al., *CD34+ leukemic subpopulation predominantly displays lower spontaneous apoptosis and has higher expression levels of Bcl-2 and MDR1 genes than CD34- cells in childhood AML.* Ann Hematol, 2008. **87**(5): p. 353-60.

152. McMahon, C.M., et al., *Clonal Selection with RAS Pathway Activation Mediates Secondary Clinical Resistance to Selective FLT3 Inhibition in Acute Myeloid Leukemia.* Cancer Discov, 2019. **9**(8): p. 1050-1063.

153. Zhou, S., et al., *Understanding gilteritinib resistance to FLT3-F691L mutation through an integrated computational strategy.* J Mol Model, 2022. **28**(9): p. 247.

154. Eguchi, M., et al., *Mechanisms Underlying Resistance to FLT3 Inhibitors in Acute Myeloid Leukemia.* Biomedicines, 2020. **8**(8).

155. Joshi, S.K., et al., *A noncanonical FLT3 gatekeeper mutation disrupts gilteritinib binding and confers resistance.* Am J Hematol, 2021. **96**(7): p. E226-E229.

156. Bedouhene, S., et al., *Neutrophil Degranulation of Azurophil and Specific Granules.* Methods Mol Biol, 2020. **2087**: p. 215-222.

157. Gierlikowska, B., et al., *Phagocytosis, Degranulation and Extracellular Traps Release by Neutrophils-The Current Knowledge, Pharmacological Modulation and Future Prospects.* Front Pharmacol, 2021. **12**: p. 666732.

158. Windisch, R., et al., *Oncogenic Deregulation of Cell Adhesion Molecules in Leukemia.* Cancers (Basel), 2019. **11**(3).

159. Melki, J.R., et al., *Hypermethylation of E-cadherin in leukemia.* Blood, 2000. **95**(10): p. 3208-13.

160. Histology, A.o.P.a.A. *Actin filaments.* Dec 30, 2022]; Available from: https://mmegias.webs.uvigo.es/02-english/5-celulas/7-actina.php.

161. Lone, A.M. and K. Tasken, *Proinflammatory and immunoregulatory roles of eicosanoids in T cells.* Front Immunol, 2013. **4**: p. 130.

162. Czumaj, A. and T. Sledzinski, *Biological Role of Unsaturated Fatty Acid Desaturases in Health and Disease.* Nutrients, 2020. **12**(2).

163. Donato, R., et al., *Functions of S100 proteins.* Curr Mol Med, 2013. **13**(1): p. 24-57.

164. Wang, S., et al., *S100A8/A9 in Inflammation.* Front Immunol, 2018. **9**: p. 1298.

165. Farahani, E., et al., *Cell adhesion molecules and their relation to (cancer) cell stemness.* Carcinogenesis, 2014. **35**(4): p. 747-59.

166. Karjalainen, R., et al., *Elevated expression of S100A8 and S100A9 correlates with resistance to the BCL-2 inhibitor venetoclax in AML.* Leukemia, 2019. **33**(10): p. 2548-2553.

167. Yang, X.Y., et al., *High expression of S100A8 gene is associated with drug resistance to etoposide and poor prognosis in acute myeloid leukemia through influencing the apoptosis pathway.* Onco Targets Ther, 2016. **9**: p. 4887-99.

168. Zavorka Thomas, M.E., et al., *Gilteritinib-induced upregulation of S100A9 is mediated through BCL6 in acute myeloid leukemia.* Blood Adv, 2021. **5**(23): p. 5041-5046.

169. Nichols, J.M., et al., *Cell and molecular transitions during efficient dedifferentiation.* Elife, 2020. **9**.

170. Kawamura, K., T. Yoshida, and S. Sekida, *Autophagic dedifferentiation induced by cooperation between TOR inhibitor and retinoic acid signals in budding tunicates.* Dev Biol, 2018. **433**(2): p. 384-393.

171. Liu-Kreyche, P., et al., *Lysosomal P-gp-MDR1 Confers Drug Resistance of Brentuximab Vedotin and Its Cytotoxic Payload Monomethyl Auristatin E in Tumor Cells.* Front Pharmacol, 2019. **10**: p. 749.

172. Rajagopal, A. and S.M. Simon, *Subcellular localization and activity of multidrug resistance proteins.* Mol Biol Cell, 2003. **14**(8): p. 3389-99.

173. Zhitomirsky, B., H. Farber, and Y.G. Assaraf, *LysoTracker and MitoTracker Red are transport substrates of P-glycoprotein: implications for anticancer drug design evading multidrug resistance.* J Cell Mol Med, 2018. **22**(4): p. 2131-2141.

174. Zhitomirsky, B., et al., *Lysosomotropic drugs activate TFEB via lysosomal membrane fluidization and consequent inhibition of mTORC1 activity.* Cell Death Dis, 2018. **9**(12): p. 1191.

175. Efeyan, A., R. Zoncu, and D.M. Sabatini, *Amino acids and mTORC1: from lysosomes to disease.* Trends Mol Med, 2012. **18**(9): p. 524-33.

176. Jiao, F., B. Zhou, and L. Meng, *The regulatory mechanism and therapeutic potential of transcription factor EB in neurodegenerative diseases.* CNS Neurosci Ther, 2023. **29**(1): p. 37-59.

177. Sardiello, M., et al., *A gene network regulating lysosomal biogenesis and function.* Science, 2009. **325**(5939): p. 473-7.

178. Qiao, X., et al., *The combination of CUDC-907 and gilteritinib shows promising in vitro and in vivo antileukemic activity against FLT3-ITD AML.* Blood Cancer J, 2021. **11**(6): p. 111.

179. Hu, X., et al., *Arsenic trioxide potentiates Gilteritinib-induced apoptosis in FLT3-ITD positive leukemic cells via IRE1a-JNK-mediated endoplasmic reticulum stress.* Cancer Cell Int, 2020. **20**: p. 250.